# Mechanical Forces in Growth Regulation: Challenging Force Measurements and Force Manipulations in the *Drosophila* Wing Imaginal Disc

---

Dissertation

zur

Erlangung der naturwissenschaftlichen Doktorwürde
(Dr. sc. nat.)

vorgelegt der

Mathematisch-naturwissenschaftlichen Fakultät

der

Universität Zürich

von

Dominik Eder

aus

Österreich

Promotionskommission:

Prof. Dr. Christof Aegerter (Vorsitz der Dissertation)

Prof. Dr. Konrad Basler (Leitung der Dissertation)

Prof. Dr. Markus Affolter

Dr. Frank Schnorrer

Zürich, 2017

***"The hardest thing of all is to find a black cat in a dark room,***

***especially if there is no cat."***

(attributed to Confucius, 551-479 BC)

# TABLE OF CONTENTS

# TABLE OF FIGURES

# *ZUSAMMENFASSUNG*

Jede lebende Zelle ist in ihrer dreidimensionalen Mikroumgebung eingebettet, durch welche sie ständigen mechanischen Reizen ausgesetzt ist. Aktuelle wissenschaftliche Studien weisen darauf hin, dass diese physikalischen Parameter - zusätzlich zu den biochemischen Signalen - einen starken Einfluss auf die Entwicklungsvorgänge in der Zelle haben. Es wurde zum Beispiel gezeigt, dass mechanische Kräfte Migrationsprozesse lenken, Morphogenese vorantreiben oder Wachstum kontrollieren. Die vorliegende Arbeit konzentriert sich auf die Untersuchung von physikalischen Parametern in der Flügelscheibe der Fruchtfliege *Drosophila melanogaster*. Die Flügelscheibe, welche vor allem als klassisches Modellsystem für genetische Prozesse gilt, erfährt auch im Bereich der Biophysik steigende Beachtung. Computermodelle weisen darauf hin, dass mechanische Kräfte eine entscheidende Rolle in der Wachstumsregulierung der Flügelscheibe spielen. Diese Wachstumsmodelle stellen einen Mechanismus vor, indem eine ständige Interaktion zwischen biochemischen Signalen und mechanischen Kräften das Wachstum mit der Scheibengrösse abstimmen. Dieses Zusammenspiel stellt einen intrinsischen, robusten Mechanismus dar welcher zu homogenem Wachstum führt und eine angemessene endgültige Grösse der Flügelscheibe gewährleistet.

Diese Doktorarbeit versucht empirische Belege für die Rolle von mechanischen Reizen in der Wachstumsregulierung der Flügelscheibe nachzuweisen. Die vorliegende Arbeit besteht aus drei Teilen. Die Einleitung beinhaltet einen Review zur gängigen Literatur über mechanische Kräfte und deren Einfluss auf Organwachstum. Im Ergebnis- und Diskussionsteil werden zwei experimentelle Ansätze vorgestellt, um mechanische Reize in der Flügelscheibe entweder zu messen oder zu manipulieren.

Das erste Kapitel (Introduction) umfasst Literatur, welche die Rolle von mechanischen Reizen im Organwachstum unterstreicht. Es beinhaltet klassische Arbeiten aus Experimenten in Zellkultur und auch Studien zum Knochenumbau in Säugetieren. Die Beispiele demonstrieren, dass extern zugeführte mechanische Reize das Wachstum und die Formbildung von Geweben und Organen beeinflussen können. Folgend werden die Fortschritte, aber auch die Herausforderungen von wissenschaftlichen Arbeiten zu

mechanischen Kräften und Wachstum in der Flügelscheibe zusammengefasst, wobei ein besonderer Schwerpunkt auf Methoden gelegt wird.

Im zweiten Kapitel (Results and Discussion I) wird die Studie beschrieben, einen auf FRET-basierenden mechanischen Sensor zu entwickeln. Der Sensor sollte es uns ermöglichen, mechanische Spannungen an den Zell-Zell Kontakten in der Flügelscheibe zu messen. Dafür wurde ein bestehendes FRET-Sensor Modul in das *Drosophila* E-Cadherin Protein integriert. E-Cadherin ist ein Adhesionsmolekül welches das Zytoskelett zweier benachbarter Zellen verbindet und von dem vermutet wird, dass es eine aktive Rolle in der Kraftübertragung zwischen Zellen spielt. Mit diesen Konstrukten wurden transgene Fliegen generiert und der Sensor in drei verschiedenen Geweben auf seine Funktionalität getestet: in der Flügelscheibe, in den Amnioserosa Zellen währen dem Dorsalschluss (*dorsal closure*) und den migrierenden Zellen während der Oogenese (*border cell migration*). Jedoch waren die Messungen weder sensitiv gegenüber den dynamischen Spannungsänderungen während den normalen Entwicklungsprozessen, noch gegenüber den experimentell zugeführten mechanischen Manipulationen - der Sensor war also nicht funktionell. In den Messungen konnten technische Schwierigkeiten aufgezeigt werden, welche allgemeine Probleme von FRET Messungen darstellen könnten. Ich hoffe mit dieser Arbeit die technischen Schwierigkeiten aufzeigen zu können, um zukünftige Studien zu einem besseren Design und zur Verwendung geeigneter Kontrollen zu inspirieren, und damit künftige falsch-positive Ergebnisse zu verhindern.

Im dritten Kapitel (Results and Discussion II) beschreibe ich die Studie, mit einer vorher entwickelten Streckbank die Flügelscheibe in Kultur mechanisch zu manipulieren. Mit dieser Streckbank, in Kombination mit Zellzyklusmarkern oder einem Microarray, wurde in dieser Arbeit der Einfluss von mechanischem Stress auf Proliferation und Genexpression untersucht. Allerdings konnte durch die spezifische mechanische Reizsetzung weder die Proliferationsrate, noch das Genexpressionsmuster beeinflusst werden. Auch hier waren technische Schwierigkeiten ein Teilgrund für die negativen Ergebnisse.

Die zusammengefasste Literatur in der Einleitung hebt hervor, dass mechanische Signale einen wichtigen Einfluss auf verschiedenste Entwicklungsstadien ausüben und höchst relevant für das Organwachstum sind. Trotzdem bleibt es noch offen, wie stark mechanische Kräfte zwischen den einzelnen Zellen der Flügelscheibe auftreten und in

welchem Ausmaß sie das Wachstum beeinflussen. Die vorliegende Arbeit ist durch technische Schwierigkeiten eingeschränkt in ihrer Aussagekraft und lässt somit keine klare Schlussfolgerung über die zugrundeliegende Hypothese, dass mechanische Reize in der Flügelscheibe das Wachstum regulieren, zu. Stattdessen zeigen aber beide Studien methodische Herausforderungen klar auf, welche zukünftige Arbeiten hoffentlich positiv beeinflussen können und ein besseres Studiendesign ermöglichen.

# *SUMMARY*

Every living cell is embedded in a 3D-microenvironment where it is exposed to a variety of mechanical cues. Recent studies strongly emphasize the importance of these physical parameters – apart from biochemical ones - for developmental processes. Cellular and tissue wide forces have been shown to direct migration, to drive morphogenesis or to control growth. In the present thesis I focused on the wing imaginal disc of *Drosophila melanogaster* to decipher the role of mechanical forces in growth regulation. Being a classical model system to study genetic networks, the wing disc currently also gains attention in the field of biophysics. Computational modelling has provided evidence for a crucial role of mechanical forces in controlling growth of the wing disc. These growth models suggest feedback loops between biochemical signaling and mechanical forces to modulate growth according to size. This interplay provides a robust and intrinsic mechanism to ensure for homogenous growth and a proper final size of the wing disc.

In this thesis I aim to find empirical evidence for a growth promoting role of mechanical forces in the wing disc and to elucidate molecular mechanisms mechanosensation. The thesis is subdivided into three parts. The introduction contains a review of the current literature about mechanical forces in organ growth. The results and discussion part comprises two experimental approaches which aim to either measure or to manipulate mechanical forces in the wing disc.

In the first chapter (Introduction) I review the literature supporting the importance of mechanical forces in the regulation of growth. This review constitutes classical work of *in vitro* systems and bone remodeling which reveal that external mechanical signals affect tissue shape and growth. Further, the review summarizes the achievements and challenges of research on mechanical growth regulation in the wing disc – with special emphasis on methodologies.

The second chapter (Results and Discussion I) describes an approach to develop a FRET-based tension sensor to measure mechanical forces across the wing disc. Similar FRET sensors have previously been used to study forces at adhesion sites in mammalian cells. Here, we introduce the sensor cassette into the *Drosophila* E-

Cadherin, an adherens junction protein which connects the cytoskeleton of adjacent cells and is thereby supposed to transduce mechanical signals between neighboring cells. With this construct I generated transgenic flies and assessed the sensitivity of the sensor in three *Drosophila* tissues: the wing disc, the amnioserosa cells during dorsal closure and the migrating border cells. I carefully tested the sensor by measuring dynamic developmental processes and mechanical modifications, but the sensor was not functional. Additionally, I could not reproduce the results from a previous publication which used a similar FRET sensor in border cell migration. In all these experiments I encountered technical problems of FRET measurements, which represent general problems for FRET analysis in living tissues. By emphasizing these pitfalls I hope to help future studies to better design and control their FRET analysis and to prevent false positive outcomes.

The third chapter (Result and Discussion II) illustrates an approach to modify mechanical stress in the wing disc by using a previously developed stretching device. Combining this setup with *in vitro* culture and cell cycle analysis, I addressed the interaction between mechanical stress and growth. Further, I assessed the transcriptional profile in response to mechanical stress by a microarray and qRT-PCR. However, stretching the wing disc in culture did not affect cell cycle progression or gene expression in these experiments. One reason for the negative outcome was the limitation of the *in vitro* culturing technique which did not allow us to perform manipulation experiments for more than one hour.

In conclusion, there is general agreement in the scientific field that mechanical forces influence growth in various developmental contexts. But it still remains elusive how strong the forces are in the wing imaginal discs and to which extent they stimulate growth. The methodological approaches in this thesis tackled this question but revealed technical limitations. Rather than contributing to the question about forces in growth regulation, the present thesis highlights technical problems which challenge the progress in the field and will hopefully inspire subsequent studies for better design and performances of experiments.

# 1. INTRODUCTION – Forces Controlling Organ Growth

This section constitutes a manuscript that was submitted as a review article.

## Forces Controlling Organ Growth and Size

Dominik Eder, Christof Aegerter, Konrad Basler

## 1.1. ABSTRACT

One of the fundamental questions in developmental biology is what determines the final size and shape of an organ. Recent research strongly emphasizes that besides cell-cell communication, biophysical principals govern organ development. The architecture and mechanics of a tissue guide cellular processes such as movement, growth or differentiation. Furthermore, mechanical cues do not only regulate processes at a cellular level but also provide constant feedback about size and shape on a tissue scale. Here we review several models and experimental systems which are contributing to our understanding of the roles mechanical forces play during organ development. One of the best understood processes is how the remodeling of bones is driven by mechanical load. Culture systems of single cells and of cellular monolayers provide further insights into the growth promoting capacity of mechanical cues. We focus on the *Drosophila* wing imaginal disc, a well-established model system for growth regulation. We discuss theoretical models that invoke mechanical feedback loops for growth regulation and experimental studies providing empirical support. Future progress in this exciting field will require the development of new tools to precisely measure and modify forces in living tissue systems.

## 1.2. INTRODUCTION

Precise regulation of organ growth is fundamental for life. For example, it would be hard for us to walk if our legs were not roughly of the same length. Similarly, an insect would have problems flying if its wings were not scaled to body size. What are the mechanisms that ensure that organs and extremities acquire the right size and shape during development? Biologists in the early 20$^{th}$ century tackled this question with grafting experiments in salamanders. The zoologists Twitty and Schwind removed prospective leg anlagen from a big salamander species, and grafted them to embryos of a smaller salamander species. Interestingly, the grafted limbs grew to the large size they would have reached in their bodies of origin, while the host's other limbs remained small (Twitty and Schwind, 1931). Similar experiments were performed in mice with fetal thymus glands yielding similar results – the organs grew to their original size, even in a different environment (Metcalf, 1963). These experiments reveal that organs contain intrinsic information about their destined size. But what role do extrinsic factors, such as nutrition and hormones, play? In the above mentioned studies the feeding plan during the experiments also influenced the speed and extent of growth of the grafted organ. Thus, the interplay of intrinsic and extrinsic factors defines the final size of an organ.

Cell growth, death, proliferation and cell polarity constitute an organ's toolkit to grow and sculpt its shape. Growth is generally defined as the increase in mass. In an organ, the most common cause for this is cell proliferation, which results in an increased cell number. In addition to proliferation, tissue growth can also occur without cell division and an increase in cell size alone can significantly contribute to overall growth (Conlon and Raff, 1999). Although proliferation and cell growth are often used interchangeably, they are two separate processes as shown in the *Drosophila* wing imaginal disc (Neufeld et al., 1998; Weigmann et al., 1997). If proliferation is experimentally enhanced or blocked in the disc, the tissue still reaches its appropriate size. Hence, the tissue compensates for the reduced or increased cell number with increased or decreased cell growth, respectively. This indicates that the mechanism controlling organ size regulates the *overall* size rather than cell growth or proliferation alone. Further, it is not only the rate of growth but also its orientation that shapes an organ. Studies on the *Drosophila* wing have revealed a clear causal relationship between the orientation of cell divisions in the larval wing epithelium and the morphology of the

adult wing (Baena-Lopez et al., 2005; Aigouy et al., 2010). In addition to growth, apoptosis also plays a role in shaping the final size of an organ. Apoptosis helps shaping organs e.g. by separating digits in the mammalian limb (Raff, 1998) or by reducing the amount of neurons in the developing brain (Roth and D'Sa, 2001).

In recent years, a vast amount of molecular factors has been described which drive and control cell growth, death, proliferation and cell polarity. However, in order to understand the regulation of the final organ size we need to understand how growth is stopped at the appropriate time-point. As mentioned above, grafting experiments revealed that final organ size seems to be an inherent property. This requires an organ to continuously monitor its dimensions to determine when the final size is reached.

In the prevailing hypotheses the mechanisms for size regulation and pattern formation are interconnected. Signaling proteins are secreted, form a gradient and act in a concentration dependent manner to provide positional information. Such morphogens are responsible for patterning organs and are able to restrict or promote growth (Day and Lawrence, 2000). This has been best studied in the *Drosophila* wing disc. Two prominent morphogens - Wingless (Wg) and Decapentaplegic (Dpp) - are important patterning factors in this system (Zecca et al., 1995; Zecca et al., 1996). Overexpression of either morphogen also leads to overgrowth, whereas discs lacking Dpp or Wg are significantly smaller (Day and Lawrence, 2000; Wartlick et al., 2011). These observations indicated the interplay between patterning and growth regulation. Nonetheless, despite being an attractive system for intrinsic size regulation, morphogenetic growth models alone fail to explain numerous experimental observations in the wing disc (Schwank and Basler, 2010; Restrepo et al., 2014).

It has become widely accepted that in addition to biochemical signals, mechanical cues have an impact on growth regulation (reviewed by LeGoff and Lecuit, 2015). Therefore, tissue mechanics was integrated into various growth models to explain observations which the instructive role of biochemical growth factors alone could not account for (Aegerter-Wilmsen et al., 2007; Hufnagel et al., 2007; Egginton, 2011; Uyttewaal et al., 2012).

In this review we will discuss mechanical forces that regulate growth and review experimental approaches to investigate them. Although there is a vast amount of literature about mechanics in plant systems, we will focus exclusively on animal model

systems here. In the first part we will present evidence for the growth regulating roles of mechanical forces in different experimental systems. In the second part we will focus on the *Drosophila* wing disc, starting with mechanical feedback growth models and then describe technical means to measure and alter mechanical forces.

## 1.3. MECHANICAL FORCES IN GROWTH

The idea that the mechanical environment influences size and shape of a tissue is not new. Biologists recognized the importance of physical forces for establishing a functional organ a long time ago. D'Arcy Thompson's "On Growth and Form" is a popular book from the early twentieth century discussing biophysical principles during animal development (Thompson, 1917). Later on, the rapid technical progress in molecular biology directed the focus of developmental biologists onto genetically encoded information rather than physical one. Additionally, the lack of tools to measure and manipulate mechanical properties in a living tissue rendered research on the physical principles in development challenging. In the 1970s the discovery of focal adhesion provided a mechanism by which a cell can sense its mechanical microenvironment (Izzard and Lochner, 1976). This, together with findings about the actomyosin machinery attached to these adhesion sites, stimulated work on mechanotransduction between a cell and its surrounding (Heath and Dunn, 1978).

Subsequently the implementation of new techniques allowed the investigation of the growth promoting effects of mechanical forces. Early evidence came from cancer cells that were grown in increasing agarose concentrations that increased the compressive stress onto the spheroid tumors (Helmlinger et al., 1997; Cheng et al., 2009). These experiments revealed that increased mechanical stress inhibited growth: compression of the spheroid suppressed proliferation and induced apoptosis. Another elegant study with endothelial cells, seeded on varying substrate rigidities, indicated that individual cell growth was influenced by the geometry of the cell, rather than the direct contact with the substrate (Chen et al., 1997).

These studies illustrate that cellular growth is dependent on its mechanical environment. In the following chapter we will briefly describe the mechanical architecture of an epithelial cell and its contact points to the physical surrounding.

### 1.3.1. Mechanics of an epithelial cell

#### 1.3.1.1. Epithelial architecture

The majority of tissues in metazoans are organized as epithelia. Epithelial cells are defined by their polarity along an apical-basal direction (Fig. 1.1A): the apical side is exposed to the outside or luminal space whereas the basal side is attached to a substrate (Tepass, 2012). The adhesion between neighboring cells happens mostly at the apical side, with the adherens junctions playing a major role. E-cadherin is the most prominent adhesion protein and governs the connection between a cell and its neighbors as well as to its cytoskeleton. Nectins (Takai et al., 2008) and desmosomes (Green and Simpson, 2007) are additional complexes that allow adjacent cells to adhere to each other. Together, these adhesion complexes ensure tissue integrity (Tepass, 2012). Moreover, due to its association with the cytoskeleton, E-cadherin is believed to transduce mechanical signals between cells. At the basal side the focal adhesion complex (FA) has an analogous function: integrins - at the core of the FA - form strong attachments to the ECM and anchor to the cytoskeleton at the other end. Thus, integrins connect the cytoskeleton to the mechanical environment at cell-ECM adhesion points in a similar fashion as E-cadherin does at the cell-cell junctions (Geiger et al., 2009).

The shape of an epithelial cell is governed by internally and externally generated forces. In order to minimize mechanical damage to a cell and to ensure tissue integrity, internal and external forces must be balanced. Therefore, the actomyosin cytoskeleton constantly adjusts to the internal hydrostatic pressure and to mechanical stresses from outside the cell. Two cytoskeletal structures share this responsibility: actin cortex and stress fibers (SF). Lying under the apical cell membrane and more rarely at the basal side, the actin cortex comprises a mesh of actin filaments, myosin motors and actin binding proteins (Salbreux et al., 2012). The actin cortex is considered to be the main determinant of cell surface stiffness and to associate with the adherens junctions; cortical actin senses external forces and responds by remodeling. Accordingly, SF form a highly dynamic actin network when forces are required. SF can sense and respond to the external environment via attachment points at the FA. In contrast to cortical actin, SF span most of the cell and therefore can transmit forces over a longer distance range (Smith et al., 2014). Due to the high activity of actin crosslinkers and myosin motors, the turnover of the actin cortex and SF happens within seconds, enabling a fast response to an applied stress (Salbreux et al., 2012).

The activity of the actomyosin network, however, does not only passively resist against internal or external stress, but also actively shapes the cell. In concert with other cytoskeletal components, such as microfilaments and intermediate filaments, actin filaments stimulate cellular shape changes by altering apical, basal or lateral domains of the cell (Huber et al., 2015; Mao and Baum, 2015). The simultaneous activation of such transformations in a group of cells alters tissue architecture and contributes to morphogenetic development. A good example for this is apical constriction in which shortening of the apical cortex results in a wedge like shape of the cell. If coordinated tissue-wide, this can trigger the folding and invagination of a tissue such as in ventral furrow formation during *Drosophila* gastrulation or in *Caenorhabditis elegans* (Mao and Baum, 2015). Alternatively, actomyosin and/or microtubule activities modify the lateral dimension of a cell which causes flattening. If happening tissue-wide, epithelial flattening elongates a tissue as in the amnioserosa of *Drosophila* (Pope and Harris, 2008).

#### *1.3.1.2. Types of mechanical stress and mechanotransduction*

Here, we will briefly outline the types of external forces to which an epithelial cell is exposed and how the mechanical cues are transduced to generate a cellular response (Fig. 1.1B, C). An epithelial cell is constantly exposed to tensile stresses from adjacent cells. By definition, tensile stress leads to expansion or compression in the direction of the force. This can be caused by active shape and volume changes of the neighbors or through proliferation or apoptosis. According to current knowledge, mechanical cues from adjacent cells are transduced via E-cadherin to the actin filaments. The cytoskeleton directly senses the stress and causes a relevant response. It is further hypothesized that α-catenin, which links E-cadherin to actin, acts as mechanosensor and triggers a biochemical signaling cascade (Nowotarski and Peifer, 2014; Rooij, 2014). An epithelial cell is also sensitive to the rigidity of the ECM. Mechanical cues from the ECM are transferred via integrins to SF, which sense and respond directly to the stress by remodeling. Alternatively, the actin adapter protein Talin acts as a mechanosensor – when stretched it exposes buried binding sites for effector proteins (Austen et al., 2015). Finally, mechanical stresses can be exerted from outside the epithelium or the lumen. For example in endothelial tubes, cells are exerted to a shear stress which is caused by the frictional force of a flowing fluid. In contrast to tensile stress, shear stress is oriented longitudinally to the surface. Mechanotransduction of a

shear stress is thought to be mediated via cilia bending, stretching sensitive ion channels or junctional proteins (Roman and Pekkan, 2012).

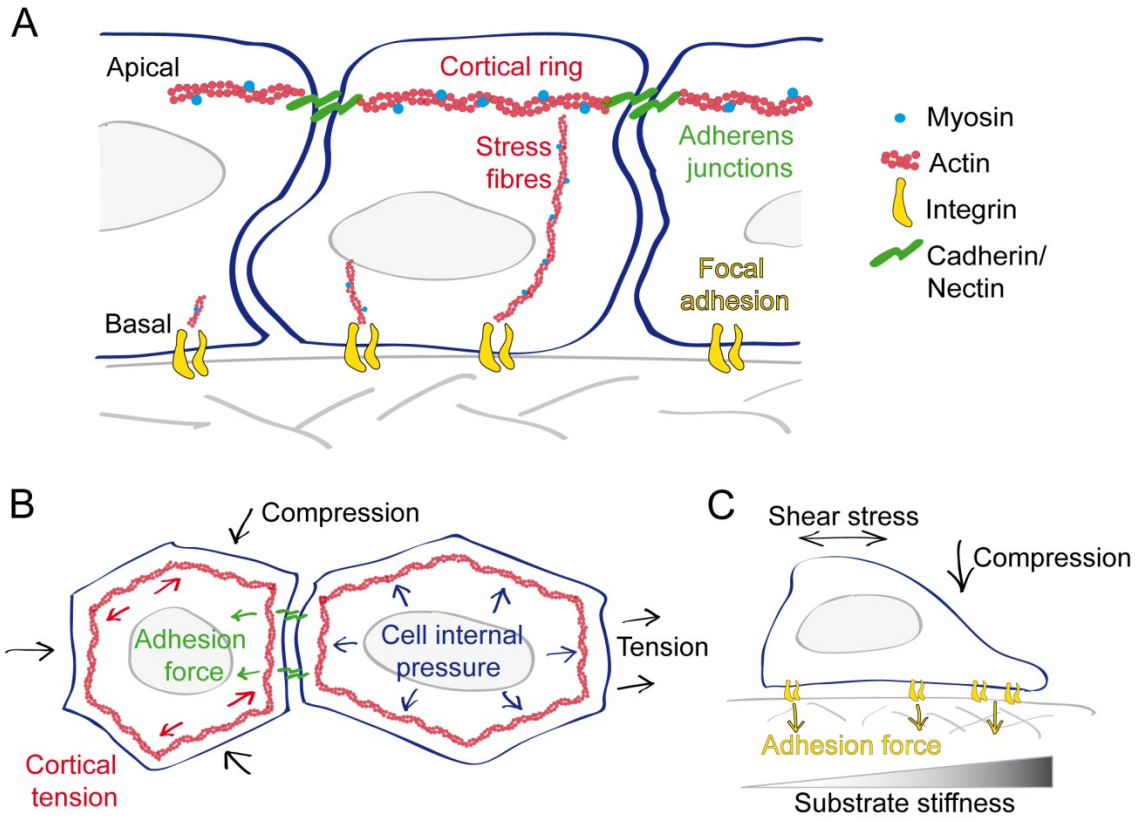


**Figure 1.1. Schematic representation of an epithelial cell and its mechanical environment.** (A) A polarized epithelial cell is connected via adherens junctions to its neighboring cells and via focal adhesion to the substrate. Desmosomal, septate and tight junctions are not shown because they do not appear in all epithelial cell types. (B, C) Epithelial cells are exposed to various types of mechanical stresses from intrinsic forces, neighboring cells and the extracellular space. (C) Cells respond to increasing substrate stiffness by reinforcing adhesion and active spreading on the substrate in an actomyosin- dependent process.

### *1.3.2. Models for mechanical growth control*

#### *1.3.2.1. Bone remodeling*

The function of bones is to give a framework for the body, to provide attachment sites for skeletal muscles and to protect inner organs. Bones are therefore exposed to varying mechanical loads.

Bones are constantly remodeled by the balanced activity of their constituent cell types, resulting in gain or loss of bone mass. The bone-forming osteoblasts and the bone-resorbing osteoclasts reside on top of the mineralized bone matrix beneath the

periosteum (Fig. 1.2A). Osteoblasts produce the organic bone matrix and support mineralization, whereas osteoclasts dissolve bone matrix. The osteoblast-derived osteocytes are dispersed throughout the bone matrix and form dendritic networks between each other, osteoblasts and osteoclasts. Osteocytes stimulate osteoblast and osteoclasts to form or resorb the bone matrix (Bonewald and Johnson, 2008; Crockett et al., 2011).

Several observations indicate that bone remodeling strongly depends on the mechanical load: the playing arm of professional tennis players is enriched in bone mass whereas persons with long-term bed rest have reduced bone mass, as do astronauts (Armbrecht et al. 2011; Vico et al., 2000). *In vivo* studies in mice show an increased bone mass of the caudal vertebrae following increased loading (Christen et al., 2014). These studies reveal the strong response to mechanical loads on the level of the tissue. On the other side, *in vitro* studies on single osteocytes indicate a change in cellular behavior if exposed to mechanical stress (Crockett et al., 2011). It has been reported that osteocytes activate Nitric Oxide (NO) signaling and Wnt signaling upon the application of mechanical stress (Jacobs et al., 2010; Crockett et al., 2011). In the absence of osteocytes bone remodeling does not respond to mechanical loading (Tatsumi et al., 2007). Osteocytes are therefore the mechanosensors which mediate instructive signals for bone remodeling.

The current model of bone adaption to mechanical load is a multiscale process (Fig. 1.2A). Initially, a mechanical load onto the organ causes a tissue–level strain. But the transmitted tissue-level strains are too small to activate a cellular response (You et al., 2001). Thus, it has been proposed that mechanical loading induces a fluid flow in the extracellular fluid surrounding the osteocytes (Klein-Nulend et al., 2012). The fluid flow enhances the mechanical strain and thus serves as the mechanical stress which is sensed by the osteocytes. *In vitro* models indicate that shear stress of the fluid interacts with membrane-associated proteins which stimulate signaling pathways such as BMP, Wnts and NO (Jacobs et al., 2010; Klein-Nulend et al., 2012). The signaling factors from the osteocytes modulate the activity of osteoblasts and osteoclasts and promote their bone forming and resorbing potential, respectively (Crockett et al., 2011).

Apart from correlational studies, this multiscale process is very difficult to analyze *in vivo*, hence most evidence was derived from either *in vitro* studies or theoretical modelling. As a consequence the relationship between bone remodeling and its

mechanical environment remains under debate. Concerns were raised whether osteocytes *in vivo* are stimulated by mechanical stress or whether regulation could be explained by an altered biochemical environment due to different flow dynamics in the bone (Jacobs et al., 2010). With the current methods it is difficult to separate cellular responses that are triggered by mechanical versus biochemical cues. Recent studies combined advanced high resolution computer tomography with computational methods to calculate local strain distributions and microstructural changes: a strong correlation was observed between bone remodeling and local strain patterns in murine vertebrae and human tibiae *in vivo* (Schulte et al., 2013; Christen et al., 2014). This supports the hypothesis of a multi-scale process: Organ-scale stresses provoke a change in the local microenvironment which in turn drives the adaption of specific micro-structures. These mechanisms allow bones to resist to external forces and to adjust to these forces by remodeling of the organ.

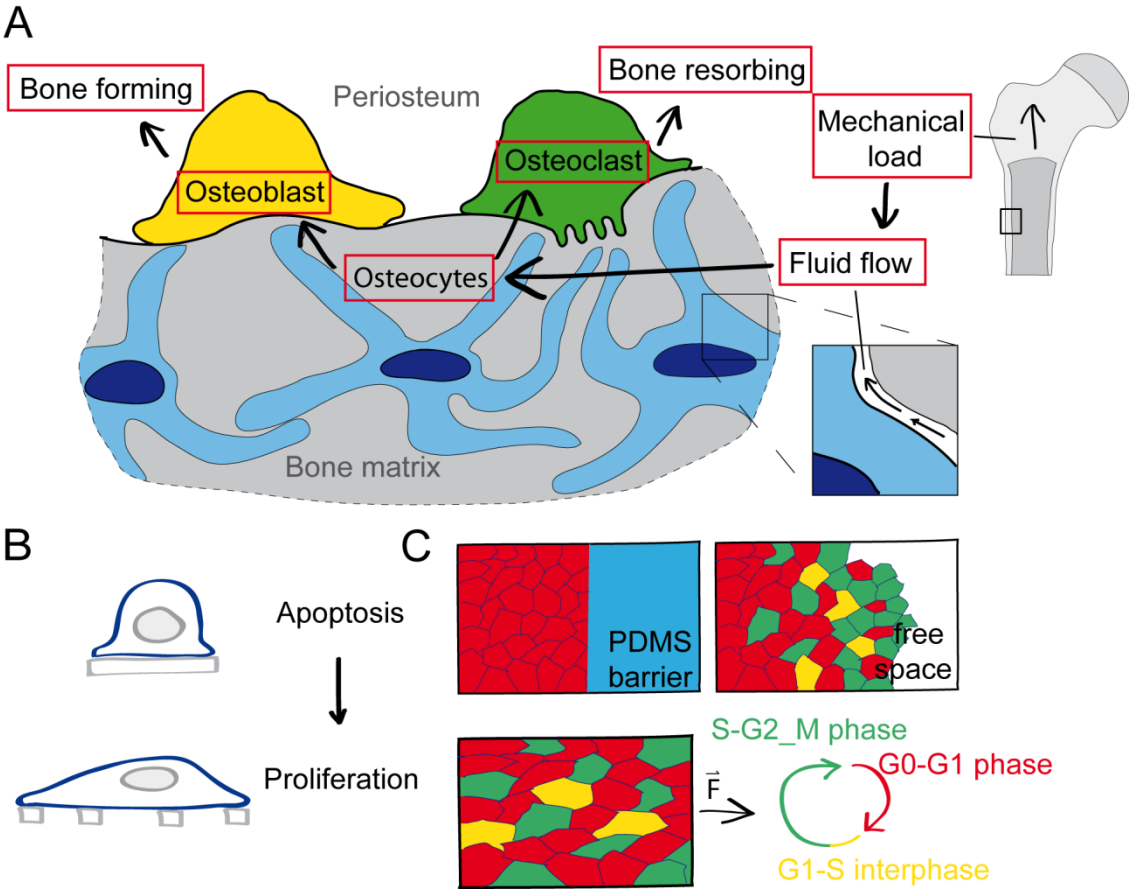


**Figure 1.2. Model systems for mechanical growth control.** (A) Mechanical load is driving bone remodeling in a multi-scale process: Mechanical load on the bone leads to fluid flow surrounding the osteocytes. Subsequently, shear-stress induced activation of osteocytes stimulates osteoblasts or osteoclasts to form and resorb the bone matrix, respectively. (B) Endothelial cells switch from proliferation to apoptosis when cell size is decreased by using micropatterned islands of adhesive

substrate (Chen, 1997). (C) Proliferation patterns of MDCK cells analyzed with Fucci cell cycle marker. Cells constrained with a PDMS barrier do not proliferate, but progress in cell cycle when the barrier is removed. Similarly, when cell area is increased by stretching the substrate, cells continue in the cell cycle (Streichan et al., 2014).

#### *1.3.2.2. Epithelial culture systems*

Systems such as the culture of epithelial monolayers allow controlled mechanical manipulation to be performed to investigate the behavior of multicellular tissues in response to force patterns. It has been shown for endothelial cells that the mechanical properties of the substrate strongly govern cell shape which in turn influences growth and viability (Fig. 1.2B; Chen, 1997). Endothelial cells were seeded on micropatterned substrates coated with extra-cellular matrix (ECM) components. By changing the spacing between the substrate islands it was possible to alter either the cell spreading or the cell-ECM contact zone (Fig. 1.2B). The results indicated that individual cell growth was governed by the cell geometry rather than the area providing contact with the substrate. Epithelial cells also respond to substrate rigidity by changing their geometry: they spread more on stiff than on soft substrates (Pelham et al., 1997). But how do cells behave if they are not separated from each other but in contact with neighboring cells? In an interesting study, Nelson et al. grew cell sheets on micropatterned substrates to control their spatial organization (Nelson et al., 2005). These authors explored how growth generates a global mechanical stress pattern in the tissue and how this feeds back to form asymmetric patterns of proliferation. When seeding cell sheets on microfabricated islands of different forms, they observed that the proliferative patterns changed according to the size and shape of the islands. Furthermore, computational modelling of the mechanical stress patterns within the tissue revealed a high correlation between mechanical stress and proliferation, suggesting that it is mechanical stress that is driving proliferation. Experimental depletion of junctional components showed that intercellular junctions are required for, and hence likely mediate, force-dependent proliferation.

Similar feedback loops between tissue mechanics and proliferation patterns were observed in studies with Madin-Darby canine kidney (MDCK) cells. The term “contact inhibition” describes the drastic decrease of motility and proliferation rate in a confluent epithelial monolayer (Fig. 1.2C) (Martz and Steinberg, 1972). Contact inhibition depends on cell-cell contact. Puliafito et al. performed a quantitative characterization of contact inhibition in MDCK cell culture by long-term tracking of

single cells and monitoring tissue behavior (Puliafito et al., 2012). An outward growing colony reaches the point where cells at the periphery cannot expand fast enough to accommodate for the proliferation in the bulk. Hence, cell density in the bulk increases as a consequence of mechanical constraints. This marks the onset of contact inhibition and mitotic activity sharply decreases. In this transition phase, cell area is reduced by cell division and converges to the critical point where proliferation is arrested. Puliafito et al. concluded that cell contacts are necessary, but not sufficient for mitotic inhibition. Rather, proliferation is arrested as a consequence of the reduced cell area, which is imposed by mechanical constraints on tissue expansion. In another study, the correlation between mechanical constraints, cell area and proliferation rate was examined by experimental perturbation of the mechanical constraints (Fig. 1.2C; Streichan et al., 2014). Restricting the overall area of the MDCK epithelial layer or actively stretching and compressing the tissue confirmed the conclusions of Puliafito et al. Furthermore, Streichan and colleagues proposed that mechanical constraint inhibits proliferation by regulating cell cycle entry at the checkpoint from G1 to S Phase.

In sum, *in vitro* proliferation is regulated by the mechanical constraints stemming from tissue dynamics. Similar mechanisms could also control tissue growth during organ development.

## 1.3.3. *Drosophila wing imaginal disc*

### *1.3.3.1. Introduction*

The *Drosophila* wing imaginal disc is currently one of the best studied model systems for which mechanical signaling is integrated into growth models; we will therefore focus on this system. The wing disc is the larval progenitor organ that develops into the wing of an adult fly (Fig. 1.3A). Development starts out with an anlage of around 30 cells and reaches roughly 50,000 cells at the onset of metamorphosis (Milan et al., 1996). The wing disc is an epithelial monolayer which forms a sac-like structure. The columnar cells on one side of the sac are the focus in most studies. At the center of the disc is the wing pouch which gives rise to the adult wing blade. Due to its relatively flat geometry and the well characterized set of morphogens and growth factors involved in its patterning, most of the growth studies have concentrated on the wing pouch.

Evidence for an integrative role of mechanical interactions in growth regulation first came from computational modelling (see 2.3.2.); these were then complemented by experimental data (see 2.3.3. and 2.3.4.). Below we first briefly describe the computational growth models that invoke mechanical forces and then discuss the options available to experimentally measure and modify mechanical forces within the wing disc.

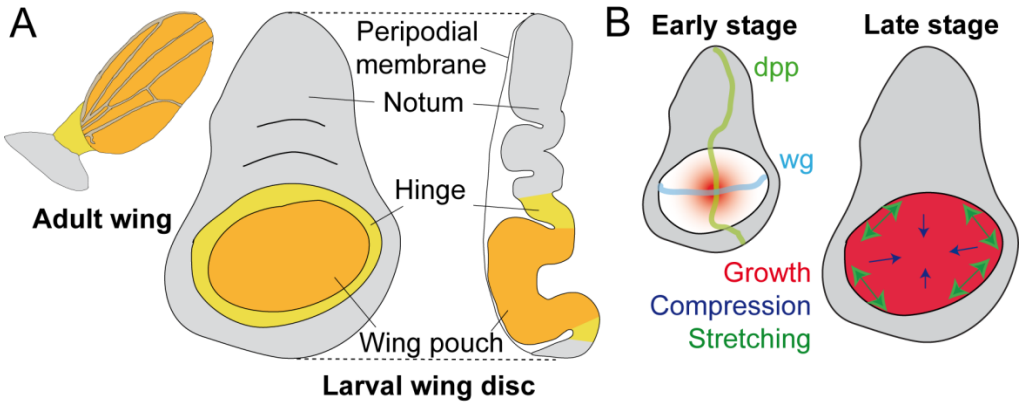


**Figure 1.3. Drosophila wing imaginal disc.** (A) Top and lateral view of the wing imaginal disc at third instar. The wing pouch will develop into the wing blade of the adult fly. (B) The concentration of morphogens is highest in the center of the wing pouch. Growth models suggest that the morphogen distribution promotes growth in the center, resulting in a growth gradient at early stages (Aegerter-Wilmsen et al., 2007; Hufnagel et al., 2007). This gradient changes the global tensions in the wing pouch which in turn stimulates proliferation at the periphery and suppresses proliferation at the center. This feedback loop leads to homogenous growth throughout the wing pouch at later stages as well as controlling size.

#### *1.3.3.2. Modelling forces*

It has been suggested that patterning and growth are coupled. In the wing disc the morphogens Dpp and Wg are supposed to play key roles in patterning and also in promoting growth (e.g. Day and Lawrence, 2000). But the role of Dpp and Wg in growth regulation remains controversial. Recent work pointed out that Dpp and Wg are only partially essential for growth and are not directly required to set the final size of the wing disc (Akiyama and Gibson, 2015, Alexandre et al., 2014, Harmansa et al., 2015). In the wing pouch Dpp and Wg form gradients perpendicular to each other with the highest concentrations in the center. The observation that proliferation is homogenous throughout the wing pouch lead to a conundrum: How can the graded morphogen distribution result in a uniform proliferation pattern (Milan et al., 1996)? This paradox inspired scientists in the field to think about alternative models for growth

control - considering mechanical signals as an additional carrier of instructive information for cells.

B. Shraiman initially postulated that mechanical interactions allow cells to compare their growth rate and trigger an appropriate cellular response (Shraiman, 2005). In a tissue with non-uniform growth certain patches of cells grow faster than the surrounding cells. Due to tissue rigidity and spatial restrictions, the faster growing cells get compressed whereas the surrounding tissue is stretched. Under the assumption that mechanical compression negatively regulates growth, the growth rate of the faster growing cells would eventually slow down until it is similar to that of the surrounding tissue. A prediction of this mechanical feedback mechanism is that in a healthy tissue different growth rates will converge and result in uniform growth. This mechanism would also prevent the local accumulation of mechanical stress and ensure tissue integrity.

This initial assumption was further integrated into two similar growth models which proposed a feedback loop between mechanical forces and morphogen induced proliferation in the wing disc (Fig. 1.3B; Aegerter-Wilmsen et al., 2007; Hufnagel et al., 2007). These models both offered a solution to the paradox of uniform growth driven by graded morphogens as well as providing a mechanism for final size determination. Hufnagel et al. suggested that cells proliferate above a certain threshold of Dpp concentration (Hufnagel et al., 2007). Although contradicted by more recent work (Hamaratoglu et al., 2011, Wartlick et al., 2011), they experimentally showed that the Dpp gradient is fixed over time and does not scale to disc size. According to the model, proliferation is arrested when Dpp levels fall below the threshold in the marginal cells resulting in increased compression in the center of the disc. This compressional stress feeds back on the proliferation rate and reduces growth. The model of Aegerter-Wilmsen et al., suggested that the high abundance of Dpp and Wg in the center of the disc initially promotes growth (Aegerter-Wilmsen et al., 2007). As the center grows, the surrounding cells are stretched, stimulating growth. Simultaneously, compression builds up in the center which leads to a competition between the growth promoting effects of morphogens and the inhibitory effects of compression. Growth stops when the stimulating effects of morphogens can no longer overcome the inhibitory effects of compression; the disc has then reached its final size. According to both models, mechanical feedback can explain the homogenous proliferation pattern as

well as acting as a determinant of the final size of the wing disc. Aegerter- Wilmsen and colleagues extended their model to integrate molecular signaling pathways into the mechanical growth regulation (Aegerter-Wilmsen et al., 2012). The extended model includes tested, and also hypothetical, interactions between the factors which are known to be involved in wing disc growth. The network incorporates the morphogens Dpp and Wg, growth factors like Yorkie and Vestigial, and polarity factors such as Four-jointed and Dachsous. The model was able to make predictions of cell size and shape which were subsequently confirmed by experimental data.

Initially, the mechanical feedback model was hypothetical as it was not based on empirical evidence in the wing disc, but rather extrapolated from different studies in other tissues (see 2.2.2). Consequently, parameters were not derived from underlying experimental data but were fitted manually. In the next two chapters we will highlight experimental approaches that are being used to directly assess the role of mechanical forces in wing disc growth.

#### *1.3.3.3. Measuring forces*

The underlying premise of the mechanical feedback models is that mechanical tensions are distributed heterogeneously over the wing disc. Initially, cell area was used as a read-out for mechanical stress. As predicted, a gradient of cell area can indeed be observed in the wing disc, with smaller cells in the center and larger, tangentially elongated cells at the periphery (Aegerter-Wilmsen et al., 2012). However, cell area can also be affected by other mechanisms; therefore it is a somewhat unspecific measure for mechanical stress.

A purely visual and non-invasive method is based on birefringence, which is an optical response of the tissue to stress anisotropies (Fig. 1.4A). Birefringence refers to the differences in refraction index of differently oriented material axes and can be measured by the retardance of polarized light transmitted through the tissue. Since forces can influence the material orientation, birefringence provides an indirect readout for mechanical stress (Nienhaus et al., 2009; Sugimura et al., 2016). Birefringence maps of the wing disc revealed that the retardance in the center is highest and decreases towards the edges, indicating a mechanical stress gradient with the maximal value in the center, which is predicted by the models (see 2.3.2., Nienhaus et al., 2009). However, the interpretation of these data is complicated by the fact that besides

mechanical stress, birefringence also depends on the thickness and density of the sample or on tissue anisotropies not induced by mechanical forces. It is difficult to correct for these additional parameters in a biological tissue. Further, it has to be considered that the measurement takes the entire tissue into account, which comprises two cell layers and two ECMs in the case of the wing disc. Thus, birefringence measurements alone do not allow a differentiation between mechanical tensions in overlapping layers.

Force inference (FI), another non-invasive method, is a computational approach which infers mechanical tensions from the analysis of cell shape (Fig. 1.4C). Given that the tissue is at mechanical equilibrium, the cell shapes are determined by the balance of contact forces between cells and the internal pressure. Thus, deviations from regular cell geometry enable the estimation of cellular tension and pressure (Sugimura et al., 2016). From any image which represents an apical surface marker, FI infers a map for junctional tension as well as internal pressure. In the wing disc FI confirmed the presence of a global mechanical gradient with highest compression in the center (Chiou et al., 2012; Ishihara and Sugimura, 2012). The advantage of FI is that it gives an overview over global mechanical patterns resolved at the cellular edge level. However, the limiting factor of the technique is that it has to rely on several assumptions. First, a requirement for FI is that cellular forces are dominating at the apical side because cell geometries are obtained from the apical cell surface. This neglects the contribution of more basally located cell-ECM junctions to cell mechanics. Further, FI greatly depends on prior assumptions of mechanical equilibrium, force balance and homogenous mechanical properties. Video force microscopy (VFM) relaxes some of these assumptions by using temporal cell shape changes rather than static images (Brodland et al., 2014). Finally, FI only provides relative information about pressure and tension and does not give absolute values.

The findings of FI in the wing disc were supported by laser ablation (LA) experiments (Fig. 1.4B). In contrast to the above described methods, LA is an invasive measurement. For LA, a focused two-photon-laser ablates a cellular structure which is under tension and the reaction of the cell is recorded. In the wing disc LA has been used to disrupt the cortical actomyosin in order to measure the recoil velocity of the remaining cell edges (LeGoff et al., 2013; Mao et al., 2013). The recoil velocity provides a measure of the tension state of the cortical actomyosin. LA confirmed that

cells in the center of the wing disc are compressed and cells at the periphery are stretched tangentially, in accordance with all previously observations.
In addition to its invasiveness, LA has two limitations. First, when interpreting results it has to be considered that only the tension of the cortical actomyosin is measured; adhesion strength and hydrostatic pressure are neglected in this analysis. Second, the recoil velocity does not only depend on the cortical tension, but also on the material properties of the structure. More precisely, the measurement only provides the ratio of force/viscosity, which means that no absolute values of forces can be gained from LA (Campas, 2016).

FRET based sensors were used in different systems to measure mechanical forces between cells (Fig. 1.4D). In contrast to other methods, FRET sensors measure forces along specific proteins. The core of a FRET sensor is two fluorophores connected by an elastic linker. Analysis of the FRET efficiency reveals the distance between the fluorophores, which correlates with the tension on the sensor. Being genetically encoded, such sensors were integrated into several proteins which are known to be involved in mechanotransduction and used for *in vitro* studies: Vinculin, Talin and E-cadherin (Grashoff et al., 2010; Borghi et al., 2012; Austen et al., 2015). We tested a sensor for the wing disc to measure tensions across E-cadherin at adherens junctions, but could not reliably measure mechanical forces (manuscript in preparation). The general problems of this method are: (1) FRET efficiencies not only depend on the distance between the two fluorophores but also on their microenvironment and their conformation to each other. This complicates the interpretation of the results. (2) Technical limitations impede the ratiometric method - the most commonly used scheme for FRET analysis. Being an intensity-based method it works well in cell culture but includes measurement artifacts when applied in living tissues. We believe that currently FRET based sensors are not an optimal tool for force measurements in the wing disc.

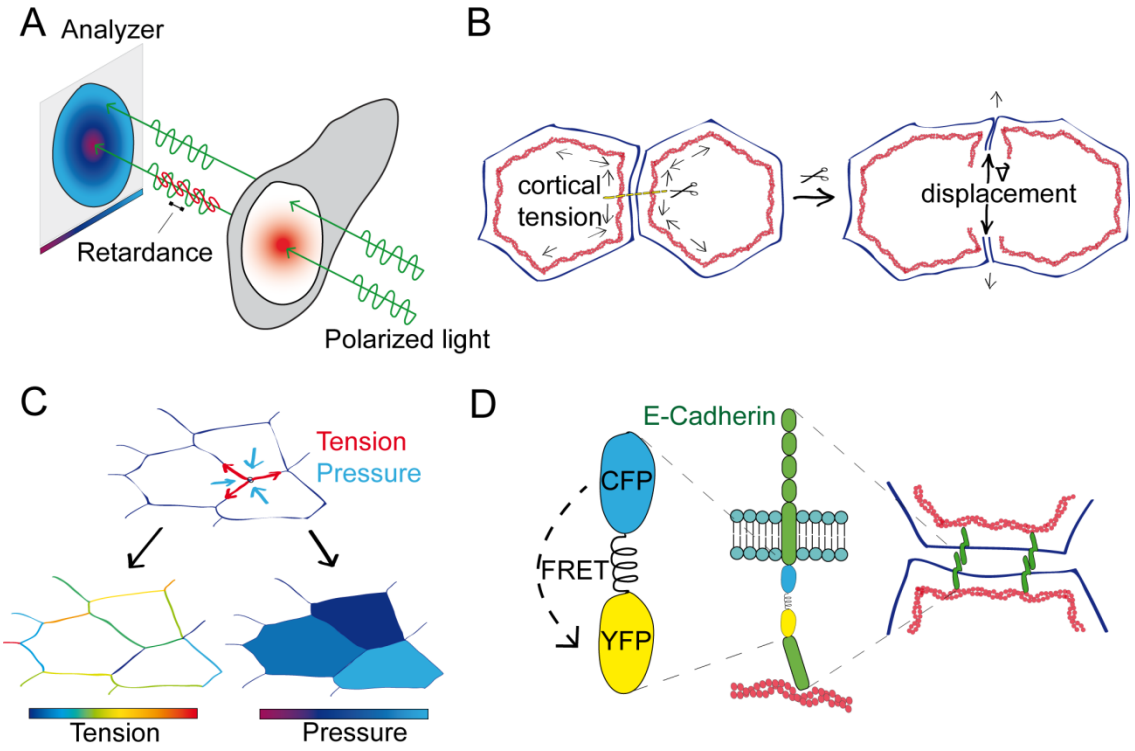


**Figure 1.4. Methods to measure forces in the wing disc.** (A) Birefringence measurement: The polarization state of a linearly polarized beam of light is changed when passing through a birefringent material. This is described by a phase difference in the different states called retardance and can be due to stress anisotropies in the material. (B) Laser ablation: When the actomyosin cortex is cut with a focused laser beam, the remaining edges retract, indicating a positive tension at the cortex. The velocity of the displacement provides a measure for this tension. (C) Force inference: The cell geometries of the input image reflect the balance between internal pressure and apical tensions. Solving force balance equations returns maps of cell pressure and tensions at cell-cell junctions. (D) FRET tension sensor: Sensor module is composed of two fluorophores connected by an elastic linker. The module is genetically integrated to a protein of choice, here E-cadherin. E-cadherin mechanically connects adjacent cells, thus tension between neighboring cells is transduced via E-cadherin. This moves the two fluorophores apart and can be measured by FRET efficiency.

#### *1.3.3.4. Modifying forces*

Measurements of force distributions show a clear circumferential pattern of mechanical stress with compressed cells in the center and stretched cells in the periphery of the wing disc, supporting the mechanical feedback models. In order to show a causal relationship between mechanical cues and growth, however, methods to experimentally modify tensions over the wing disc are required. For this, improvements of *in vitro* culturing techniques are essential, as they allow for long term *ex vivo* studies of wing discs (Zartman et al., 2013).

The most direct approach to evaluate the relationship between forces and growth has been the mechanical stretching of the wing disc *in vitro* (Fig. 1.5A). For this, the disc was attached with poly-L-lysine onto two movable coverslips which are pulled apart with a defined force. Imaging the dynamics of mitotic cells during stretching, an increase in proliferation upon mechanical stretching was observed in the wing pouch (Schluck et al., 2013).

While suggesting a link between mechanical tension and proliferation, the time-window for this experiment was one hour - the minimum length of one cell cycle is 8 hours (Milan et al., 1996). Thus currently, a major drawback of this method of the relatively short experimental window provided by the *in vitro* culturing technique. An additional concern is that *in vitro* cultivation interferes with cell cycle progression (Handke et al., 2014). This also limits the potential of wing disc culture to investigate growth and proliferation. Further efforts have to be made to either improve the culturing conditions of the wing disc or to establish manipulation techniques *in vivo*. *In vivo* imaging approaches have already been developed, but the handling and manipulation of the wing disc *in situ* is hampered by the accessibility in the larvae (Nienhaus et al., 2012; Heemskerk et al., 2014).

The induction of clones of overproliferating cells is one approach to increase mechanical tensions in the wing disc (Fig. 1.5B). Manipulation of the Hippo pathway in a patch of cells stimulates these cells to overgrow and surrounding tissue is stretched (LeGoff et al., 2013; Mao et al., 2013). This induced a tension pattern resembling that of the entire wing pouch. Consequently, adjacent cells that were stretched oriented their division plane according to the force field (Mao et al., 2013). Interestingly, in an analogous experiment in the *Drosophila* pupal notum, cell clones were stimulated to grow by overexpression of the oncogene RasV12. But instead of stretching the adjacent cells, tissue crowding was observed around the clone. Tissue crowding compressed the neighboring cells and drove apoptosis and cell delamination (Levayer et al., 2016). Thus, the effect of overproliferating clones on tissue mechanics is unclear, as it remains unresolved whether this discrepancy is an outcome of different biological or analytical tools.

Mechanical tension in the wing disc has also been modified indirectly by targeting cytoskeletal components (Fig. 1.5C). Genetic perturbations or pharmacological drugs were used to alter the actomyosin cytoskeleton. Inducing extra actin formation by the

loss of actin capping proteins stimulated overgrowth in the wing disc. Analogous to experiments in mammalian cells (Aragona et al., 2013) this overproliferation was mediated by Yorkie (Fernandez et al., 2011; Sansores-Garcia et al., 2011). The downregulation of myosin by targeting the myosin regulator Rho-associated protein kinase (ROCK), either via RNAi or the drug Y-27632, also reduced wing disc growth. Similar to actin dependent overgrowth, the growth effect was mediated by increased Yorkie activity (Rauskolb et al., 2014). Thus, there is a clear link between the actomyosin cytoskeleton, Yorkie activity and growth. This suggests that mechanical stretching of a cell is enhancing cytoskeletal assembly which in turn promotes proliferation (Rauskolb et al., 2014). However, this mechanism remains hypothetical. Actin and myosin are essential for a plethora of cellular processes. Therefore it remains to be assessed whether the growth promoting effect of actin and myosin activation is mechanically driven or initiated by another cellular process.

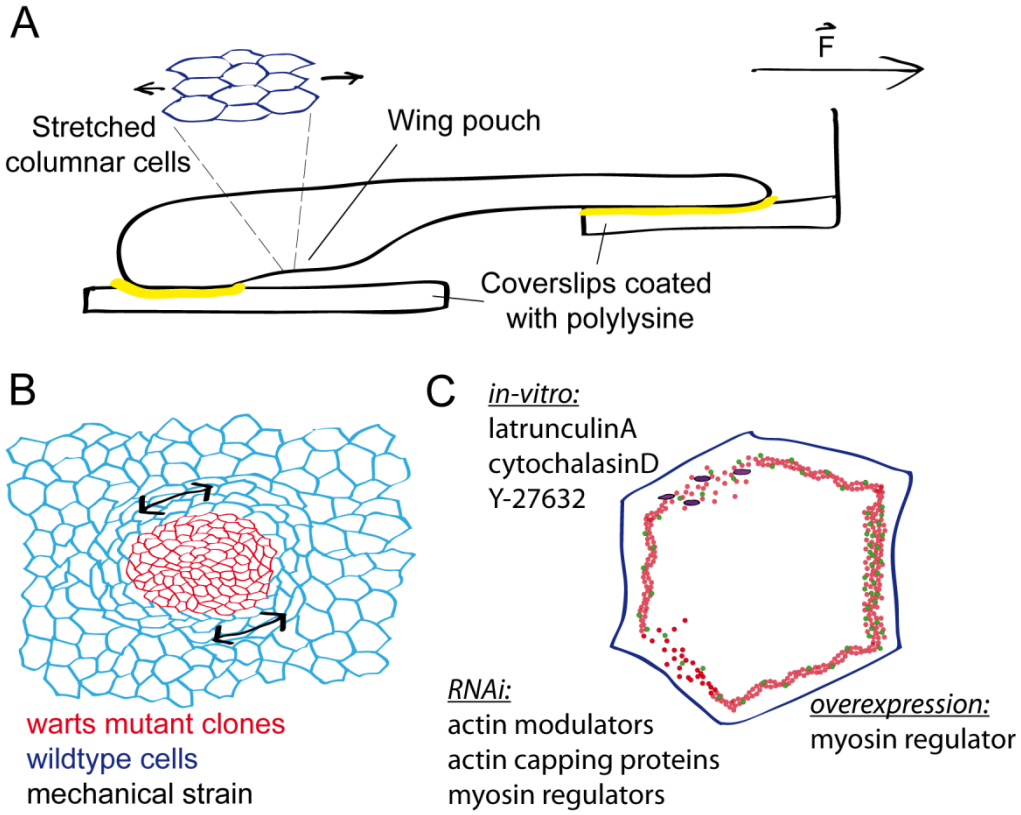


**Figure 1.5. Methods to manipulate forces in the wing disc.** (A) Stretching device: The wing disc is attached *in vitro* onto two flexible coverslips with poly-lysine. The coverslips can be moved apart with a defined force to stretch the wing disc tissue. (B) Overproliferating clone: Clonal manipulation of the Hippo pathway stimulates a patch of cells to overproliferate. Cells within the clone are compressed and the surrounding tissue is stretched tangentially. (C) Cytoskeletal modification: Pharmacological drugs applied *in vitro* or RNAi against actin or myosin regulators reduces tension of the actomyosin network, especially at the apical cortex. Overexpression of myosin regulators increases the tensional state.

## 1.4. CONCLUDING REMARKS

There is increasing evidence that in addition to biochemical signaling events, mechanical forces also impact on cellular processes in developing organs. *In vitro* experiments have shown that mechanical cues and tissue architecture have the potential to modulate cellular behavior and therefore to actively drive developmental events. Mechanical signals can coordinate cell movement, stimulate proliferation (Chen, 1997; Helmlinger et al., 1997), orient cell division (Campinho et al., 2013; Mao et al., 2013) and trigger differentiation (Guilak et al., 2009). Do mechanical cues also similarly affect the development of organs *in vivo*?

For the mammalian bone it was confirmed by long-term studies that size and shape are determined by mechanical loads (Christen et al., 2014). Mechanical forces feedback onto bone remodeling in a multi-scale process to ensure that the bone adapts to mechanical loads (see 2.2.1). Similarly, during remodeling of vertebrate blood vessels, blood pressure and flow shape the developing vessels in order to preserve their integrity (Hoefer et al., 2013). In the bone and the vascular system, mechanical stress originates from outside the tissue and is clearly of biological relevance. In other developmental systems, mechanical stress that is internally generated by tissue growth is also supposed to play a role as developmental regulator (see 2.3.2.; Campinho et al., 2013; Uyttewaal et al., 2012). Computational growth models, like those developed for the *Drosophila* wing disc, integrate mechanical feedback loops to modulate growth according to size (see 2.3.2). However, despite intense efforts, causal empirical evidence for the contribution of mechanical signaling *in vivo* remains elusive. For a deeper understanding of the complexity of mechanics *in vivo*, new tools are needed to quantify and modify mechanical cues (see 2.3.3. and 2.3.4.)

An epithelial cell is exposed to mechanical forces from different origins, which in turn lead to stresses on different subcellular structures. Additionally, the material properties of the tissue, such as viscosity or elasticity, also contribute to the mechanics of a cell (see 2.1.; Campas, 2016). Because different mechanical stresses could affect the cellular behavior in a different manner, it is important to consider that most experiments affect or measure only one of these mechanical quantities (see 2.3.2. and 2.3.3.). For example it was shown in mammalian cell culture and in the *Drosophila* wing disc that the homologs Yorkie/YAP are activated by increasing cytoskeletal

tension, which would suggest a similar mechanism operates in the two systems (Aragona et al., 2013; Rauskolb et al., 2014). However, experiments in mammalian cells were performed by changing substrate stiffness, whereas in the wing disc the cytoskeleton was manipulated at cell-cell junctions. Substrate stiffness is sensed at the basal side while alterations of cell-cell junctions act at the apical side of a cell – which suggests two potentially different mechanisms exist.

Further, the time-scales of developmental processes are relevant to understand the interplay of mechanics and cellular behavior. Mechanical perturbations can change cellular structures within a few seconds (Le Duc et al., 2010, Salbreux et al., 2012, Tabdili et al., 2012) while transcriptional events or cell divisions take several hours. Fast cytoskeletal turnover could therefore relax and dissipate mechanical stresses on a short time scale. Then it would be unclear how mechanical information can be stored in the long-term to trigger a response over a longer period (Salbreux et al., 2012). However, it was shown that mechanical stress can remain and influence cellular behavior over long time scales (Schluck et al., 2013, Wyatt et al., 2012), possibly with stresses being stored in less viscous structures such as the ECM (Wyatt et al., 2016).

In conclusion, it has been shown that mechanical forces have the potential to regulate growth and size of tissues. But we are just beginning to understand the underlying mechanisms. In order to deepen our knowledge of mechanobiology in organ growth, techniques to precisely quantify and modify forces need to be further developed.

## *1.5. ACKNOWLEDGEMENTS*

We would like to thank Amarendra Badugu and George Hausmann for useful discussions and comments on the manuscript. Funding for this work was provided by a SystemsX IPhD project.

# 2. RESULTS AND DISCUSSION I – Measuring Forces

This section constitutes a manuscript to be submitted for publication

## Challenging FRET-based force measurements in Drosophila

Dominik Eder, Konrad Basler, Christof Aegerter

## 2.1. ABSTRACT

Mechanical forces play a critical role during embryonic development. Cellular and tissue wide forces direct cell migration, drive tissue morphogenesis and regulate organ growth. Despite the relevance of mechanics for these processes, our knowledge of the distribution and dynamics of mechanical forces in a tissue remains scarce. Recent studies have tried to address this problem with the development of tension sensors based on Förster resonance energy transfer (FRET). These sensors are integrated into force bearing proteins and allow the measurement of mechanical tensions on subcellular structures. Here, we developed such a FRET- based sensor to measure tensions in different *Drosophila* tissues *in* and *ex vivo*. Similar to previous studies, we integrated the sensor module into E-cadherin, a transmembrane protein which is known for its role in mechanotransduction. E-cadherin is supposed to transmit forces throughout an epithelial tissue. We generated transgenic flies with the sensor and assessed its sensitivity in three *Drosophila* tissues: the wing imaginal disc, the amnioserosa cells and the migrating border cells. We carefully tested the sensor by measuring dynamic developmental processes and mechanical modifications of the tissues. However, these assays revealed that the sensor is not functional in the three tissues. Moreover, we encountered technical problems with the measurement of FRET which might represent more general pitfalls with FRET sensors in living tissues. These insights could help future studies to better design and control their experiments.

## 2.2. INTRODUCTION

Every living cell is embedded in a 3D- microenvironment where it is exposed to a variety of mechanical cues. It is getting clearer that – apart from biochemical cues – the physical parameters from the cellular environment strongly influence the cellular behavior. These cues originate either from neighboring cells or from extracellular structures like the extracellular matrix (ECM) or liquid flow in the lumen. Cells harbor machinery allowing them to sense and respond to these mechanical cues thereby ensuring their survival and the maintenance of tissue integrity and function. *In vitro* studies on single cells revealed that mechanical cues regulate cell migration (Borghi et al., 2010), cell differentiation (McBeath et al., 2004; Engler et al., 2006), the orientation and rate of cell division (Chen, 1997; Fink et al., 2011) and the activation of signaling pathways (Dupont et al., 2011). In multicellular culture systems mechanics also influenced growth (Helmlinger et al., 1997; Nelson et al., 2005; Streichan et al., 2014) and migration (Gjorevski et al., 2015). As these findings derive from *in vitro* experiments, it is of interest whether such force-dependent behaviors also occur *in vivo* during tissue development (Schluck et al., 2013). Advances in image acquisition techniques allowing the tracking of cell and tissue shapes *in vivo* revealed the relevance of mechanical cues for the regulation of developmental and morphogenetic processes (Keller, 2013). Tissue mechanics has been shown to drive morphogenetic events during gastrulation by altering cell mobility and the orientation of division plane in zebrafish, *Drosophila* and *C.elegans* (Martin et al., 2010; Roh-Johnson et al., 2012; Campinho et al., 2013). For the *Drosophila* wing imaginal disc, a well-established model for growth regulation - computational growth models (Shraiman, 2005; Aegerter-Wilmsen et al., 2007; Hufnagel et al., 2007; Aegerter-Wilmsen et al., 2012) and mechanical stimulation experiments (Schluck et al., 2013) suggested a key role of mechanical forces for growth and size regulation. These models propose a mechanical feedback loop allowing the wing disc to constantly monitor its size to ensure homogenous growth and a proper final size.

Despite increasing interest and technical advancements in the field of biomechanics, the measurement and quantification of mechanical quantities remains challenging. For *in vitro* studies there are a variety of tools to measure cellular forces and to modulate the mechanical properties of the environment (reviewed in Campas, 2016; Sugimura et al., 2016). For *in vivo* and *ex vivo* studies most of the techniques are not applicable:

they either rely on direct contact with the structure to measure force – which is mostly impossible for living tissues; or the measurement has a time resolution that is not appropriate for living processes. That is why for the measurement of physical properties in living tissues imaging-based methods are most convenient. Laser-ablation is the most popular method for whole tissues, where a cellular structure is ablated with a focused laser beam to probe the tension state before the cut. In the *Drosophila* wing disc laser ablation has provided insights in the distribution of tensions throughout the tissue (LeGoff et al., 2013; Mao et al., 2013); these results corroborated previous reports using stress-birefringence (Nienhaus et al., 2009) and cell shape analysis (Aegerter-Wilmsen et al., 2012). However, the invasiveness of laser ablation makes it unsuitable for measuring dynamic processes over time. Force inference, a non-invasive, computational tool, determines mechanical forces by analyzing the cell shapes. If the tissue is at mechanical equilibrium, every deviation from regular cell geometry enables the estimation of edge tension and pressure. Force inference greatly depends on these prior assumptions of mechanical equilibrium, force balance and homogeneous mechanical properties. Hence, it requires further validation of its results with other methods. A promising alternative are FRET (Förster Resonance Energy Transfer)-based tension sensors. Such sensor modules usually consist of two fluorophores linked with an elastic spacer. The FRET efficiency of these modules correlates with the tension exerted onto the sensor (Meng et al., 2008; Grashoff et al., 2010). Being genetically encoded, the sensor module can be integrated into the protein of choice, where the tension is of interest. The sensor has already been integrated in proteins which are expected to be involved in mechanotransduction, e.g. Vinculin, Talin or E-Cadherin (Meng et al., 2008; Grashoff et al., 2010; Borghi et al., 2012; Cai et al., 2014; Austen et al., 2015).

Here, we generated a FRET-based sensor for use in various tissues in *Drosophila melanogaster*. To address the role of mechanical tensions at the cell-cell contacts during development, we integrated a FRET module into E-Cadherin. E-Cadherin connects the apical cortices of adjacent cells and therefore plays an active role in tissue dynamics and the transduction of tissue-wide forces (Lecuit and Yap, 2015). In order to assess the functionality of our sensor, we measured FRET values in the wing imaginal disc, the amnioserosa cells and the border cells. To our surprise, the FRET values neither represented the expected tension patterns, nor responded to mechanical manipulations. Hence, the FRET module was not sensitive to mechanical forces in

these *Drosophila* tissues. This work reveals the technical challenges of FRET tension sensors and highlights common pitfalls with the interpretation of FRET results, especially in dense, living tissues.

## 2.3. RESULTS

### 2.3.1. Development of a new E-Cadherin tension sensor

It is widely accepted that mechanical forces are propagated across an epithelial tissue from cell to cell via the adherens junction complex (reviewed in Leckband and Rooij, 2014; Ladoux et al., 2015; Lecuit and Yap, 2015). According to the current model, the transmembrane protein E-Cadherin forms homophilic bonds with E-Cadherins from adjacent cells whereas the cytoplasmic domain recruits α- and β- catenins which in turn associate with F-actin. Hence, E-Cadherin physically links neighboring cells to the cytoskeleton and is likely an appropriate protein to measure mechanical forces across epithelial tissues. We designed a tension sensor based on FRET in a fashion similar to the well- estabilised TSMod sensor (Grashoff et al., 2010). Our sensor cassette consisted of ECFP and mEYFP which were connected by an elastic linker $(GPGGA)_8$ derived from spider silk (gift from Alexander Dunn)(Fig. 2.1A). If the tension on the sensor is low, the two fluorophores are close enough to allow for FRET. With increased tension, the distance between the fluorophores increases and the FRET efficiency decreases. Hence, the FRET efficiency should correlate with the tension across the sensor. In contrast to previously published sensors, we used ECFP instead of mTFP1 as donor fluorophore because mTFP1 forms aggregates in wing disc and amnioserosa cells which might interfere with its function as a sensor. We inserted the sensor cassette into the cytoplasmic domain of E-Cadherin, into the unstructured region between the transmembrane domain and the β- catenin binding domain (shgFRET) (Fig. 2.1B). Additionally, we generated a control construct in which the sensor cassette was attached at the C-terminus, which lies outside of the force transmitting region (shgContr) (Fig 2.1B). This construct should control for any FRET influencing effect other than the mechanical forces across the protein, such as conformational changes, molecular crowding, etc. With these constructs we generated transgenic flies by a *knock-in* into the endogenous *shotgun* locus. Hence, the sensor was integrated into the endogenous E-Cadherin and in homogzygous flies no other E-Cadherin interfered with the measurements. Co-staining with β- catenin (Armadillo) showed that the two

constructs were localized properly to the adherens junctions (Fig. 2.1C). Further, flies homozygous for shgFRET or shgContr were fertile and viable without any obvious phenotype, indicating that the constructs were fully functional.

In order to measure FRET we developed a workflow including confocal microscopy and image processing. We used the ratiometric method to calculate the FRET index by detecting sensitized emission, which partially corrects for variability in confocal image acquisition (VanReenen2004, see Material and Methods). It is important to consider that this method is very dependent on image acquisition parameters. Therefore the resulting FRET index obtained in this way is a relative value which can only be used to compare values within one experiment with exactly the same conditions, and not values from different experiments. To test whether this workflow is applicable to various *Drosophila* tissues, we used an established ATP (Adenosine triphosphate) FRET sensor as a positive control (Fig. S1, Tsuyama et al., 2013). We were able to reproduce the published results in the salivary gland, the wing disc and the border cells (see supplementary information). As a proof of principle we measured FRET indices of shgFRET and shgContr in the *Drosophila* wing imaginal disc showing that FRET is taking place when the sensor was expressed in the wing disc (Fig. 2.1D). The average FRET index in the wing pouch region of the wing disc was higher for shgFRET (0.240 ± 0.005) than shgContr (0.227 ± 0.007) (Fig. 2.1E).

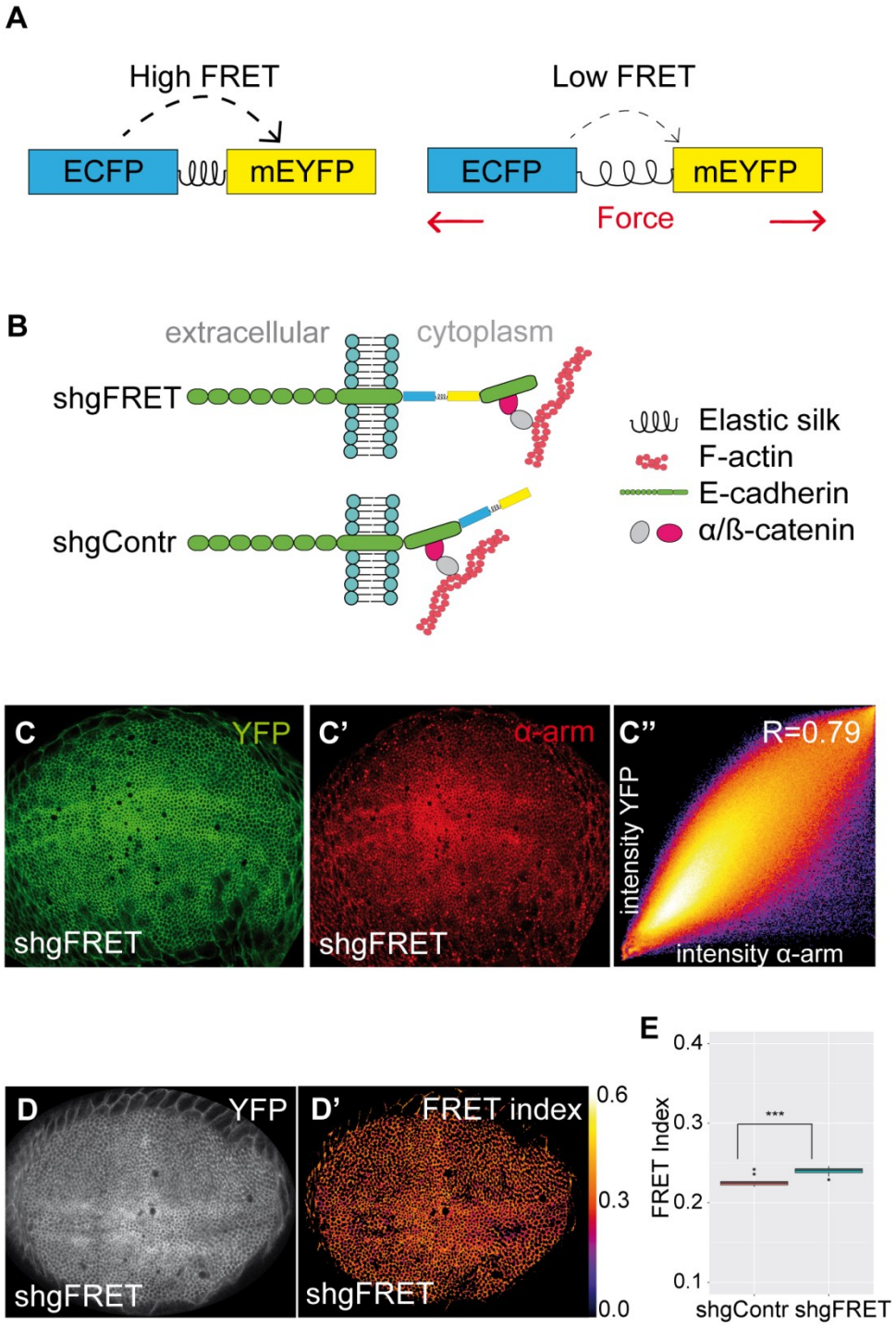


**Figure 2.1. Developing a FRET tension sensor for E-Cadherin.** (A) The tension sensor consists of ECFP and mEYFP connected by an elastic linker $(GPGGA)_8$. FRET efficiency is high in a relaxed state but should decrease if external forces extend the sensor module. (B) The sensor module was either integrated into the cytoplasmic domain of E-Cadherin adjacent to the transmembrane domain (shgFRET) to measure forces along the protein. The sensor module was also attached at the C-terminus of E-Cadherin (shgContr) lying outside of the force transducing domain to serve as a zero-force control. (C) Expression pattern of the sensor (YFP channel) and immunostaining for Armadillo (C') revealed high degree of co-localization in the wing pouch (C''). (D) YFP expression (D') and corresponding FRET index (D'') of shgFRET shows that FRET was detectable in the wing pouch. (E) FRET index in the wing pouch of shgContr (0.227, n=10) was significantly lower than for shgFRET (0.240, n=10).

### 2.3.2. FRET measurements in the wing disc

In order to evaluate the sensors functionality in the wing disc, we tested whether FRET distributions mirror the tension patterns across the wing pouch. It has been shown previously, that cells in the center of the wing pouch are mechanically compressed, whereas cells at the periphery are circumferentially stretched (Nienhaus et al., 2009; Ishihara and Sugimura, 2012; LeGoff et al., 2013; Mao et al., 2013). Compressed refers here to cells with less cortical tension than the stretched ones. Heat maps of FRET distributions in the wing disc did not reveal any obvious pattern (Fig. 2.1D), so we further analyzed the results in more detail. It was shown before that the stretched cells were bigger and more elongated than the compressed cells (Aegerter-Wilmsen et al., 2012; Mao et al., 2013) (Fig. 2.2A). But the FRET indices did not correlate with cell size in the wing pouch of shgFRET and shgContr flies (Fig. 2.2A', Fig. S2A). Further, we distinguished the cells of the wing pouch by shape between round and elongated cells, because we expected the elongated ones to be stretched (Fig. 2.2A''). However, FRET indices did not change between round and elongated cells. It could be possible that an effect averaged out because the shorter edges of a stretched cell were under higher perpendicular tension than the long edges. But FRET indices also did not vary between the long and short edges of the cells (Fig. 2.2A'''). Thus, by analyzing the FRET index distribution of our sensor lines, we could not detect any evidence of the global tension patterns reported in the wing pouch.

To further test whether the FRET index represents mechanical tensions in the wing disc, we performed manipulations to experimentally modify the tension on E-Cadherin. We decreased the cortical tension in the wing disc cells by adding 10µM LatrunculinB to the medium, which effectively inhibits actin polymerization (Fig. 2.2B). We confirmed the efficiency of the treatment by imaging Moesin and Myosin dynamics (Fig. S3A, Fig. S3B). Instead of an increase in FRET index due to LatrunculinB treatment, we observed a decay of the FRET indices in the shgFRET and the shgContr lines (Fig. 2.2B'). Having a negative control without treatment revealed that FRET indices decrease over time in culture even without any treatment or manipulation. We observed also in other experiments that the FRET indices decay over time in tissue culture, which is a more general "culturing artifact" in our setup. That is why we staged all experiments precisely in time and always added controls without treatment to monitor the time-dependent decay. However, the effect of LatrunculinB treatment on

shgFRET did not differ from these negative controls. Hence, the decrease in FRET index seemed to be a more general effect rather than tension specific.

Because shgFRET did not react to a decrease in tension, we applied an external tensional force onto the entire wing disc to increase the tension across the cells. For this we used a previously developed stretching setup which allowed us to stretch the cultured wing disc longitudinally with a defined force (Fig. S3C, Schluck and Aegerter, 2010). We measured the FRET index at two different forces: (1) In a pre-stretched state we applied a force of 10μN in order pull until the disc was taut and the folds were partially removed; (2) In a second step we applied a force of 25 μN to further stretch the disc. With higher forces the wing disc would have detached from the stretching device. Alternating between these two states, we measured the FRET index within the hinge region (Fig. 2.2D). We again observed a time-dependent decrease of FRET for shgFRET and shgContr, but the alternating forces did not affect the observed FRET index.

Additionally, we experimentally increased tension by treatment with distilled water. E-Cadherin is supposed to connect the cortical acto-myosin rings of adjacent cells, and therefore an increase in cell volume by the osmotic shock should expand the distance between the rings and stretch E-Cadherin (Fig. S2B, Fig. S2C). Following the osmotic shock and the volume increase FRET indices did increase, and not decrease as expected. Again, this was the case for both shgFRET and shgContr wing discs (Fig. S2D).

Thus, not only did the distribution of FRET across the wing disc not resemble the reported patterns of mechanical tensions that have been described earlier, but direct mechanical manipulations only altered the FRET index of shgFRET to the same extent as for the negative control shgContr. This indicates that changes in FRET index are directly influenced by the experimental procedure rather than specifically by mechanical tensions in the wing disc.

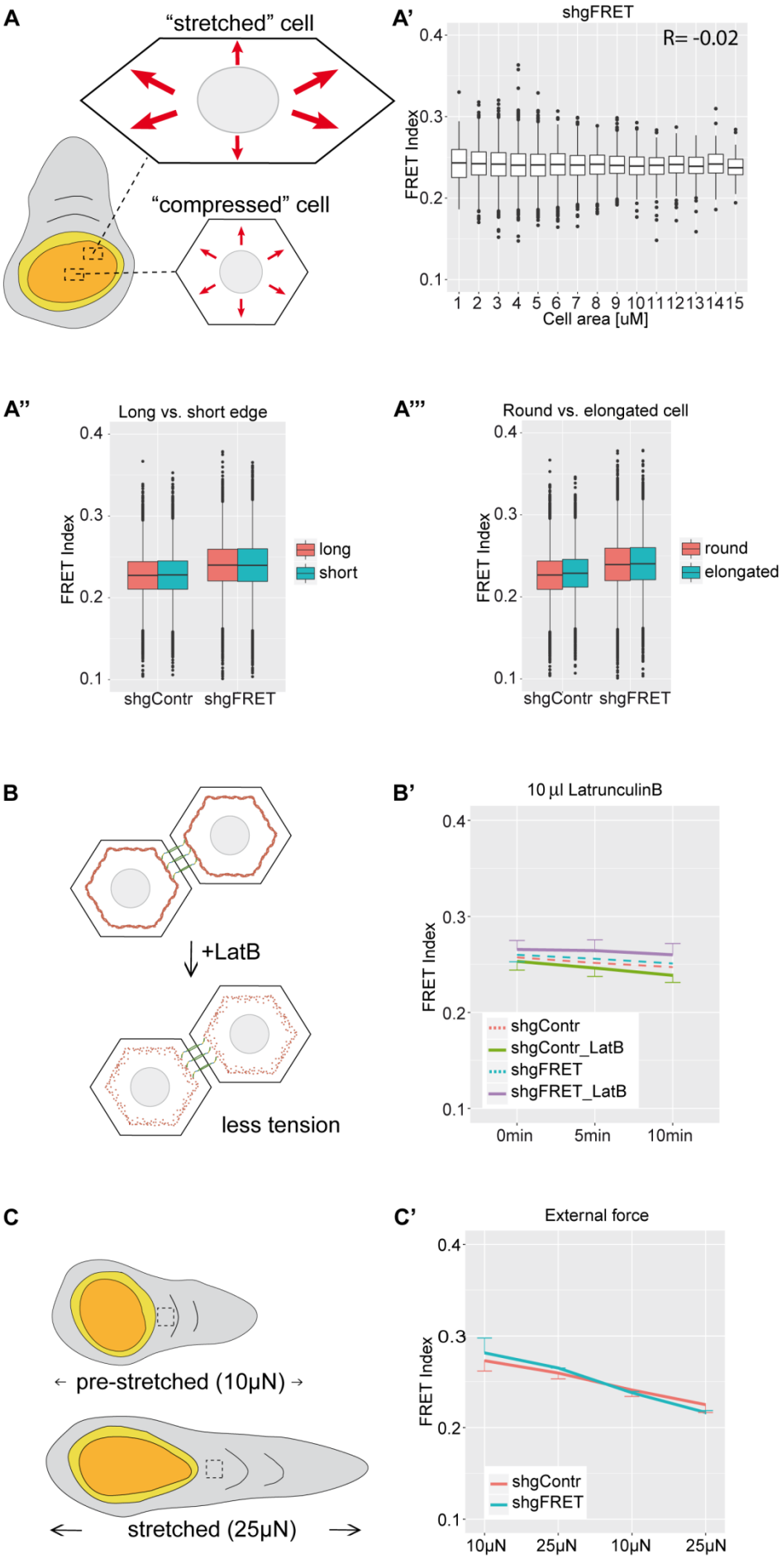
A
"stretched" cell
"compressed" cell
A'
shgFRET
R= -0.02
FRET Index
Cell area [uM]
A''
Long vs. short edge
FRET Index
long
short
shgContr shgFRET
A'''
Round vs. elongated cell
FRET Index
round
elongated
shgContr shgFRET
B
+LatB
less tension
B'
10 µl LatrunculinB
FRET Index
shgContr
shgContr_LatB
shgFRET
shgFRET_LatB
0min 5min 10min
C
← pre-stretched (10µN) →
← stretched (25µN) →
C'
External force
FRET Index
shgContr
shgFRET
10µN 25µN 10µN 25µN

**Figure 2.2. Single cell analysis and functional experiments in the wing disc.** (A) Schematic drawing illustrates that cells in the center of the pouch are small, round and supposed to be mechanically compressed, whereas marginal cells are larger, elongated and mechanically stretched. In the marginal cells, the short edges are exposed to more mechanical stress than the long edges. These assumptions lead to following comparisons: (A') The FRET index did not correlate with cell area in the wing pouch (here shown for shgFRET). (A'') The FRET index did not differ between long and short edges for shgContr (0.228 vs. 0,227) and shgFRET (0.240 vs. 0.240). (A''') The FRET index did not differ between round and elongated cells for shgContr (0.229 vs. 0.226) and shgFRET (0.240 vs. 0.240). (data for A', A'' and A''' were pooled from 14 wing discs). (B) LatrunculinB treatment reduces cortical tension. (B') FRET index decreased for shgContr (6%, n=18) and shgFRET(2%, n=18) upon treatment within 10 minutes. But also without treatment (dashed lines) the FRET index decreased over time for shgContr (4%, n=9) and shgFRET (3%, n=9). (C) Using a stretching device, a pre-stretched (applied force of 10µN) and a stretched (25 µN) wing disc were compared. The dashed rectangle indicates the analyzed area. (C') When cyclically altered between the two states every 5 minutes, a strong decay over time was observed for shgContr (18%, n=2) and shgFRET (23%, n=2), but no impact of the force change.

### *2.3.3. FRET measurements in the amnioserosa cells*

In the wing disc, mechanical tensions build up due to tissue growth and are therefore changing over long time scales. In contrast, in the amnioserosa cells during dorsal closure, mechanical tensions are highly dynamic and play an active role in morphogenesis. The amnioserosa cells underlying the dorsal gap undergo rapid waves of contraction and expansion on the time scale of minutes (Fig. 2.3A). These pulses are driven by the actomyosin cytoskeleton and pull the surrounding epidermal cells to subsequently close the dorsal opening (Gorfinkiel et al., 2009; Solon et al., 2009; Saias et al., 2015). E-Cadherin as a key mechanotransducer in epithelial cells is very likely required for the transmission of the forces generated during dorsal closure (Gorfinkiel and Arias, 2007; Mateus and Martinez Arias, 2011). Therefore, we expect that FRET values of our tension sensor would decrease in a contracting amnioserosa cell and increase if the cells are expanding, in the context of dorsal closure.

We imaged cells over seven minutes to determine their pulsing stage according to their apical cell size (Fig. 2.3B). For every cell we analyzed the FRET values of two different time points and considered cells that were in opposing cycle stages. Hence, we categorized FRET indices of contracted and expanded cells for both shgFRET and shgContr (Fig. 2.3B'). But instead of a decrease in FRET index upon contraction, there was no significant difference in the FRET index between contracted and expanded cells. A problem of the analysis of single cells was that we could not discriminate between E-Cadherin from two neighboring cells which share an edge. Thus, also the neighboring cells pulsing stage influenced the analysis. Further, mechanical forces are

anisotropic in a cell, meaning that one region of a cell could be contracting while another one is expanding. This could have averaged out the effect.

Therefore, we analyzed single edges and sought for edges that either contract or expand within one minute (Fig. 2.3C). Thereby, we were certain that in this specific region forces are generated and that at both sides of the edge the force is propagated. But also with this type of analysis, we did not see a response of the tension sensor to the changed mechanical state of the edge (Fig. 2.3C'). There was no significant difference between long and short edges regarding the FRET index of shgContr and shgFRET.

To conclude, in the amnioserosa cells it is known that forces are generated and changed cyclically over short time-scales, which can be observed by the shape changes of the cells and edges by live imaging. However, our tension sensor did not respond to these dynamics and FRET values did not change accordingly.

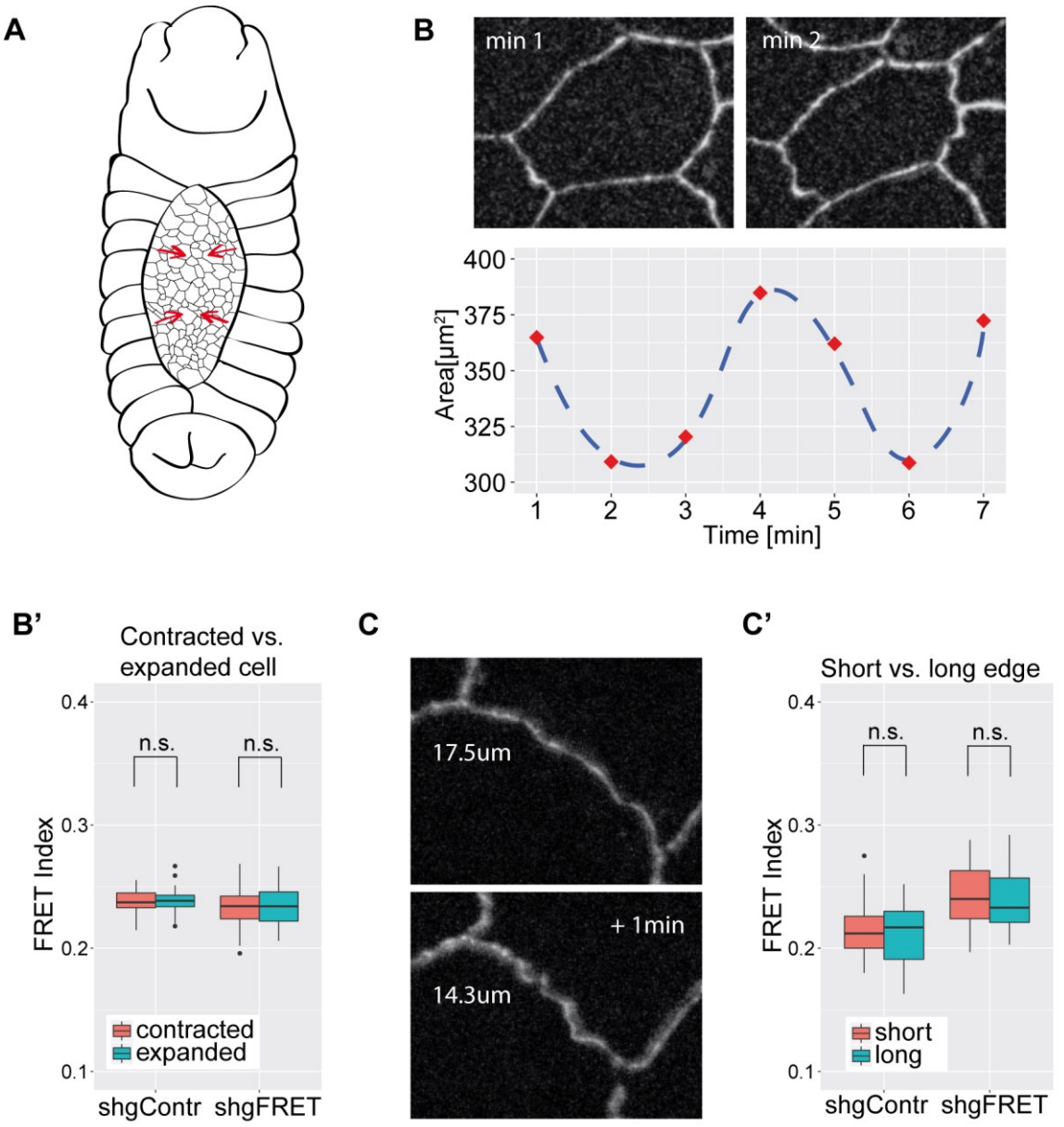


**Figure 2.3. FRET analysis of the amnioserosa cells during dorsal closure.** (A) In the early *Drosophila* embryo, the dorsal gap of the epidermis is closed by contractions of the underlying amnioserosa cells. (B) Amnioserosa cells undergo cycles of contraction and relaxation taking around four minutes. Here we show an example of one cell with measured values (red) and a guide to the eye (blue). (B') FRET index did not significantly differ between contracted and expanded cells for shgContr (0.239 vs. 0. 239, n=24) and shgFRET (0.233 vs. 0.235, n=26). (C) If two neighboring cells contract, the conjunctive edge also contracts. (C') For edges that contracted or expanded within one minute, the FRET index did not significantly differ between the shortened and elongated state for shgContr (0.216 vs. 0. 214, n=31) and shgFRET (0.243 vs. 0.241, n=29).

### 2.3.4. FRET measurements of border cell migration

Border cells of the *Drosophila* ovary have emerged as a model system for collective cell migration (Montell et al., 2012). The border cells constitute a cell cluster of six to eight cells which detach from the anterior follicular epithelium at stage 9 of the egg chamber (Fig. 2.4A). Subsequently, the cluster navigates with protrusions of the leading cell between the surrounding nurse cells and migrates posterior towards the oocyte (Fig. 2.4A). E-cadherin is expressed in all cell types in the egg chamber and is required for border cell migration and especially for direction sensing of the cluster (Niewiadomska et al., 1999; Cai et al., 2014). It was reported that E-cadherin is under higher tension in the front of the cluster, compared to the back of the cluster (Cai et al., 2014). This difference in tension is processed in a feedback loop with the actin cytoskeleton and leads to a persistent and directed movement.

We analyzed the border cell cluster with our sensor and were expecting to see a difference between the front and the back of the moving cluster. As tension of E-cadherin is supposed to be higher in the front, the FRET index should be lower in the front. Therefore we calculated the front to back ratio by choosing small areas of around $20\mu m^2$ in the leading and the rear cell. The ratio of the shgFRET sensor line was 1.00±0.110 [mean±stdev] which does not reveal any difference in FRET index between front and back. In contrast, the shgContr line had a front to back ratio of 0.95±0.128 and was lower than the ratio of shgFRET (Fig. 2.4C). Therefore, we looked at the absolute values of FRET indices, where no significant difference between the cells in the front and the back of the cluster were detectable, neither for shgFRET nor for shgContr (Fig. 2.4D).

Hence, we did not observe the expected difference in tension between front and back in the border cell cluster. We further asked whether the FRET index of our sensor represents at all mechanical tensions across E-cadherin in the border cell. We performed a treatment with the Rho kinase inhibitor Y-27632 which inhibits myosin activity and indirectly reduces the tension on E-cadherin (Cai et al., 2014). We measured the FRET index of the border cells before and after the treatment. But for shgFRET and shgContr the treatment with Y-27632 did not have a significant effect on the FRET index.

To conclude, the shgFRET sensor did not report the expected difference of mechanical tension between the front and the back of the cell cluster. Because inhibiting myosin did not affect the sensor, we concluded that the FRET values that we measured did not represent mechanical tensions during border cell migration.

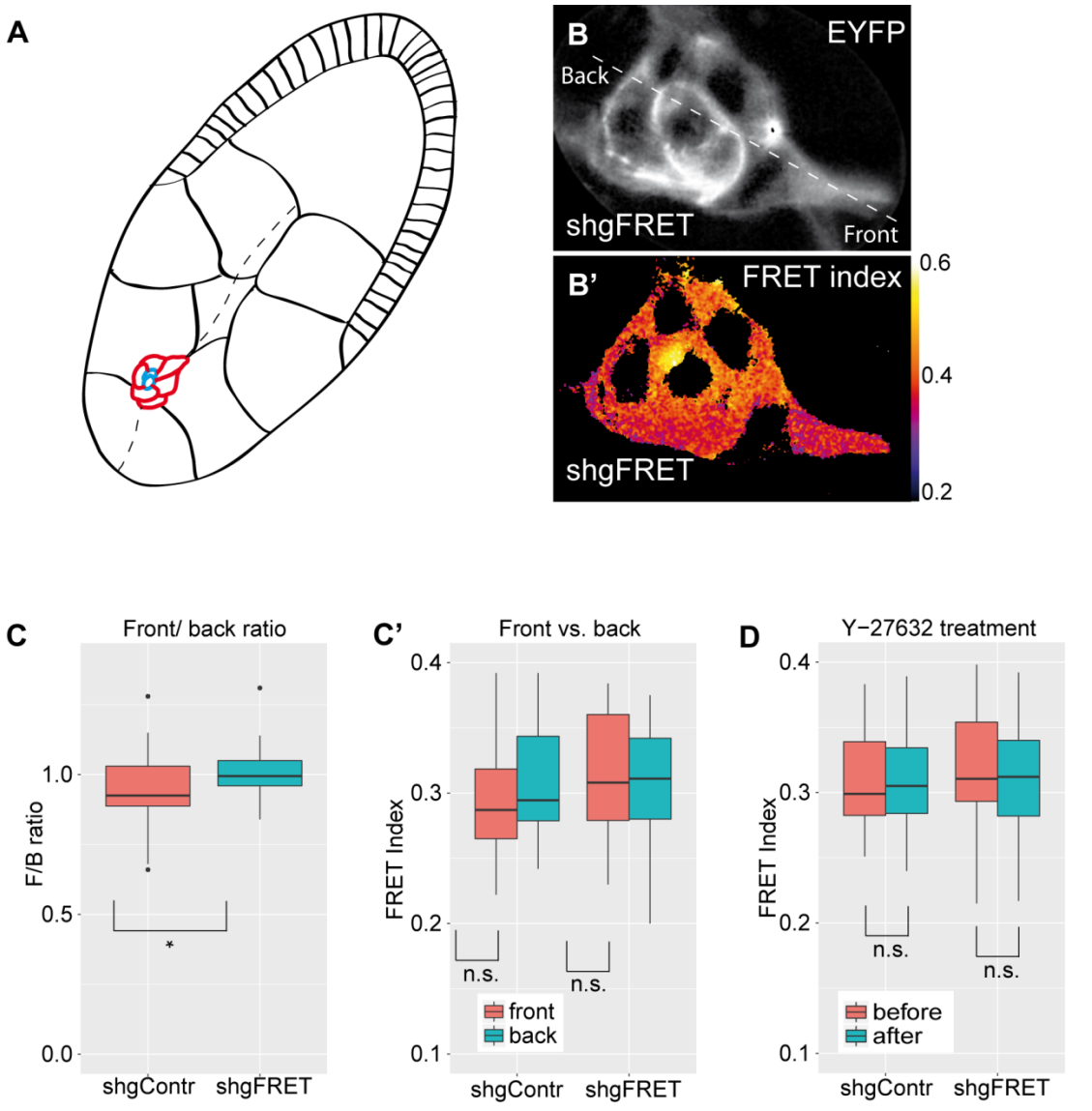


**Figure 2.4. FRET analysis of border cell migration.** (A) During stage 9 in the egg chamber, a cluster of six to eight border cells (red) and two polar cells (blue) migrate from the anterior pole through the nurse cells towards the oocyte (path as dashed line). (B) Border cell cluster forms protrusions at the leading cell to navigate between the nurse cells. FRET index was detectable in the entire cluster, here illustrated in the YFP channel and the corresponding FRET index. (C) The relative front to back ratio of the FRET index was significantly lower for shgContr (0.95, n=40) than for shgFRET (1.01, n=38). (C') But the absolute values between front and back did not differ significantly for shgContr (0.294 vs. 0.310, n=40) nor for shgFRET (0.313 vs. 0.311, n=38). (D) The release of tension upon the treatment with the myosin blocker Y-27632 did not significantly change the FRET index for shgContr (0.312 vs. 0.317, n=40) nor for shgFRET (0.320 vs. 0.313, n=38).

### 2.3.5. Fluorescence lifetime imaging microscopy to measure FRET efficiency

In order to test whether the negative outcome of the functional tests is due to a lower sensitivity of the ratiometric method, we repeated experiments with Fluorescence Lifetime Imaging Microscopy (FLIM), an alternative method of FRET determination. FLIM is based on the fact that every fluorophore has a characteristic lifetime, which is the average time between the excitation and the emission of fluorescence. The lifetime of a fluorophore is sensitive to its molecular environment, which includes FRET dependent quenching. Hence, the lifetime is a direct read-out for FRET (Berney and Danuser, 2003; van Rheenen et al., 2004; Wessels et al., 2010; Becker, 2012). There are two main advantages of FLIM over the ratiometric methods: (1) Because the lifetime is independent of the fluorescence intensity, FLIM is less susceptible to imaging artifacts and variation in microscopy parameters and has therefore a much better signal to noise ratio – or in short, it is a more sensitive measure of FRET. (2) Because perfect calibration of the imaging system in a biological tissue is almost impossible, the ratiometric method remains semi-quantitative and provides only a relative value of FRET. With FLIM we obtain the absolute FRET efficiency. The absolute FRET efficiency represents the fraction of energy absorbed from the donor and transferred to the acceptor. Being an absolute value it allows comparing values between different experiments with different settings.

For technical reasons, we only measured FLIM in the wing imaginal disc. To estimate the absolute FRET efficiency of the sensor in the wing disc we compared the fluorescence decay curves from shgFRET, shgContr and shgCFP (a sample which only included the donor and not the acceptor). The divergence of the curves of shgCFP with shgFRET and shgContr confirmed that donor and acceptor were close enough that FRET could take place (Fig. 2.5A). Calculating the FRET efficiency from the lifetimes revealed that FRET was higher in shgFRET (0.12±0.006) compared to shgContr (0.09±0.007) (Fig. 2.5B, Fig. S4B). This was in agreement with our data from the ratiometric method, but somewhat contradicted the design of the sensor, where the zero-force control shgContr was expected to have higher FRET due to lower tension. Furthermore, we tested whether lifetimes correlated with the size of the cells because size depends on the tension of a cell. But no correlation between lifetime and cell size was detectable (Fig. 2.5C, Fig. S4A). Neither did the shape of a cell or the length and

orientation of an edge affect the lifetimes significantly (Fig. S4E, Fig. S4F). When performing LatrunculinB treatment, we observed the same effect as with the ratiometric method (Fig.2.2B): the lifetimes of shgContr and shgFRET both increased and hence the FRET efficiency decreased (Fig.2.5D). Because FRET efficiency decreased similarly for the sensor and the zero –force control (p=0.37), the effect seemed to be an unspecific affect which was independent of tension. Time controls for shgFRET and shgContr without treatment had the same decrease of FRET over time as the treated samples (p=0.14 and p=0.17), indicating a more general effect of culturing the wing disc *ex vivo* (Fig. S4C). With this we confirmed that the above described "culturing artifact" is no measuring artifact from the ratiometric method but that culturing the wing disc indeed affects the FRET efficiency over time (Fig. S4C). Also the treatment with distilled water had an effect on the FRET efficiencies of both, shgContr and shgFRET, indicating that this is a force-independent effect (Fig. S4D).

Together, the data obtained from FLIM measurements confirmed the results from the ratiometric method in the wing disc. Surprisingly, the FRET efficiencies calculated from lifetimes of shgFRET were higher than the ones of shgContr which was not in accordance with the idea of shgContr presents a zero-force control in which the fluorophores should be closer together and FRET efficiency therefore higher. Also, lifetimes and consequently FRET did not correlate with size and shape of cells and they did not respond force- specifically to mechanical manipulations of the cells.

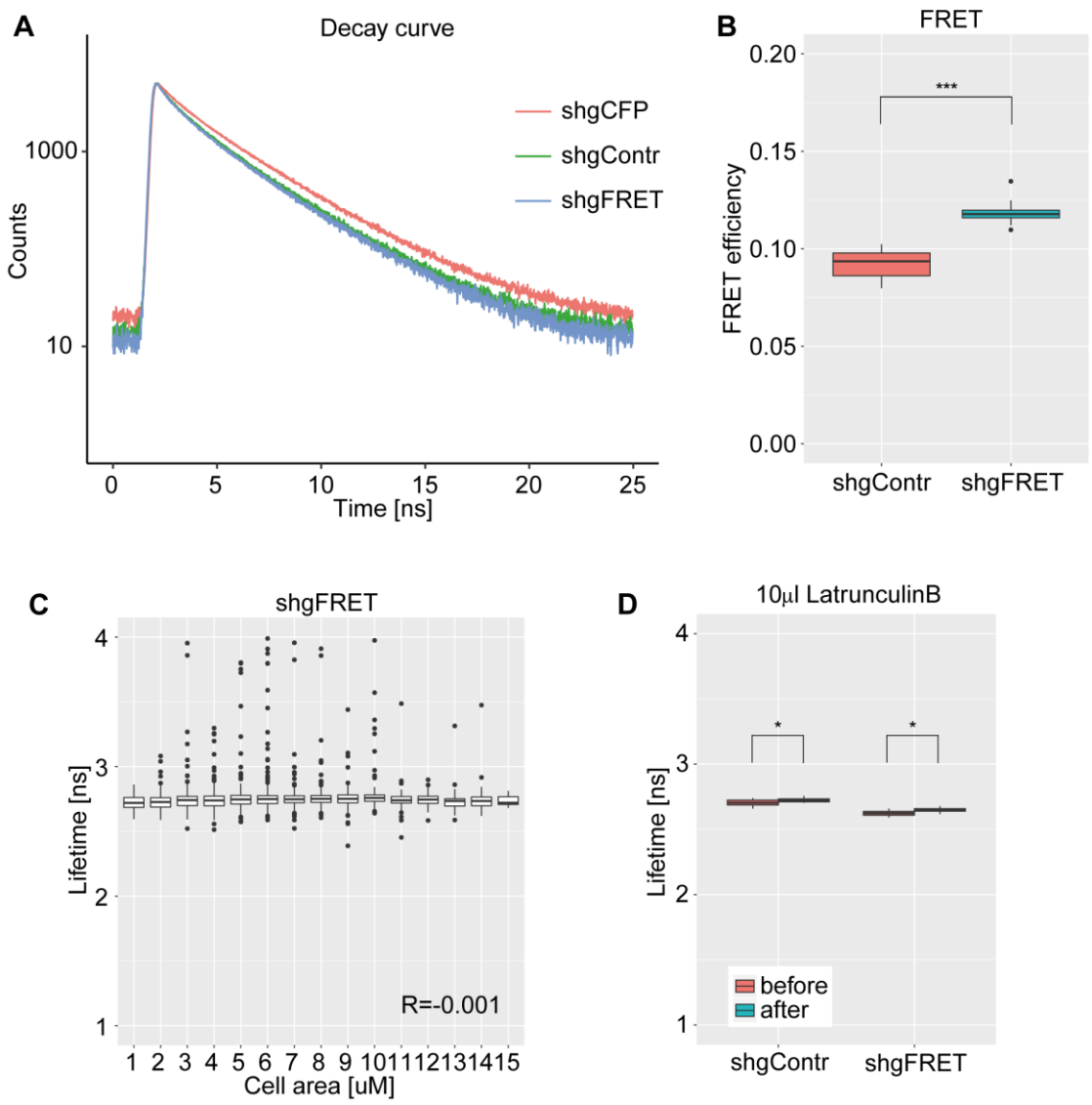


**Figure 2.5. FLIM measurements in the wing disc.** (A) Fluorescence decay curves of shgContr and shgFRET were almost overlapping, and both revealed lower lifetimes than shgCFP (n=5). (B) Calculated FRET efficiency was significantly lower for shgContr (0.09, n=15) than for shgFRET (0.12, n=14). (Corresponding lifetimes are shown in Fig. S4B.) (C) Lifetimes of single cells in the wing pouch did not correlate with cell size (here for shgFRET, n=8 wing discs). (D) Lowering tensions by LatrunculinB treatment similarly increased lifetimes of shgContr and shgFRET for 1% (n=9).

## 2.4. DISCUSSION

To test the hypothesis that mechanical forces play a crucial role in tissue development of *Drosophila*, we aimed to develop a sensor that will allow us to measure mechanical tensions across a tissue. Using a similar FRET tension sensor strategy as previously published (Grashoff et al., 2010), we generated transgenic flies with the FRET sensor integrated into the endogenous E-Cadherin locus. This was an improvement compared to E-Cadherin sensors in other systems, in which the sensor was overexpressed in addition to the endogenous E-Cadherin (Borghi et al., 2012; Cai et al., 2014). The modified sensor E-Cadherin might not experience the same forces as the endogenous one when both are expressed at the same membrane, especially because the cytoplamsmic domain with the sensor module is much larger than the endogenous cytoplasmic domain (707aa vs. 141aa). Further, we exchanged the mTFP1 with ECFP as donor fluorophore for FRET. mTFP1 strongly forms aggregates in the *Drosophila* tissues which we did not observe with ECFP, resulting in a more intense signal with less background. With our sensor line, we aimed to measure mechanical tensions in three different tissues: the wing imaginal disc, amnioserosa cells and border cells. For all these tissues it has already been known that cellular tensions change over space or time (Gorfinkiel et al., 2009; Nienhaus et al., 2009; Solon et al., 2009; Aegerter-Wilmsen et al., 2012; Ishihara and Sugimura, 2012; LeGoff et al., 2013; Mao et al., 2013; Cai et al., 2014; Saias et al., 2015). However, our sensor did not display the expected tension patterns. Further validation of the sensor's functionality by using cytoskeletal blockers also did not reveal a change. Because the negative outcome might be due to the low sensitivity of the ratiometric method, which we used for FRET analysis, we additionally applied FLIM in the wing disc. Also with FLIM, the sensor did not differ from the negative controls. Additionally, we repeated all the experiments with an already published tension sensor that had been tested for the border cell migration in *Drosophila* (Fig. S5, Fig. S6, (Cai et al., 2014). Surprisingly, even this sensor did not seem to be sensitive for mechanical forces in the wing disc, the amnioserosa and the border cells. To confirm that our methods could detect differences in FRET, we used a formerly published ATP-FRET sensor as positive control (Tsuyama et al., 2013). We successfully applied the ATP sensor with the ratiometric method and FLIM verifying our analysis pipelines. Thus, we tested two different E-Cadherin sensors in three *Drosophila* tissues with two alternative methods, but did not achieve any indication that these two sensors are functional.

In the following chapters we would first like to discuss some technical challenges that arose during our experimental approaches. These difficulties seem to be more general pitfalls during FRET data acquisition and might be sources for false positive results. Subsequently, we will discuss possible explanations of why E-Cadherin FRET sensors might not be suitable in *Drosophila* tissues.

### 2.4.1. Ratiometric method – source for measuring artifacts

The most commonly used technique to measure FRET is the ratiometric method (Borghi et al., 2012; Conway et al., 2013; Cai et al., 2014). Thereby, the FRET index is calculated by the ratio of the donor intensity and the acceptor intensity upon donor excitation. The obvious problem is that the method is intensity-based and therefore the donor/acceptor ratio does not only depend on FRET. The intensities obtained from confocal microscopy additionally depend on a plethora of factors, e.g. penetration depth into the tissue, autofluorescence, laser fluctuations, microscopy settings and all the parameters during image processing. As most of these factors are wavelength dependent, they strongly bias the ratio which is used as a FRET index. Especially the factors during image acquisition are somewhat difficult to control and therefore present a likely source of variability and measuring errors. To control for this variability, we used the negative control shgContr.

In our experiments the correlation between intensity of the signal (direct acceptor excitation) and the obtained FRET index was highest in border cells (r=0.44) followed by the wing discs (r=0.39). In border cell migration the problem is that for imaging the cell cluster, the laser and emission light migrates through the egg chamber, where scattering and autofluorescence take place. In the amnioserosa cells the correlation was not obvious (r=0.16), although the strong autofluorescence of the epidermis and the underlying yolk caused noise in the measurements.

Furthermore, we observed that for wing disc culture, the FRET index decreased over culturing time. One reason was that the intensity dropped over time, which due to the correlation between intensity and FRET index provoked a corresponding drop in FRET index. However, FLIM confirmed that also the actual FRET efficiency decreased over time in tissue culture, indicating that either the distance or orientation between the two fluorophores changed in a time dependent manner.

In sum, the intensity-dependence and the time-dependence of the FRET index caused non-random measuring artifacts, for which the statistical tests cannot control. Hence, statistical significance of apparent differences from the analysis could simply be explained by variation in intensity of the sensor or by timing differences, rather than by changes in the distance between acceptor and donor or by different tensions. These pitfalls have to be considered when comparing different samples and especially illustrate the importance of the proper controls to reduce the risk of false positive results.

### *2.4.2. Dynamic range of FRET sensor module*

The sensitivity of the FRET module is limited to only a small range of mechanical forces. The dynamic range depends on the elastic properties of the linker peptide and the principle that FRET only takes place at distances below 10nm. Grashoff et al. estimated that the FRET module is sensitive in the range of 1-6 pN, which is adjusted to the forces exerted onto focal adhesions (Grashoff et al., 2010). But are the forces onto adherens junctions also covered by this dynamic range? Measurements with atomic force microscopy characterized the binding strength of mouse VE-cadherin, a homolog of E-Cadherin that is expressed in the vascular endothelium (Baumgartner et al., 2000). This study revealed that the binding strength of the trans-interactions of the extracellular domain is between 35 and 55 pN. These forces would be far above the sensors range and would theoretically be out of the range of FRET sensors because the fluorophores unfold at forces around 35pN (Austen et al., 2015). In a different study, mouse N-cadherin (neuronal), which was expressed in C2 myogenic cells, exerted an estimated force of 10pN on an N-Cadherin coated substrate (Ganz et al., 2006). More recently, it was shown that α- catenin, which connects the adherens junction complex to F-actin, only stably binds to F-actin under force. An optical trap based assay revealed that the adherens junctions complex stably bind to F-actin with a force of around 10pN (Buckley et al., 2014). Currently, we do not know the amplitude of forces which are exerted onto E-cadherin *in vivo* in *Drosophila* epithelia. However, these absolute values from previous studies indicate that forces might be higher than the dynamic range of our sensor. More recently, another FRET sensor module was developed which used another linker to connect the two fluorophores allowing to measure forces between 6-11pN (Austen et al., 2015). Studies with this new sensor module uncovered that, although the focal adhesion adapter protein Vinculin is under 2.5pN forces

(Grashoff et al., 2010), Talin, a linker between FAs and the cytoskeleton, is exposed to forces between 7-10pN (Austen et al., 2015). This shows that junctional proteins are exposed to a broad range of forces demonstrating the likelihood that E-Cadherin might not fall into the range of 1-6 pN.

### *2.4.3. Conformation governed FRET*

If the forces across E-Cadherin were higher than 6pN, we would expect that the sensor module is stretched too far and FRET would be very low. In this case, FRET of the shgContr should be higher than shgFRET, as shgContr represents the sensor without mechanical load. However, this is not the case as FRET index was always lower for shgContr than for shgFRET in our experiments. Therefore, something else must influence the FRET index in our systems rather than the forces across the protein. It is well established that FRET is very sensitive to the distance between the fluorophores, because the FRET efficiency depends on the sixth power of the distance. The idea behind the design of our FRET tension sensors is that the distance increases with increasing forces. However, another important feature of FRET is the dependence on the relative orientation of the two fluorophores $\kappa^2$ (Esposito and Wouters, 2004). In the majority of FRET studies $\kappa^2$ is random and estimated by the average of 2/3. But this is only valid if the fluorophores are free to rotate in all possible rotations (VanBeek et al., 2007; Munoz-Losa et al., 2009). Because our sensor is monomolecular, meaning that the fluorophores are linked together, the relative orientation is biased and not random any more. In this case, it has been shown that the distance and the orientation are strongly dependent and that apart from the distance also the orientation has a significant impact on FRET efficiency (VanBeek et al., 2007). Hence, ignoring the orientation of the FRET pair could lead to errors in the interpretation of data.

In a study with a very well calibrated monomolecular FRET pair it was shown that the relative orientation even had a comparable impact on FRET as the distance (Meng et al., 2008). This was further illustrated by the approach to generate an orientation-dependent force sensor which turned out to be even more sensitive to forces around 5-10pN than the distance-dependent sensor (Meng et al., 2008; Meng and Sachs, 2012). So far, we can only speculate about the orientation of our FRET sensor *in vivo*, but it is very likely that conformation of E-Cadherin or neighboring proteins affect the relative orientation of the FRET pair. This could in turn explain the difference in FRET

between shgContr and shgFRET and could also explain why similar changes in FRET occurred with shgContr and shgFRET in some experiments. Hence, it would be incorrect to attribute every change in FRET index to changes in mechanical forces across E-Cadherin.

Finally, it is also known that FRET is slightly sensitive to pH and the refractive index of the medium surrounding the FRET pair (Esposito and Wouters, 2004; Meng and Sachs, 2012). This could partially explain why the FRET efficiency is changing upon *in vitro* culturing of the wing disc or the application of an osmotic shock with distilled water, which both affect the intracellular environment.

### 2.4.4. Does E-Cadherin transduce the applied forces?

So far we discussed factors that interfere with the FRET measurement and therefore cause noise in our analysis. Additionally, it is also plausible that the forces we aim to observe are not transmitted across the sensor. Therefore, it is important to mention that the sensor module is much bigger than the cytoplasmic domain (566aa vs. 141aa). In previously published E-Cadherin FRET sensors the sensor E-Cadherin was expressed in addition to the endogenous E-Cadherin (Borghi et al., 2012; Cai et al., 2014). Because the endogenous cytoplasmic domain is much smaller than the modified one, it is very likely that forces are only transmitted via the endogenous protein and that the sensor E-Cadherin is not participating in mechanotransduction. In our transgenic flies, the sensor E-cadherin is expressed in the absence of the endogenous protein. However, other junctional proteins could take over the force transducing function. Especially Echinoid, the *Drosophila* ortholog of Nectin, is part of the adherens junction complex and connects adjacent cells with the cytoskeleton in a similar fashion as E-Cadherin (Wei et al., 2005; Takai et al., 2008). It would be possible that, due to its size, the sensor protein is attached loosely to the cytoskeleton whereas Echinoid transmits the mechanical load instead.

Furthermore, we expected forces to change spatially or temporally during the development of the wing disc, dorsal closure or border cells. Mostly, these variations in forces have been measured by laser ablation experiments, which indicate altered tensions in the cortical actomyosin ring (Solon et al., 2009; LeGoff et al., 2013; Mao et al., 2013). Hypothetically, these forces might be dissipated in other structures without

passing through E-Cadherin. Hence, the alteration of forces in certain cellular substructures does not necessarily mean that they also occur across E-Cadherin.

In conclusion, our *in vivo* approach to develop a FRET based tension sensor revealed several technical challenges. Even though we used an improved version of previously published tension sensors, we did not observe any sign that our sensor, as well an already published sensor, reproducibly measured forces in the three different *Drosophila* tissues. This study highlights very general problems and pitfalls with the analysis and interpretation of FRET based tension sensors and will hopefully encourage subsequent projects to consider these difficulties more carefully.

## 2.5. EXPERIMENTAL PROCEDURES

### 2.5.1. Drosophila strains

Fly stocks were grown on a standard cornmeal medium at 25°C. $Cad^{Contr}$, $Cad^{TS}$, Cad-Venus and Cad-mTFP (Bloomington #58368, #58365, #58367, #58366) (a gift from D. Montell) were used in experiments analogous to shgContr, shgFRET, shgYFP and shgCFP. Border cell-specific *slbo*Gal4 driver and UAS-*lifeact*-RFP (Bloomington #58435, #58362) were used to label the border cell cluster for segmentation. AT1.03RK2 and AT1.03NL2 (DGRC #117014, #117012) with the driver lines *salE*Gal4 (Denise Nellen, FBrf0211371, 4.8 kbp EcoRI fragment 2L:11459156..11454345 Dmel_r6.08 generated in our laboratory) and *slbo*Gal4 were used for experiments with ATP-FRET. For live movies, *sqh*-GFP, *moesin*-GFP, and DE-Cad-*GFP* (Bloomington #57144, (Edwards et al., 1997; Huang et al., 2009) were used.

### 2.5.2. Generation of transgenic flies

shgFRET, shgContr, shgYFP and shgCFP were generated by a knock-in of the sensor module into the endogenous locus of E-cadherin (*shotgun*), as previously described (Huang et al., 2009). We used the sensor module published by Borghi et al. 2012, but with the mTFP1 exchanged by an ECFP (a gift from Alex Dunn). Therefore we used the plasmid DE-Cad $^{(rescue)}$ from Huang et al., a pGE-attB- vector containing a fragment of *Drosophila* E-cadherin. For shgFRET, shgCFP and shgYFP we introduced the restriction sites KpnI and SphI into the cytoplasmic domain of E-Cadherin, between the

*p120*- binding site and the transmembrane domain, with the primers CGGGGTACCTGGCACGAAAAGGACATCGA (KpnI) and ACATGCATGCGCCATTCTTCTGCTTTTTCT (SphI). We inserted the FRET sensor (shgFRET), only ECPF (shgCFP) or only EYFP (shgYFP) via the restriction sites for SphI and KpnI. Following primer pairs, flanked by a KpnI or SphI, were used for amplification:

shgFRET: ACATGCATGCGGATCAGGTGGAACTGGTT
and CGGGGTACCACCTCCTGTTGAACCTCC
shgCFP: ACATGCATGCGGATCAGGTGGAACTGGTT
and CGGGGTACCGAACAGCTCCTCGCCCTT
shgYFP: ACATGCATGCGACGAGCTGTACAAGTTA
and CGGGGTACCACCTCCTGTTGAACCTCC

For shgContr we introduced KpnI and SphI before the STOP codon, with the primers CGGGGTACCTAGGAATCTTCGCCAGCC (KpnI) ACATGCATGCGATGCGCCAGCCCTGGTCAT (SphI).
The same amplicon as for shgFRET was inserted by KpnI and SphI.

These constructs, cloned into the DE-CAD$^{(rescue)}$ vector, were microinjected into the founder line DE-CadGX23w[-]/CyO (Huang et al., 2009). Microinjection was performed by the Huazhen Biotech Company.

### 2.5.3. Immunohistochemistry

Immunostaining of the wing imaginal disc was performed according to standard protocol. Primary antibody anti-armadillo (AB_528089, Developmental studies hybridoma bank) and secondary antibody goat anti-mouse Alexa Fluor 594 (Molecular Probes, 1:500) were used.

### 2.5.4. Live imaging

Wing discs and salivary glands were dissected from 3$^{rd}$ instar larvae in WM1, mounted in a glass bottom dish (Imaging dish CG, Bioswisstec) covered with a cell culture insert (Millipore), as previously described (Zartman et al., 2013). Because timing of dissection and imaging was critical, we dissected shgContr and shgFRET alternating to have best control for timing effects.

To image border cell migration, egg chambers were dissected in Schneider's medium (Invitrogen) supplemented with 15%FBS (Gibco) and 200 mg/ml insulin (Sigma-Aldrich) from 3-4 days old, well fed female flies. Egg chambers were mounted in a poly-L-lysine (Sigma-Aldrich) coated glass bottom dish (Imaging dish CG, Bioswisstec). (Adapted from Prasad et al. 2007, Methods in Mol Biol)
For dorsal closure, embryos were aged for around 18-20h at 25°C, dechorionated in 50% bleach and mounted in Voltalef 10s oil (VWR) on cover slips (Menzel Gläser).(Adapted from Jankovics and Brunner, 2006)

Images were acquired with a Zeiss LSM710 microscope with an Argon laser, if not otherwise stated.
Movies were taken with an Andor revolution spinning disc confocal microscope and an Andor iXon3 EMCCD-camera.

### 2.5.5. Pharmacological treatment

For pharmacological treatments the drugs were directly added to the culture medium for wing disc, salivary glands or border cell migration. To inhibit actin polymerization in the wing disc, Latrunculin B was added to the WM1 (10µM, Sigma Aldrich) and imaged 5 and 10minutes after. To increase cell volume of the wing disc by an osmotic shock, distilled $H_2O$ was added to a final concentration of 50% and imaged 5 minutes after. To decrease Myosin activity in the border cells, the ROCK-inhibitor Y-27632 was applied (100µM, Sigma-Aldrich) and images were taken 30-45min after. To modify the activity of the ATP-FRET sensor, Antimycin A (20µM, Santa Cruz Biotech) was added to the culture of wing disc, salivary gland and egg chamber and imaged as indicated in the figures.

### 2.5.6. Stretching device

In order to apply an external force to the cultured wing disc, we used the stretching device as described previously (Schluck and Aegerter, 2010). The wing pouch of the dissected wing disc was attached to a glass slide, whereas the notum was attached to a small, moveable cover slip. Poly-L-lysine (Sigma Aldrich) was used for adhesion. The moveable cover slip was attached to a spring sheet which we used to apply a calibrated force to the disc. The force was calculated with the formulae adopted from the equation for the spring constant of a cantilever ($L$ is the length, $a$ the thickness, $b$ the width and

*E* the elastic modulus of the spring sheet, d is the distance that the spring sheet is displaced):

$$F = -\frac{E * a^3 * b}{4 * L^3} d$$

For measuring the effect of an applied force, we alternated between a pre-stretched state (10µN), to pull the disc until it was taut, and a stretched state (25µN).

### 2.5.7. FRET analysis

#### 2.5.7.1. Sensitized emission

For FRET analysis images were taken with the Zeiss LSM710 in three different channels: (1) YFP: 514nm laser; filter: 525-570 (2) CFP: 458nm laser; filter: 463-505nm (3) FRET: 458nm laser; filter 525nm-570. To correct for the crosstalk between the channels due to spectral overlap, we calculated the sensitized emission (SE) (Youvan et al., 1997; van Rheenen et al., 2004). By bleed-through, we infer here the leak-through of CFP signal into the YFP detector. By cross-excitation we refer to the direct excitation of YFP with the 458nm laser. To correct for the bleed-through we used the shgCFP flies and calculated the correction factor $\alpha=I^{FRET}/I^{CFP}$( $I^{FRET}$= intensity FRET channel; $I^{CFP}$= intensity CFP channel; $I^{YFP}$= intensity YFP channel). To correct for cross-excitation we used the shgYFP flies and calculated the correction factor $\beta=I^{FRET}/I^{YFP}$. Depending on the tissue and the microscopy settings, the values for α and β varied between 0.05-0.15. With these factors we obtained the SE from shgFRET and shgContr by:

$$SE= I^{FRET}- \alpha*I^{CFP}- \beta*I^{YFP}$$

The FRET index was further calculated by the ratio:

$$FRET\ index= SE / (I^{CFP}+SE)$$

#### 2.5.7.2. Image analysis

Fluorescent images were analyzed with Fiji, a distribution of ImageJ, using in-house macros.

Raw images were blurred with a median filter (sigma=1), oversaturated pixels were removed and background was subtracted using the rolling ball algorithm. Further, the image stack was projected by a maximum-intensity z-projection and masked with an automated threshold from CFP and YFP channels (Otsu algorithm). Subsequently, the FRET index was calculated pixel by pixel as described above. Finally, negative pixels were deleted and the look up table "Fire" was applied for visualization of the results. For an overall FRET index of one image, the mean of the masked image was taken.

#### *2.5.7.3. Image segmentation*

To analyze cell size, cell orientation and edge length of the wing disc and the amnioserosa, we processed the images in the YFP-channel by using FIJI and Epitools (Heller et al., 2016, Icy plug-inn). First, images were blurred and background subtracted as described above, then local maxima were determined and particles segmented to obtain a segmented binary image in FIJI (*Find Maxima - Segmented Particles*). Second, the segmented binary images and the calculated FRET images were overlaid with Epitools (*CellGraph* and *CellOverlay*) and the values for FRET indices combined with cell size, edge length and orientation extracted.

To analyze amnioserosa cells, we either distinguished between cells that contract/ expand between 7 minutes (1) or cell edges that contract/relax within 1 minute (2). (1) To determine cells according to their size, we took high quality image stacks at time-point 0min and 7min to calculate the FRET index. Every minute in between (time-points 1,2,3,4,5,6 min) we took snapshots to determine the cell area. We defined time-points 0 and 7 to be in a different pulsing stage (contracted vs. expanded) if they differ in cell area for more than 10% and they differ in more than one standard deviation, calculated from all the time-points together. (2) To determine edges according to their length, we measured length as the distance between two vertices. We took two high quality image stacks within one minute and distinguished contracted and expanded edges if they differ for more than 20% in length.

To analyze border cells of $Cad^{TS}$ and $Cad^{Contr}$ ROIs, covering on average 20µm$^2$ of masked image, in the front and the back were chosen according to the channel for *slboG4::UAS-lifeact-RFP* and the information about orientation from an overall image. For shgFRET and shgContr the YFP channel was used instead of *slboG4::lifeact-RFP*.

### 2.5.8. Statistics

Statistics were performed in R. Significance was calculated by with Welch's t-test, which assumes unpaired samples with unequal variance. Significance levels were indicated as ***($p \leq 0.001$), **($p \leq 0.01$), * ($p \leq 0.05$) and n.s. ($p > 0.05$). To estimate the correlation between two samples, the Pearson's correlation coefficient R was calculated.

### 2.5.9. FLIM

#### 2.5.9.1. Image acquisition

Images were taken with a Leica SP8 confocal microscope covering a TCSPC-FLIM module from Picoquant (PicoHarp300) and the SymPho Time 64 software. For shgFRET and shgContr, a pulsed diode laser (PDL 800-B) (440nm, 40MHz) and a HyD SMD detector (450-505nm) were used. For $Cad^{TS}$ and $Cad^{Contr}$ a White Light Laser (at 470nm, 40MHz) and a HyD SMD detector (480-505nm) were used. (Imaging performed at ScopeM – Image facility at ETH Zürich)

Mounting and imaging was performed as described above for the Zeiss LSM710.

#### 2.5.9.2. Image analysis

Lifetime data were analyzed using the SymPho Time 64 software. For an overall lifetime value of one image, we fitted a double-exponential, reconvolution (calculated IRF) model to the lifetime histogram of the image and used the intensity weighted lifetime ($\tau^{\text{Av Int}}$). For spatial patterns of lifetime across the wing disc, we set a binning of 2x2 pixels and a threshold to remove the background and calculated a FLIM Fit. To calculate FRET efficiency (E), we took lifetimes from donor only ($\tau^{shgCFP}$) and the FRET pairs ($\tau^{shgFRET}$or $\tau^{shgContr}$):

$$E=1-\tau^{shgFRET}/\ \tau^{shgCFP}$$

For $Cad^{TS}$ and $Cad^{Contr}$ analysis was done accordingly.

## 2.6. ACKNOWLEDGEMENTS

We would like to thank George Hausmann for useful discussions and comments on the manuscript. We thank Alexander Dunn, Denise Montell, Damian Brunner and Yang

Hong to share fly lines and plasmids with us. We thank Flavio Lanfranconi and Davide Heller for technical support with the stretching device and the Epitools software. Laurynas Pasakarnis assisted with the work on the amnioserosa cells. The image facility centers of the University of Zürich (ZMB) and the ETH Zürich (ScopeM) helped with microscopy imaging and image analysis. Funding for this work was provided by a SystemsX IPhD project.

## 2.7. SUPPLEMENTAL INFORMATION

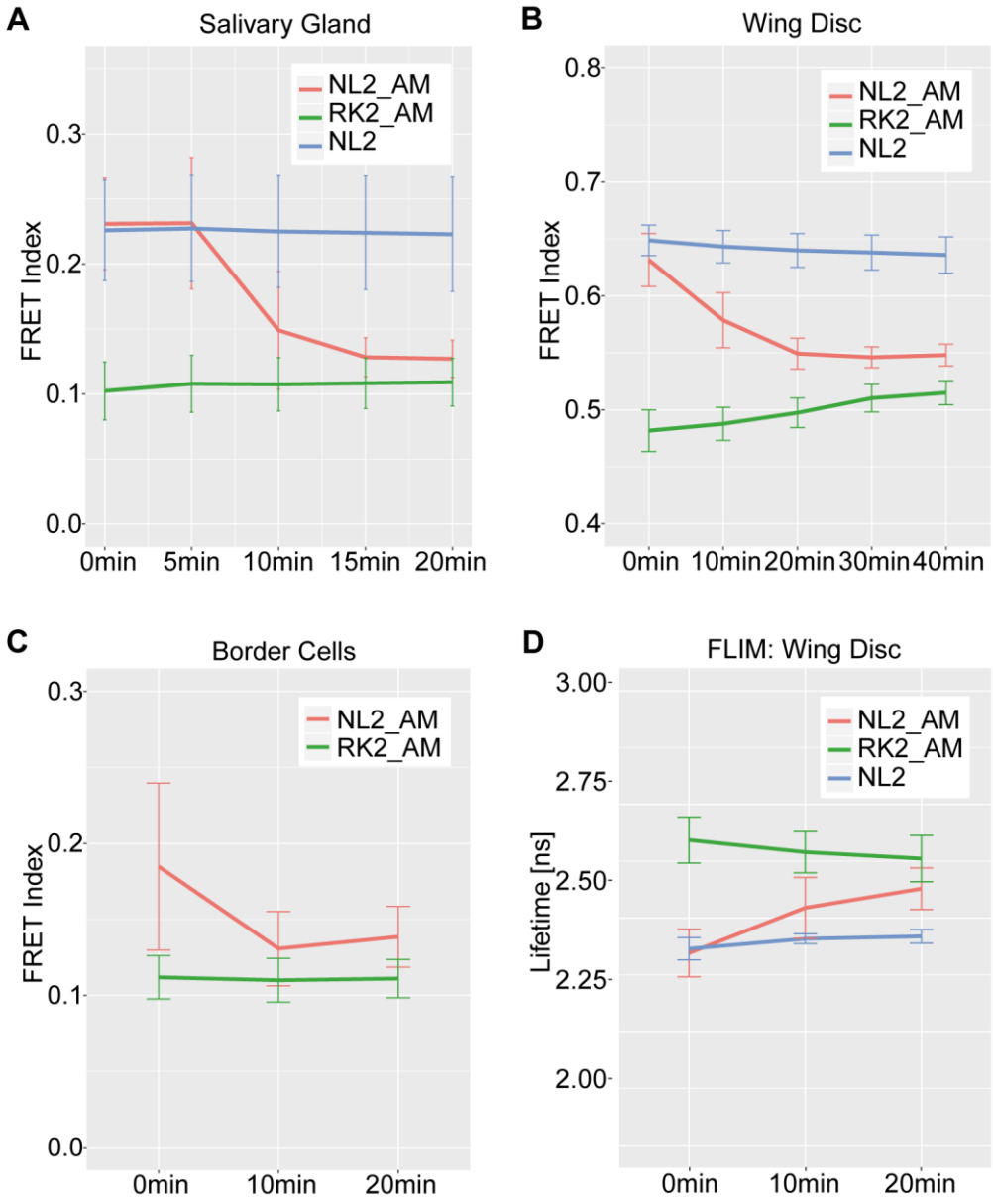


**Figure 2.6. S1. FRET analysis of ATP sensor as positive control.** We used an established FRET sensor to test our analysis workflow. This ATP (Adenosine triphosphate) activity sensor changes conformation from an open state to a closed state by binding of ATP (Tsuyama et al., 2013). Hence, an increased FRET index indicates high abundance of ATP. A functional sensor (ATP-NL2) and an

insensitive version as negative control (ATP-RL2) were used. We treated the samples with the chemical AntimycinA (AM) to decrease ATP levels. Using the ratiometic method, the sensor was applied in the salivary gland (A), as in the original publication, in the wing disc (B) and in the border cells (C). In all three tissues the FRET index decreased upon AM treatment as expected within 5- 20 minutes. The negative control RK2 was not affected or slightly increased by the treatment. (D) Similar results were obtained when FRET was measured with FLIM. These results confirmed that our FRET analysis pipelines are sensitive to FRET.

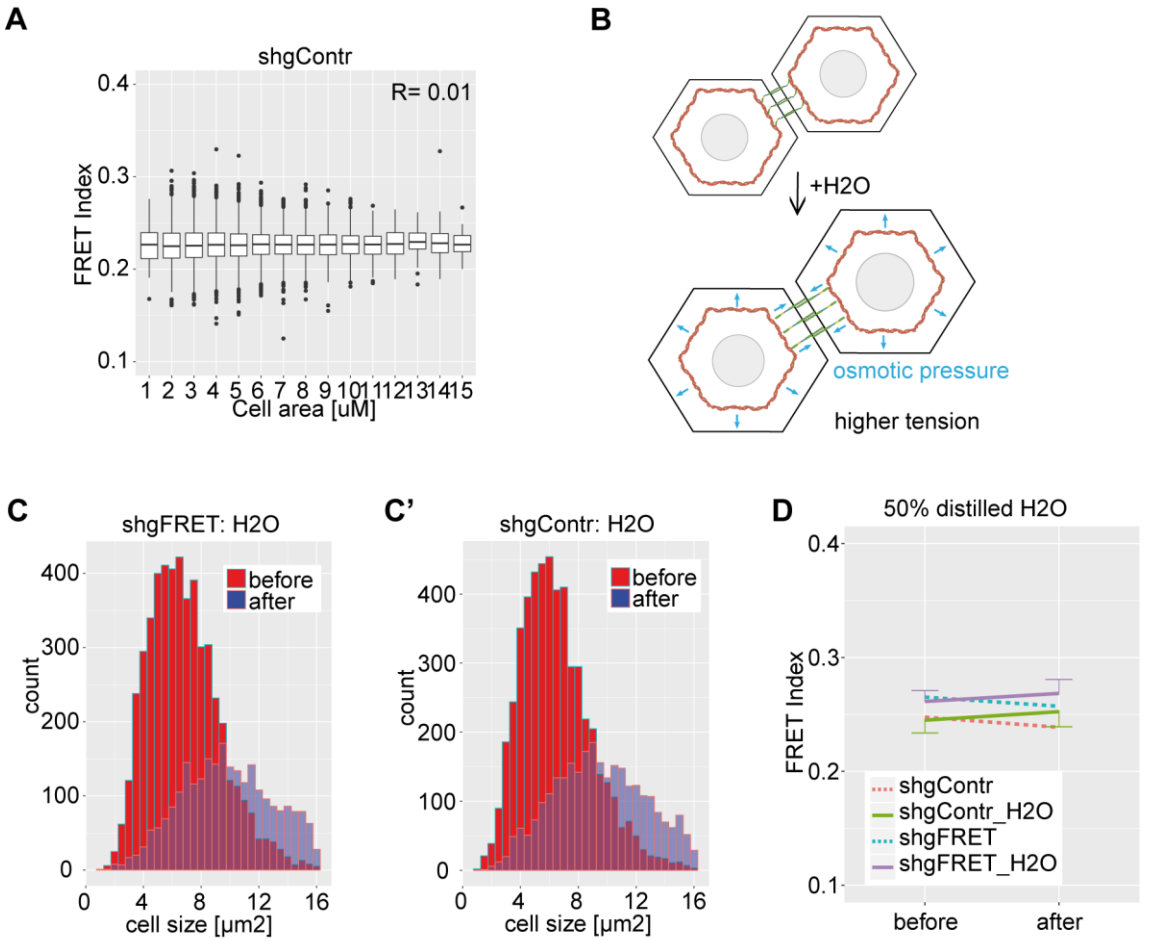


**Figure 2.7. S2. FRET analysis in the wing disc.** (A) The FRET index of individual cells did not correlate with cell area in the wing pouch (here shown for shgContr, n=14 wing discs). (B) The treatment with distilled H2O causes an osmotic shock and increases the cell volume. We expect that the distance between the acto-myosin rings of adjacent cells increases and thereby stretches E-Cadherin. This would result in a decrease in FRET index. (C, C') Upon H2O treatment, the apical cell area increased for around 40% for shgFRET and shgContr. (D) But instead of an expected decrease, the FRET index of both shgFRET (2.7%, n=24) and shgContr (3.0%, n=24) increased. The control without treatment (dashed line, n=12) decreased over the 5 minutes of experiment.

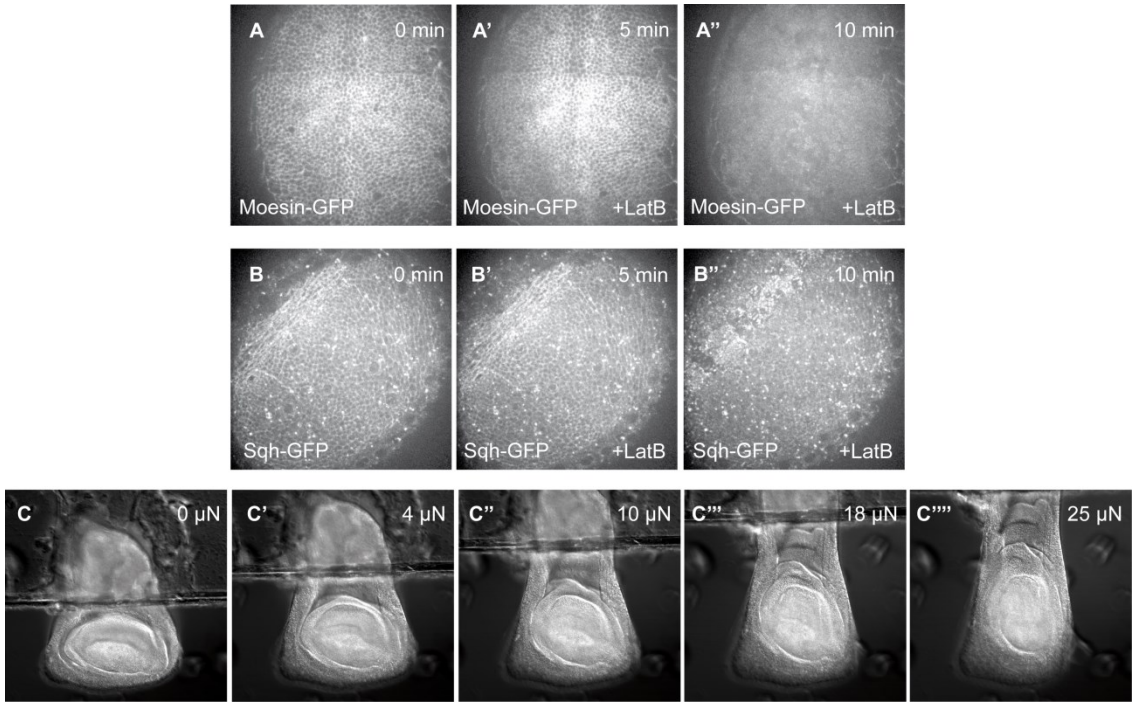


**Figure 2.8. S3. Mechanical stimulations in the wing disc.** (A, B) LatrunculinB treatment is supposed to inhibit actin polymerization and thereby decreases the cortical tension. To test the efficiency and speed of our treatment, we analyzed the dynamics of the actin-binding protein Moesin (A, A', A'') and the *Drosophila* homolog of Myosin, Spaghetti squash (sqh) (B, B', B''). For both, the intensity of the signal dropped and the signal disappeared from the membranes within the first 10 minutes. (C-C'''') Here, we show an example of a wing disc which was stretched with an increasing force. Images show the transmission light channel. (C'') and (C'''') represent the applied forces which were used for the experiment, 10µN and 25 µN (Fig. 2.2).

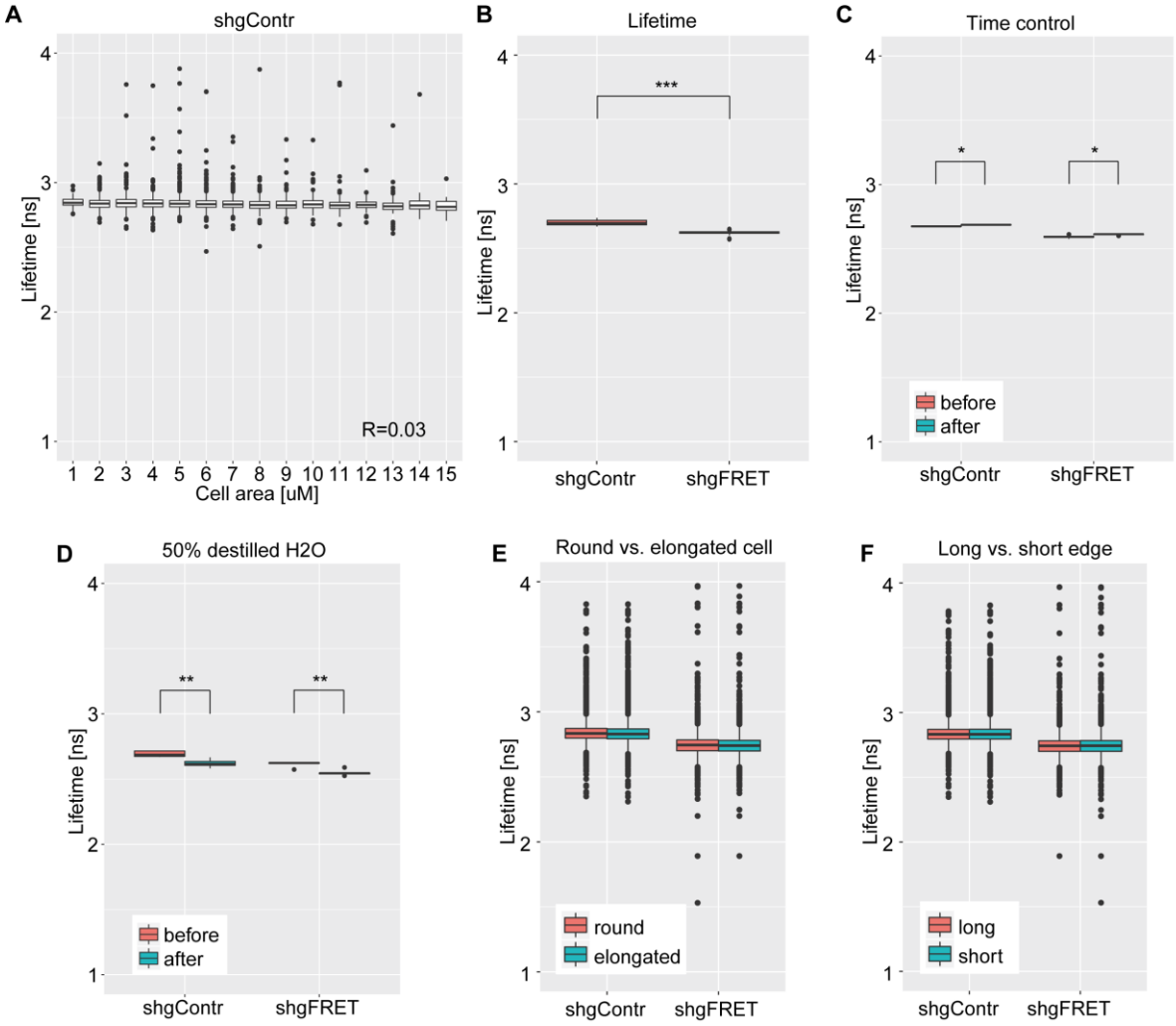


**Figure 2.9. S4. FLIM measurements in the wing disc.** (A) The fluorescence lifetimes of individual cells did not correlate with cell area in the wing pouch (here shown for shgContr). (B) Lifetimes of the entire wing pouch were significantly higher for shgContr (2.7, n=15) than for shgFRET (2.6, n=14). (C) The lifetimes of shgContr (2.68 vs. 2.69, n=4) and shgFRET (2.59 vs. 2.61, n=4) increased over the 5 minutes of the experiment, even without any treatment. (D) The application of an osmotic shock by adding distilled H2O decreased the lifetimes for shgContr (2.69 vs. 2.62, n=5) and shgFRET (2.61 vs. 2.55, n=9). (E) Lifetimes did not differ between round vs. elongates cells for shgContr (2.83 vs. 2.83) and shgFRET (2.74 vs. 2.74), neither between long vs. short edges (F) for shgContr (2.83 vs. 2.83) and shgFRET (2.78 vs. 2.78). (Data for A, E and F were pooled from 8 wing discs.)

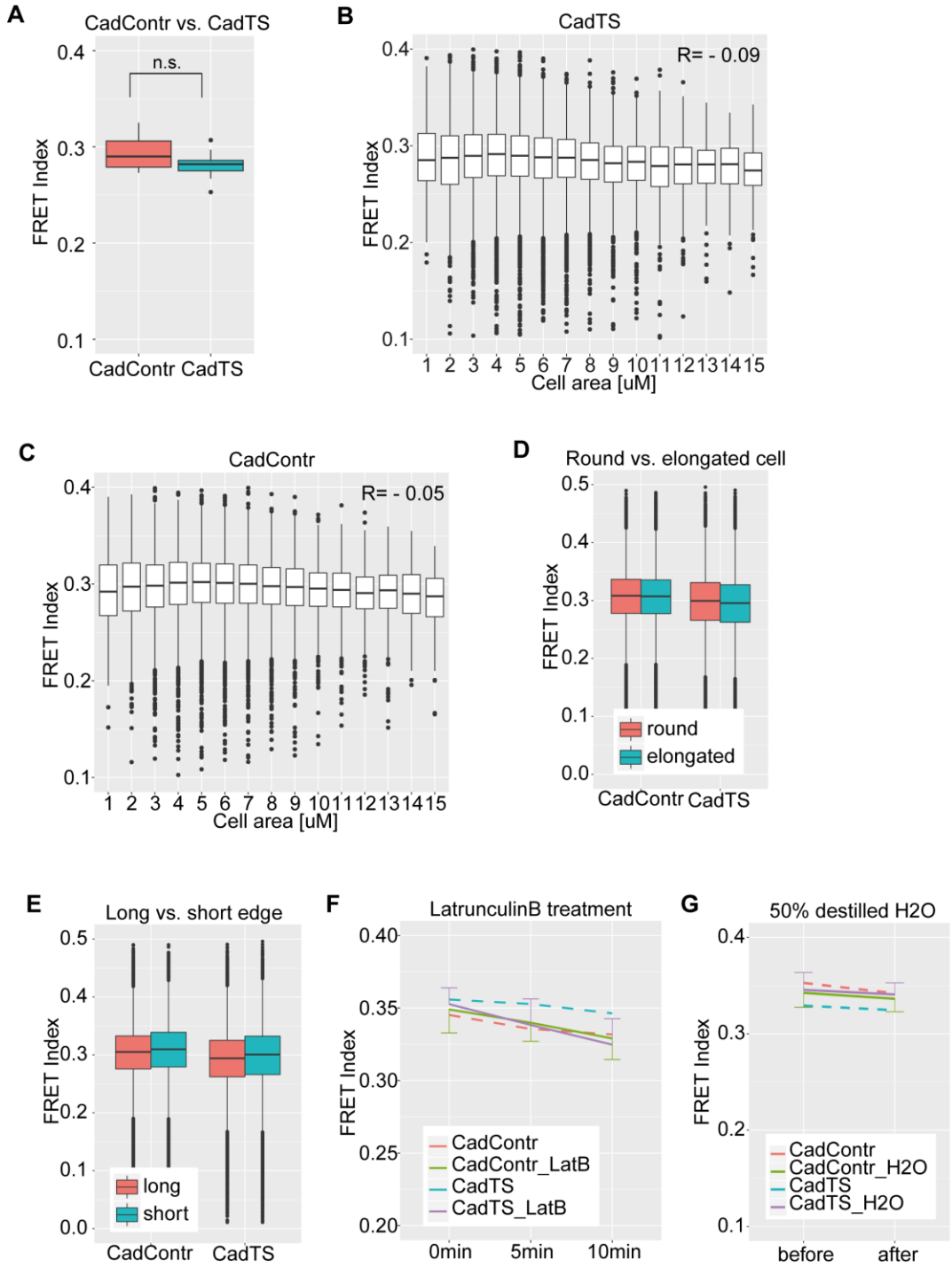


**Figure 2.10. S5. FRET analysis of CadTS sensor in the wing disc.** (A) The FRET index in the entire wing pouch for CadContr (0.292, n=13) is 4% higher than for CadTS (0.281, n=13). (B, C) For both, CadTS and CadContr, the FRET index of individual cells does not correlate with cell size. (D) The FRET index of individual cells is similar between round and elongated cells for CadContr (30.6 vs. 30.5), but they differ around 1.5% for CadTS (29.7 vs. 29.3). (E) The FRET index of an individual edge is around 1.5% lower for long than for short edges, for CadContr (30.2 vs. 30.7) and CadTS (29.2 vs. 29.7). (Data for B, C, D and E were pooled from 13 wing discs.) (F) After LatrunculinB treatment, the FRET index for CadContr and CadTS decreases slightly more than for the time control without treatment (dashed line). (G) After treatment with distilled H2O, the FRET index decreases for CadContr and CadTS slightly less than for the time controls (dashed line). ((F, G) n=18 for treated samples and n=9 for time controls)

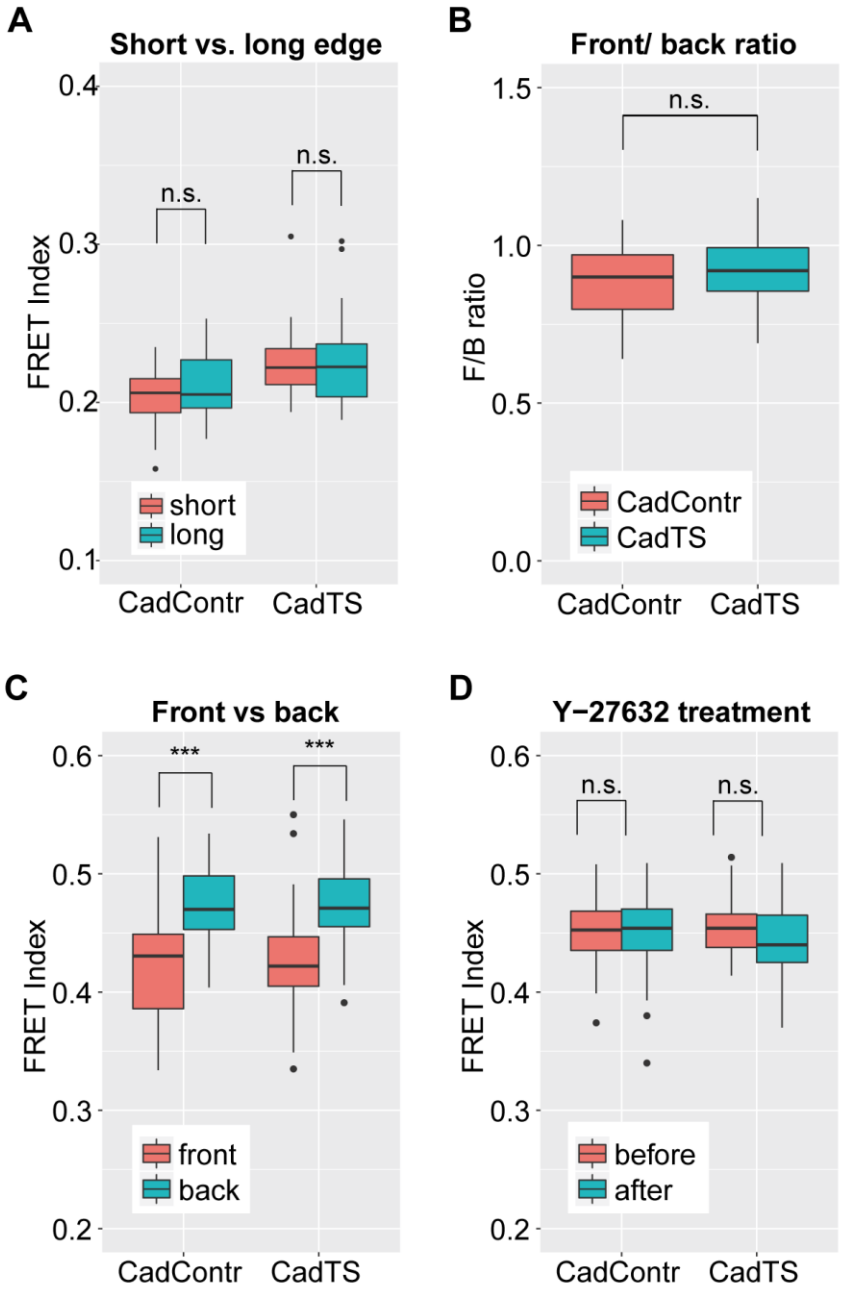


**Figure 2.11. S6. FRET analysis of CadTS in the amnioserosa cells and in the border cells.** (A) Cells which during dorsal closure either elongate or shorten within one minute do not change their FRET index. (CadContr n=55, CadTS n=44). (B, C) Both CadContr (0.89) and CadTS (0.92) have a front to back ratio below one, which shows that the FRET index is higher in the back than in the front of the border cell cluster. But CadContr and CadTS do not significantly differ in their front to back ratio. (D) Myosin downregulation by Y-27632 treatment does not significantly change the FRET index for CadContr and CadTS. ((B, C, D) n=26 for CadContr and n=30 for CadTS)

# 3. RESULTS AND DISCUSSION II – Modifying Forces

## Force manipulation in the wing disc and its implications for growth and gene expression

### 3.1. ABSTRACT

How growth and size is regulated in the *Drosophila* wing imaginal disc remains an open question. Although several molecular factors have been shown to be involved in growth regulation – with Dpp as the most prominent one – growth models based on these molecular factors fail to describe several empirical observations. To explain homogenous proliferation patterns and the cessation of growth once the final size has been reached, mechanical feedback models have been proposed. These growth models include mechanical forces as central regulators of growth. The underlying assumptions about the interaction of mechanical forces and growth derive mainly from mammalian cell culture systems. Here, we aimed to find empirical evidence for a growth promoting effect of mechanical forces in the wing imaginal disc. Therefore, we used a previously developed stretching device to apply external forces to the wing disc. With this device, we investigated the impact of the applied force on the number of proliferating cells within the wing disc. Further, we performed transcriptome analysis to find candidate genes that are differentially expressed upon mechanical stress. We could not detect any specific effect of mechanical stress, neither on the number of proliferating cells, nor on the transcriptome with this experimental setup.

## 3.2. INTRODUCTION

In the present study we performed force manipulations to investigate the growth promoting potential of mechanical stress and to elucidate molecular mechanisms of mechanotransduction. We focus on the *Drosophila* wing imaginal disc which is the larval Anlage which eventually gives rise to the adult wing. Starting from around 50 cells in the first instar larva, it reaches about 30.000 cells at the onset of the pupal stage (Martin et al. 2009). Growth and size of the wing disc are tightly regulated. If cell size or cell numbers are experimentally altered in parts of the disc, the size of the final wing disc remains constant (Weigmann et al., 1997; Neufeld et al., 1998). This indicates that the final size is controlled on the level of the overall dimension rather than on the size or number of single cells. Further, classical transplantation experiments have shown that if immature wing discs are grafted into an adult female abdomen, they autonomously grow to their characteristic final size (Bryant and Levinson, 1985). Together, these studies reveal that the wing disc contains a very robust, intrinsic mechanism to control its size.

Growth models aiming to explain this intrinsic size control mechanism attribute a central role to the morphogen Dpp. Dpp is secreted by a stripe of cells next to the A-P boundary from where it spreads to generate a gradient (reviewed by Affolter and Basler, 2007; Restrepo et al., 2014). Several studies provide considerable evidence that Dpp plays a role in growth regulation of the wing disc. Wing discs lacking Dpp activity are reduced to small stumps whereas ectopic activation of Dpp leads to significantly larger wing discs (Zecca et al., 1995; Burke and Basler, 1996; Nellen et al., 1996; Akiyama and Gibson, 2015; Harmansa et al., 2015).

Growth models for the wing disc fall into two categories (reviewed by Wartlick et al., 2011a; Hariharan, 2015). In the first category, Dpp is instructive for growth which means that Dpp directly drives cell growth or division. These models are challenged by the observation that proliferation is distributed homogenously throughout the wing disc. Hence, the question arises of how a morphogen with a graded distribution can account for a homogenous proliferation pattern? An early model assumed that Dpp levels at the center and at the margins of the wing pouch are fixed, resulting in the flattening of the gradient over time (Day and Lawrence, 2000). Cells are supposed to sense the steepness of the gradient: they proliferate with a sufficiently steep gradient,

but stop dividing if the gradient drops below a certain threshold. Another instructive growth model proposed that the proliferation rate is dependent on the relative change of Dpp levels over time (Wartlick et al., 2011b). Based on the observation that the concentration of Dpp in the center increases over time, the model suggests that cells divide when their Dpp levels increase by 50% to the levels of the preceding cell cycle. Both intrinsic growth models account for the homogenous proliferation patterns and partially explain the cessation of growth when the disc has reached a certain size. However, the importance of a graded Dpp activity in the two models was questioned by experiments in the absence of a Dpp gradient. If Dpp is blocked and in addition Brinker, a transcription factor that is negatively regulated by Dpp, is removed the wing discs grow relatively normal (Schwank et al., 2008).

This observation fostered the second category of growth models: In permissive growth models Dpp promotes growth indirectly. Dpp enables growth above a certain threshold, but the more precise regulation is instructed by other factors. According to the "growth equilibration model", Dpp indirectly promotes growth in the center of the wing disc by suppressing Brinker, a growth inhibitor (Schwank and Basler, 2010). With the parallel activity of another reverse gradient, supposedly of the Fat/Hippo system, Dpp/Brinker leads to homogenous growth throughout the wing disc.

Another set of permissive growth models incorporates mechanical forces into growth regulation. As discussed in detail in chapter 1, mechanical forces affect growth and proliferation in various tissues. In these models, mechanical forces act as a long range signal to instruct tissue wide growth patterns (Shraiman, 2005; Aegerter-Wilmsen et al., 2007; Hufnagel et al., 2007). The mechanical growth models require a high concentration of growth factors in the center of the pouch for initiation. This high concentration occurs at the intersection of the Dpp and the Wingless expression domains and promotes growth in the center. Growth in the center causes a tangential stretching of the surrounding tissue, whereas cells in the center get compressed. Based on the assumption that stretching induces growth and compression reduces growth, the lateral cells are driven to proliferate - even in the absence of growth factor. In contrast, compression in the center opposes the growth induction of the growth factors. When the growth factors can no longer overcome the inhibitory effect of mechanical compression, an equilibrium has been reached and the wing disc stops growing. A more recent version of the mechanical model also incorporated molecular signaling

pathways into the regulatory network (Aegerter-Wilmsen et al., 2012). This network comprises already established interactions between Notch, Dpp, Wg and Vestigial, as well as the activation of Yorkie via Four-jointed/Dachsous signaling. These mechanical growth models give an explanation for the conundrum of how growth can occur homogenously in the presence of non-uniformly distributed growth factors. Further, mechanical forces are part of a feedback mechanism that provides information about the overall wing disc size and triggers the termination of growth once the final size has been reached.

Experimental evidence supports the predictions of force distributions in the wing disc. Cells in the center are compressed whereas the ones at the periphery are stretched (Nienhaus et al., 2009; Ishihara and Sugimura, 2012; LeGoff et al., 2013; Mao et al., 2013). Laser ablation experiments and clonal analysis reveal that global force distributions indeed emerge from proliferation patterns and that these force distributions feedback to guide the orientation of tissue growth (Mao et al., 2013). Further, studies indicate that mechanical perturbations could have an impact on cell proliferation via the Hippo pathway (Dupont et al., 2011; Aragona et al., 2013). In mammalian cell culture experiments, stretching cells increased YAP activity and lead to higher proliferation rates. Similarly in the wing disc, perturbations of the actin cytoskeleton affect the YAP homolog Yorkie and induce overgrowth (Fernandez et al., 2011; Sansores-Garcia et al., 2011; Fletcher et al., 2015). More recently, a mechanism has been proposed for the wing disc: experimentally increased mechanical tension at the apical side recruits Ajuba. Ajuba in turn activates Yorkie by sequestering Warts, the negative regulator of Yorkie (Rauskolb et al., 2014).

However, it still remains elusive whether the mechanical forces occurring during normal wing disc development are sufficient to trigger proliferation and to antagonize the growth factors. Here, we use a previously developed device to mechanically stretch the wing disc *in vitro* and to test the growth promoting effect of mechanical stress (Schluck and Aegerter, 2010; Schluck et al., 2013). Further, we aim to find molecular factors which are involved in the transduction of the mechanical cues to generate an appropriate cellular response.

## 3.3. RESULTS

In order to apply an external force to the wing disc, we used a previously developed stretching device (Schluck and Aegerter, 2010). The dissected wing disc was attached with the peripodial membrane directed downwards onto two poly-L-lysine-coated glass slides (Fig.1A). Around half of the pouch was attached to a stationary microscopy slide, whereas the notum was attached to a small, movable cover slip. The cover slip was connected to a spring sheet which was fixed at the other end. Upon the application of a controlled force, the spring sheet bends which moves the small cover slip to stretch the wing disc. Fig.1B illustrates a wing disc with a stepwise increased tension. We induced GFP expressing clones in order to have landmarks within the wing disc. These landmarks revealed that some areas, which are initially not visible, got exposed upon stretching. This indicates that a proportion of the applied force was used to stretch out folds and to flatten the tissue.

In order to test how harmful the procedure of stretching was to the wing disc, we performed a simple assay with the molting hormone Ecdysone. When applied to the wing disc culture overnight, Ecdysone drives evagination of the wing pouch (Fig. 1C) (Fristrom and Chihara, 1978). In stretched wing discs, which were removed from the device after one hour and subjected to an overnight Ecdysone treatment, the wing pouch still evaginated (Fig. 1C'). This showed that the wing disc survived the manipulations and was still viable for several hours after stretching to allow for evagination.

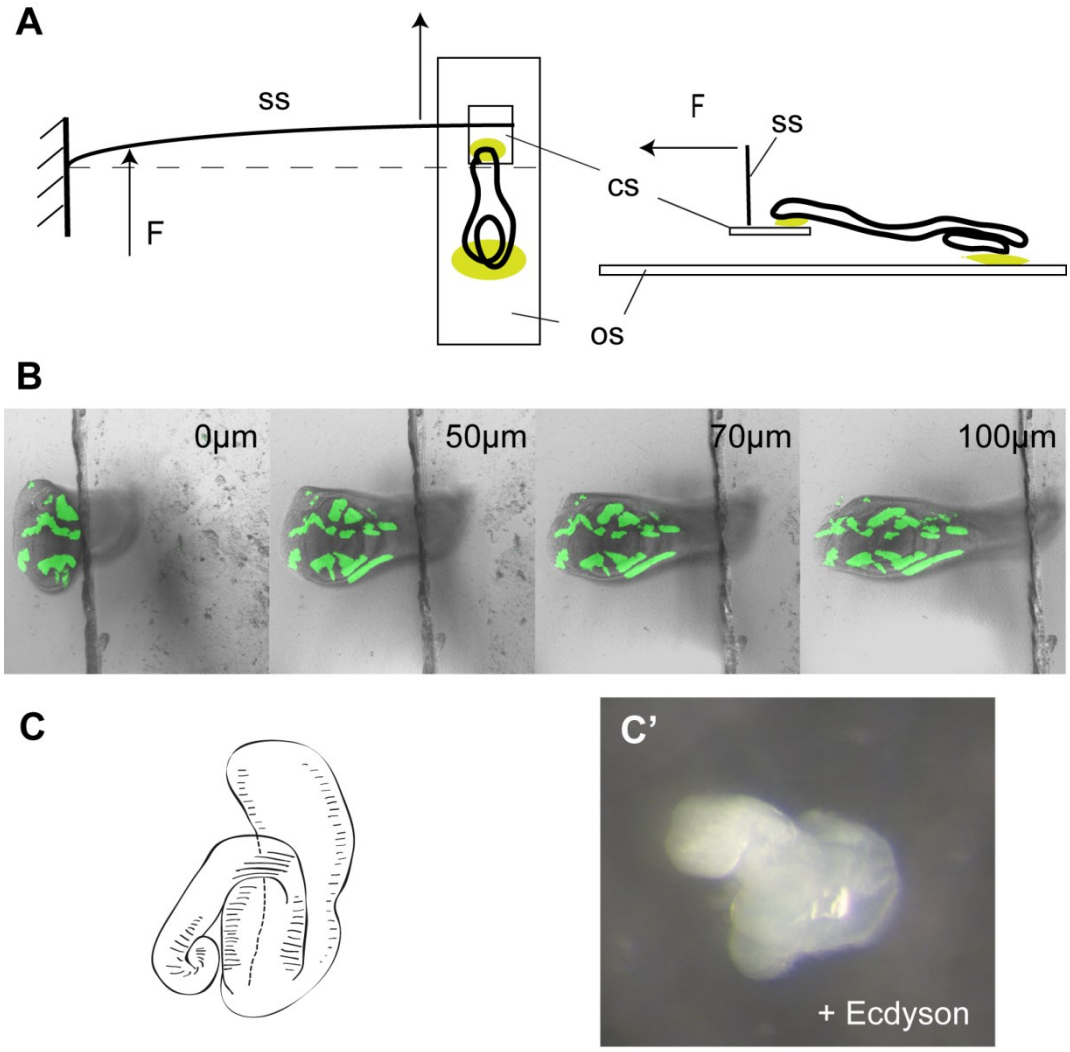


**Figure 3.1. Application of an external force to the wing disc.** (A) Schematic drawing of the stretching device from top (left) and lateral (right). Using poly-L-lysine (yellow), the wing disc is attached with the wing pouch downwards to a big objective slide (os) and with the notum to a small cover slip (cs). The cover slip is connected to a spring sheet (ss) which is fixed at the other end. Application of a force to the spring sheet moves the small cover slip and stretches the wing disc. (B) Example of a wing disc with increasing force application. Numbers indicate the displacement of the spring sheet. GFP labeled clones (green) serve as a landmark on the transmission light image. For geometrical and optical reasons, clones are only visible around the wing pouch region and not at the notum. (C) Schematic drawing illustrates the evaginated wing pouch after Ecdysone treatment (adapted from Fristrom and Chihara, 1978). (C') A wing discs which was stretched for one hour and removed from the stretching device evaginated after an overnight treatment with Ecdysone.

### *3.3.1. Cell cycle regulation upon mechanical stretching*

An earlier study with the stretching device suggested that one hour of stretching had an observable effect onto the proliferation rate (Schluck et al., 2013). For this, they performed live-imaging of the wing pouch during stretching while counting dividing cells. These were identified by their increased apical area. This directly yields a

proliferation rate given by the relative increase in the number of cells over time. The results of this study suggested that proliferation rate increased in wing discs upon the application of mechanical stress relative to control discs, where no mechanical stress was applied.

We further investigated this effect by using other cell-cycle markers. After stretching the wing discs for one hour, we performed phospho-Histone3 (pH3) immunostaining - a marker for mitotic cells (Hans and Dimitrov, 2001) - to measure cell cycle progression at that time. As a control, the second disc of the same larva was attached to an identical setup without the application of a force. We counted pH3-positive cells in a defined area (circle of 120µm diameter) in the center of the pouch (Fig. 2A). Wing discs which were fixed directly after stretching had on average 30±2 (mean ± stdev) mitotic cells, whereas for stretched (19±6) and control (22±10) wing discs the numbers decreased (Fig. 2B). However, stretched and control wing discs did not differ significantly. Thus, stretching the wing disc for one hour had no detectable effect onto the absolute amount of mitotic cells in this assay.

Labelling the cells of the S-phase with EdU is another way to assay proliferation. Therefore, we stretched the wing disc for one hour and then added EdU for 30min to allow incorporation by S-phase cells. Wing discs were then stained with an antibody against EdU. Because segmentation of S-phase nuclei was difficult due to the high number of positive cells, we took the overall intensity of the immunostaining as a read-out (Fig. 2C). Again, we used the second wing disc of the larva as a control without force application. Comparing the stretched discs to the controls did not reveal any effect of stretching on the amount of S-phase cells.

Because we did not obtain an effect after one hour of stretching, we extended the duration of the experiment. The external force was applied for two hours before immunostaining with pH3. Again, no difference in the number of pH3 positive cells between stretched and control discs was observed (Fig. 2E). However, the number of pH3 positive cells in the stretched and the control wing discs decreased around 70% compared to directly dissected wing discs (Fig. 2E). Thus, the negative effect of the culturing and stretching procedure over two hours was too strong to make a robust statement about the effect of mechanical stress.

Compared to values in the literature (Zartman et al., 2013; Handke et al., 2014), the decrease in the number of mitotic cells over time in culture was high. To test one of the reasons for this drop in mitotic activity, we evaluated the effect of poly-L-lysine attachment on the number of proliferating cells. Therefore, wing discs were either attached with poly-L-lysine to a conventional objective slide or alternatively mounted in a culture dish without poly-L-lysine (as described in Zartman et al., 2013). Live-imaging the wing discs with the membrane marker lac-YFP revealed that attaching the wing discs with poly-L-lysine negatively affected the proliferation rate (Fig. 2F). Hence, using poly-L-lysine might be a limiting factor of the stretching set-up that is not compatible with performing the proliferation experiments on longer time-scales.

To conclude this section, we did not detect an effect of an applied force onto the number of proliferating cells, neither with pH3 immunostaining nor with an EdU assay. The problem of these approaches, as discussed below, may be the way of characterizing cell cycle progression with a static snap-shot as well as due the fact that not the entire area of analysis may have been under increased tension. In addition, the force application was limited to one hour. Above one hour, the negative effect of the experimental procedure, especially the use of poly-L-lysine, was too strong to draw a robust conclusion about proliferation rate.

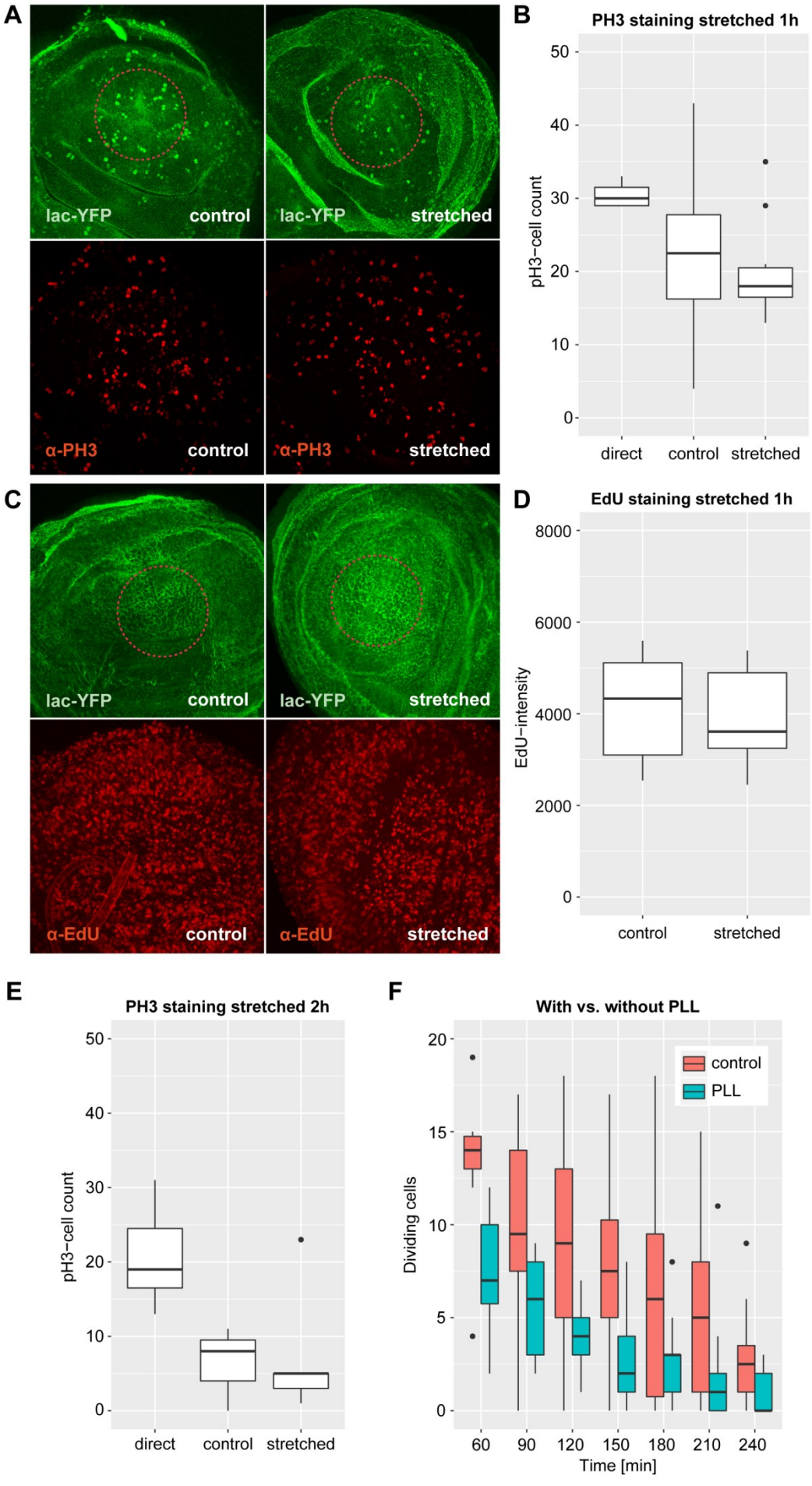
A
lac-YFP
control
lac-YFP
stretched
α-PH3
control
α-PH3
stretched
B
PH3 staining stretched 1h
pH3−cell count
50
40
30
20
10
0
direct
control
stretched
C
lac-YFP
control
lac-YFP
stretched
α-EdU
control
α-EdU
stretched
D
EdU staining stretched 1h
EdU−intensity
8000
6000
4000
2000
0
control
stretched
E
PH3 staining stretched 2h
pH3−cell count
50
40
30
20
10
0
direct
control
stretched
F
With vs. without PLL
Dividing cells
20
15
10
5
0
control
PLL
60
90
120
150
180
210
240
Time [min]

**Figure 3.2. Cell proliferation upon stretching.** (A) Immunostaining against pH3 was performed after wing discs were attached for one hour to the stretching device with (stretched) or without (control) the application of a force. The red circle in the Lac-YFP channel indicates the area used for analysis. (B) Compared to a directly dissected wing discs (30.5, n=4), control (25%) and stretched (37%) discs had a strongly decreased number of pH3 positive cells. Control (22.9, n=14) and stretched (19.5, n=15) wing discs did not differ significantly. (C) EdU incorporation and staining was performed to label S-Phase cells for control and stretched wing discs. The red circle in the Lac-YFP channel indicates the area used for analysis. (D) The intensity of the EdU staining was similar between control (4055, n=9) and stretched (4000, n=9) wing discs. (E) PH3 staining after 2h of force application (stretched) and 2h without force application (control). Compared to direct dissected wing discs (20.6, n=6), control (65%) and stretched (70%) disc revealed a drastically reduced amount of pH3-positive cells. For control (7.4, n=5) and stretched (6.3, n=3) wing discs a similar amount of pH3 cells was observed. (F) To test the impact of polylsine, we compared wing discs mounted with and without (control) polylsine. Dividing cells were detected by live-imaging the wing pouch with a membrane marker (lacYFP). Within 4h, wing discs attached to poly-L-lysine (n=13) revealed a much lower proliferation rate than in the control sample (n=12).

### *3.3.2. Transcriptional response upon mechanical stretching*

In parallel to the above experiments we used the stretching device to explore molecular factors that could be involved in sensing mechanical forces by the cells. Therefore, we performed a microarray in order to describe the transcriptional response of the tissue to an applied force. We aimed to find candidate genes which are affected by mechanical stress. The challenge with this experiment was to distinguish between a transcriptional response due to mechanical stress and the one that was due to the experimental settings itself. Therefore we performed two separate experiments (Fig. 4A): (1) First, we collected two samples of wing discs that were either stretched for one hour (str) or only attached without the application of a force (ctr I). From this comparison we gained transcriptional targets of mechanical stress. To keep variation as low as possible, we dissected the wing disc for stretching and the control from the same larva. (2) In a second experiment we aimed to detect a transcriptional response due to the sum of stresses to which a wing disc is exposed during the experiment, e.g. dissection, attachment, handling with forceps, … . Here, these stresses are referred to as culturing stress. We compared wing discs that were attached to the device without application of force (ctr II) - as in the previous experiment – and wing discs directly processed after dissection (dir). We obtained 35 genes being transcriptionally regulated due to mechanical stress and 39 genes due to the culturing stress (fold change > 1.5, p-value < 0.05) (Fig. 4A). There was an overlap of two genes between the results of the two experiments.

Around 40 genes showing up in the microarray was very few compared to the total of 20.000 genes examined. Therefore, we asked how many positive genes would randomly appear from our microarray data? We performed 200 permutations of random comparisons between three on three samples (out of the 12 that we collected). On average in these random comparisons, 30 genes revealed a fold change > 1.5 and a p-value < 0.05. This statistical experiment illustrated that from our microarray data around 30 genes might show up just by chance. This means that our expected candidate genes would be covered by a background noise of around 30 genes.

In order to filter our results we argued that if a gene was indeed transcriptionally regulated by mechanical stress, it should appear in all comparisons of samples between mechanically stressed and mechanically non-stressed wing discs: str vs. ctr l; str vs. ctr II; str vs. dir (Fig. 4B). Random results are unlikely to appear in all three comparisons. The same argument is true to filter out genes which are regulated by culturing stress. Therefore, we searched for overlaps between the comparisons of the different samples (Fig. 4B). In the cross-comparisons we obtained an overlap of 9 genes regulated upon mechanical stress and 21 genes upon culturing stress. Between these 9 and 21 genes there was an overlap of two genes which we excluded from further analysis.

To confirm the microarray results, we performed quantitative real-time PCR (qRT-PCR) with the seven candidate genes for mechanical regulation and added the genes diap1 and expanded (Fig. 4C). These two genes are commonly used transcriptional readouts for Yorkie activity (Rauskolb et al., 2014). Hence, if Yorkie played a role in the early response to mechanical forces, we would expect that these two genes to be transcriptionally upregulated. We compared the samples str vs. ctr I and str vs. ctrl II. However, only for one gene, Gr43a, did the two qRT-PCRs suggest an upregulation with a fold change > 1.5, as was shown by the microarray. Gr43a is a gustatory receptor usually expressed in the brain and other neurons and is therefore highly unlikely to be a target of mechanical stress in the wing disc (Miyamoto et al., 2012).

To conclude, the qRT-PCR did not confirm the candidates that we obtained from the microarray data. Therefore, the resulting genes from the microarray probably represent experimental background noise and are not transcriptional targets of mechanical stress.

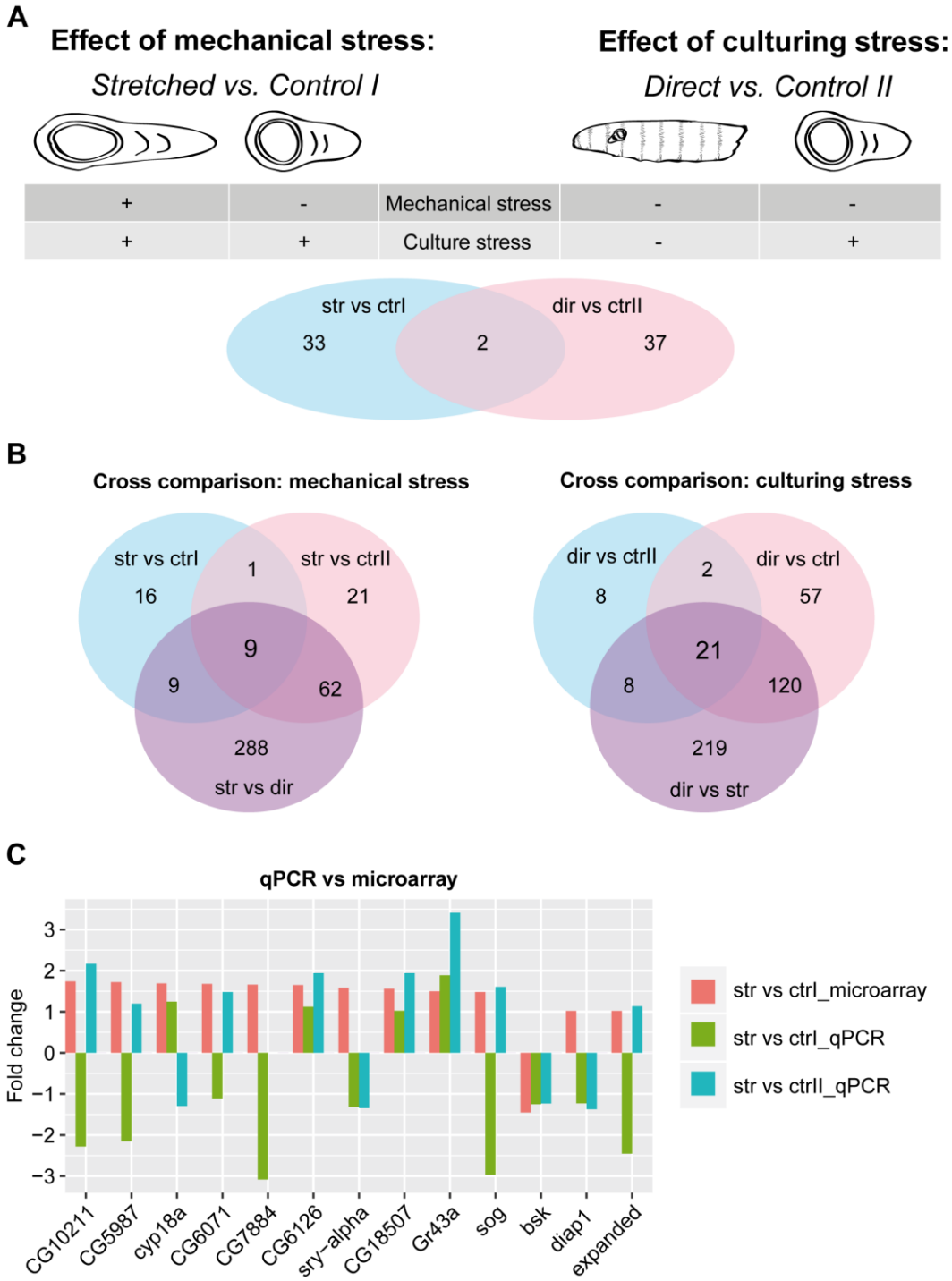


**Figure 3.3. Transcriptional response to force application.** (A) Design of the microarray: Two independent experiments were performed to either test the transcriptional response to mechanical stress or to culturing stress. Stretched samples were exposed to mechanical and culture stress, control samples only to culture stress and the directly dissected samples to no stress. The microarray revealed 35 genes regulated upon mechanical stress and 39 genes upon culturing stress, with an overlap of two genes. (B) Further, several comparisons between the four samples were performed. First, we related the comparisons of the stretched sample against all other samples to obtain candidates for mechanical stress, with an overlap of 9 genes. Second, we compared the direct sample against all other samples to obtain candidates for culturing stress, with an overlap of 21 genes. (C) The 9 genes possibly regulated upon mechanical stress were further tested by qRT-PCR, including two more genes which additionally looked promising in the microarray and two Yorkie target genes. Only for the gene Gr43a, did the qRT-PCR recapitulate the microarray data with a fold-change of >1.5.

## 3.4. DISCUSSION

The present study aimed to investigate the growth promoting effect of mechanical forces in the *Drosophila* wing imaginal disc. Computational growth models have previously suggested that mechanical forces interact with molecular growth factors to regulate growth and control size in the wing disc (Shraiman, 2005; Aegerter-Wilmsen et al., 2007; Hufnagel et al., 2007; Aegerter-Wilmsen et al., 2012). Most of the assumptions about forces in these models derive from mammalian cell culture systems. Here, we experimentally addressed whether externally applied mechanical forces are sufficient to modulate proliferation rates also in the wing disc. An earlier study in the wing disc suggested that force application for one hour had a stimulating effect onto the proliferation rate (Schluck et al., 2013). In the present study, we reproduced the experiments with different read-outs for proliferation, but did not find that mechanical forces had any effect on growth. Instead, the handling of the wing disc during the procedure of the experiment, including dissections and the attachment via poly-L-lysine, had a detrimental effect on the proliferation rate, confounding interpretation of the results. We also assessed the transcriptional profile of the wing disc after the application of a mechanical force. But microarray analysis and follow up qRT-PCR experiments did not reveal a transcriptional response specifically to mechanical stress.

The negative results of this study are somewhat difficult to interpret. They do not allow us to draw any conclusion about the underlying hypothesis, namely that mechanical forces promote growth. The negative results might be due to technical difficulties and do not necessarily disprove the hypothesis. Hence, we will further discuss the technical aspects and problems of the experiments.

### 3.4.1. Uncertainty about force propagation

One crucial aspect to consider about the stretching device is the propagation of forces from an organ-wide level to the single cells. First, the fact that a significant part of the wing disc is attached to the glass slides might preclude all cells of the wing disc from being equally stretched. For the cell cycle assays we analyzed the wing pouch region, half of which the area was attached to the objective slide. Hence, half of the analyzed cells might not even be stretched. Also for the transcriptome analysis only a subpopulation of analyzed cells was exposed to mechanical stress. This would make the analysis less sensitive because a transcriptional response is only expected in a

fraction of the tissue. Second, some of the applied force might already be dissipated by the topology of the tissue and not lead to stress on the individual cells. Although the wing disc is often seen as a flat disc, it contains folds and buckles. Hence, some force is needed to unfold the tissue and will not be exerted directly onto the individual cells. Third, the wing disc comprises two cell layers, the columnar and the peripodial cells, and additionally two ECMs at the basal side of each cell layer. Because all these layers propagate the applied forces in parallel, it is currently difficult to estimate to which extent a force is distributed over the different layers. Taken together, there is some uncertainty about how much of the applied force is transduced to the individual cells of the columnar layer, which we are interested in.

### 3.4.2. Discrepancy between studies

We repeated the experiments of Schluck et al. (2013) with different readouts for proliferation. The previous study analyzed the dynamics of proliferation over time by using live- imaging during stretching (Schluck et al., 2013), whereas here we fixed the wing discs after one hour of stretching for an immunostaining. Hence, we compare a dynamic method versus a static one. The different outcomes could be explained if mechanical stress boosts growth by accelerating cell division. Then, if the number of mitotic cells were in a steady state, every single time-point would still have the same amount of dividing cells as before force application. Such an effect would be detectable with a dynamic analysis method but remains invisible for static method such as we used.

Other than the discrepancy between the two methods, also the performance of the experiments could affect different outcomes. Because proliferation in the cultured wing disc reveals strong variation, minor differences in the experimental procedure, such as e.g. staging of larvae, differences in nutrition due to overcrowding, could lead to different inter-experiment outcomes.

### 3.4.3. No fast transcriptional response

In the present study, we did not detect any specific transcriptional response upon application of mechanical stress. However, apart from gene expression, a cellular response to mechanical stress could also be mediated e.g. by protein activation through conformational changes or phosphorylation and by redistribution of cytoskeleton or

cytosolic components (reviewed in Vogel and Sheetz, 2006). Because transcriptional responses usually take more time compared to the aforementioned responses, it is unlikely that a fast stress response is mediated by differential gene expression (Nadal et al., 2011). But on the other hand it is still possible that gene expression is altered on time scales below one hour, as shown for heat shock, oxidative or osmotic stress (Boehm et al., 2003; Capaldi et al., 2008; Shalem et al., 2008).

However, in general it is questionable whether a change in proliferation rate upon mechanical stress is expected to be fast. The average cell cycle of the wing disc increases from 5.6h during second larval instar up to 30h at the end of third instar (Martin et al., 2009). This covers the time that cells need to prepare to be ready for division. Hence, modifications which are associated with proliferation and cell cycle progression are expected to happen on longer time scales and would be missed in the short term analysis performed (Wyatt et al., 2016).

### *3.4.4. Alternative ways to apply forces*

In order to investigate the growth promoting potential of mechanical forces, one could also think about alternative ways to increase mechanical stress in the wing disc. One of the limiting experimental factors so far is the *in vitro* culturing technique, which does not allow maintaining a constant proliferation for a longer time period (Handke et al., 2014). Hence, either the *in vitro* culturing system needs to be improved to apply forces on longer time scales, or *in vivo* manipulation techniques, such as micropipette aspiration and optical or magnetic tweezers (Desprat et al., 2008; Guevorkian et al., 2011; Bambardekar et al., 2015), could be developed for the wing disc and combined with the existing *in vivo* imaging method (Nienhaus et al., 2012; Heemskerk et al., 2014). Also, indirect approaches which either genetically target cytoskeletal components (Rauskolb et al., 2014) or induce overgrowing clones to change global tensions in the tissue (Mao et al., 2013) would be alternatives methods to modulate mechanical forces on longer time-scales.

In sum, the field of mechanical forces and growth regulation remains exciting. There is a general agreement that we cannot leave mechanical forces out of consideration when talking about growth regulation. The future challenge is to develop additional tools to visualize and specifically manipulate mechanical forces. Resulting experimental

findings can then further be used to refine computational models making further predictions about the interplay of mechanical forces and growth regulation.

## 3.5. EXPERIMENTAL PROCEDURES

### 3.5.1. Drosophila strains

Fly stocks were grown on a standard cornmeal medium at 25°C. *Yw* wild-type flies were used for stainings with pH3 and EdU and for the transcriptional analysis.
To image and analyze apical cell shapes, LAC ::YFP flies (Kyoto stock center) were used to mark the septate junctions.

### 3.5.2. Immunohistochemistry

Immunostaining of the wing imaginal disc was performed according to standard protocol. Primary antibody anti-phospho-Histone H3 (Millipore, 06-570) and secondary antibody goat anti-rabbit Alexa Fluor 594 (Molecular Probes, 1:500) were used.

EdU staining was performed with Click it® EdU Alexa Fluor 647 Imaging Kit (Invitrogen) according to standard protocol. Wing discs were incubated for 20 minutes with 10μM EdU for incorporation.

Fixed samples were mounted in VectaShield (Vector Laboratories) and imaged with a Zeiss LSM710.

### 3.5.3. Live imaging

Wing discs were dissected from wandering 3$^{rd}$ instar larvae in WM1. For imaging, they were either mounted in a glass bottom dish (Imaging dish CG, Bioswisstec) covered with a cell culture insert (Millipore), as previously described (Zartman et al., 2013). Alternatively, they were attached to a microscopy glass slide coated with poly-L-lysine. Images were acquired with a Leica SP1 microscope.

### 3.5.4. Stretching device

In order to apply an external force to the cultured wing disc, we used the stretching device as described previously (Schluck and Aegerter, 2010). The wing pouch of the dissected wing disc was attached to a glass slide, whereas the notum was attached to a small, moveable cover slip. Poly-L-lysine (Sigma Aldrich) was used for adhesion. The moveable cover slip was attached to a spring sheet which we used to apply a force to the disc. The resulting mechanical strain was estimated by the distance of the cell clones as landmarks. The mechanical strain of the force we applied for all the experiments was $\varepsilon=0.75$

### 3.5.5. Transcriptome analysis

#### 3.5.5.1. Isolation of mRNA

Wing discs were stretched for one hour in WM1, removed from the stretching device and then immediately flash frozen in liquid nitrogen. For each sample, around seven wing discs were pooled and RNA was isolated using the NucleoSpin RNA kit (Machery Nagel), followed by an DNAse digest with Ambion®DNAse free.

#### 3.5.5.2. Microarray

For microarray, we collected three samples, consisting of seven wing discs, per condition. In the first experiment for mechanical stress we had the following conditions: stretched for one hour (str) vs. attached to the stretching device for one hour without application of force (ctr I). In the second experiment for the culture stress the conditions were: directly frozen after dissection (dir) vs. attached to the stretching device for one hour without application of force (ctr II). In both experiment we mostly used both discs of a larva, one for each condition.

RNA was sent to the Genomics Platform in Geneva for performance and analysis of the microarray.

#### 3.5.5.3. Quantitative real-time PCR

qRT-PCR was performed with the same samples as used for the microarray. For cDNA synthesis, we used the Transcriptor High Fidelity cDNA Synthesis Kit (Roche) with oligo-dT primers. qRT-PCR reactions were done in triplicates with the MESA

Green qRT-PCR Mastermix Plus for SYBR Assay (Eurogentec). Measurements were normalized to RB32 (Ribosomal protein L32) and TBP (TATA box binding protein).

Following primers were used:

CG10211: fw *agccgttggcttcatcat* ; rv *tcagactggaagcgcaaa*

CG5987: fw *tcaatcctcccatgaacgtc*; rv *cacgcagatggtactcttgg*

Cyp18a1: fw *tccaccattctggagtcgat*; rv *acccattgagttccacatcc*
CG6071: fw *gggctttcgtatctttaagc*; rv *ggcgatttcgtattgatcg*
CG7884: fw *tccacatgttaccgagaaatca*; rv *ggaggccaatatcaaggtga*
CG6126: fw *aggacctgatggggaaactt*; rv *agcacctgcaggaagaactg*
Sry-alpha: fw *caggacatcaaaacgaagacg*; rv *catccagggattccagtgag*
CG18507: fw *tgagaatcggctatccttgatt*; rv *tcaagtaaccaccgatcacg*
Gr43a: fw *gtgtccacctcctgtccaac*; rv *agaggaagtaggccgtagcc*
Sog: fw *aagtgtgaatgtgtggcgata*; rv *cgggcactcgtttttgata*
DIAP1: fw *gaaaaagagaaaagccgtcaagt* ; rv *tgtttgcctgactcttaatttcttc*

## *3.6. ACKNOWLEDGEMENTS*

We would like to thank George Hausmann for useful discussions and comments on the manuscript. We thank Flavio Lanfranconi for technical support with the stretching device. Funding for this work was provided by a SystemsX IPhD project.

# 4. CONCLUDING REMARKS

Physical parameters play a crucial role during most developmental processes. The literature cited in the Introduction (Chapter 1) emphasizes the relevance of mechanical forces for organ and tissue growth. But in spite of the general agreement about the importance of mechanics, we are still only beginning to understand the mechanisms of how mechanical forces affect growth and size. Computational modelling and simulations prepared the path for experimental work to unravel the work of mechanics in living tissues. But the development of appropriate tools is lagging behind and advancing only slowly. In this doctoral thesis I approached the study of mechanical forces in two different ways: by devising ways for measuring and manipulating forces in the *Drosophila* wing imaginal disc.

In the first project I aimed to develop a mechanical tension sensor to analyze force distributions across the wing disc and other tissues. Although I designed the sensor very similar to publications by other groups, the sensor was not functional. Moreover, I could not reproduce the core findings from a previous publication. Because many publications about FRET tension sensors are lacking control experiments which I consider essential for FRET measurements, I question conclusions of these studies. Especially for FRET sensors which are integrated into Cadherin proteins, I strongly doubt that these sensors provide robust and reproducible measures for mechanical tensions.

In the second project I used a previously developed setup to stretch the wing disc *in vitro*. I investigated the impact of an externally applied force on the proliferation rate and the gene expression profiles. But no effect could be observed. The obvious limitation was the short time period of the experiment. The combination of the *in vitro* culturing technique and the stretching set-up does not allow one to perform robust experiments for more than one hour. This is a short period of time in which to observe effects on proliferation rate or to expect transcriptional responses. Hence, I believe that studies using the current *in vitro* culturing technique to assay growth and transcription are ambiguous. However, the wing disc research field is progressing in the

development of new *in vitro* culturing media and is advancing with *in vivo* imaging techniques. This will surely open new possibilities for future research projects.

Because throughout my doctoral work I was confronted with presumably irreproducible research findings, I would like to finish the concluding remarks with an essay about "Reproducibility in science".

***Excursus: Reproducibility in science***

The reproducibility of research is one of the central pillars in science. Reproducibility reflects the robustness and the reliability of the scientific work. Only if scientific findings can be reproduced by other scientists do they meet the requirement for the science's claim for an objective truth. However, in recent years a discussion has spread in the scientific community announcing a reproducibility crisis. The inability to reproduce work, even published from high profile journals, lead to the suggestion that around 75%-90% of the experimental findings in biomedical sciences are not reproducible (Prinz et al., 2011; Begley and Ellis, 2012). Similar numbers are also found in other disciplines (Begley and Ioannidis, 2015). Although these numbers have to be treated with caution and might be an overestimate, the problem of irreproducibility is apparent throughout science. Even popular media flagged the topic of flawed and irreproducible scientific studies (The Economist, 2014), which is problematic for the reputation of science in the public. As the public directly or indirectly provides the money for scientific research, the support and confidence of the public for science are essential.

Here, I would like to reflect and discuss the reasons why a lot of scientific work cannot be reproduced. I define reproduction as the successful, independent verification of the core conclusion of a research finding or publication. In contrast to replication, reproduction can also be achieved with a different methodology than that used in the original publication. The very basic reasons why a study cannot be reproduced are: (1) The results cannot be repeated properly because the methodology is either technically challenging or not well documented in the original publication. (2) The interpretation of the original results is wrong. And of course, there is a large grey zone between the two cases because "true" and "wrong" often cannot be clearly defined.

For the problem of insufficiently documented studies, it is partially up to the scientific journals to offer space for a proper documentation and to urge the authors for more transparency and detail in the data acquisition and analysis. The standards of the journals are slowly changing in the right direction to increase strength and quality of the publication process (Journals unite for reproducibility, 2014). Additionally, transparency and openness between scientific competitors is required to facilitate others to repeat and reproduce an original work. But of course, the competition for high impact papers and the resulting scientific culture of confidentiality complicates this prospect (Fang and Casadevall, 2015).

Below, I would like to discuss why scientific literature includes many false positive results which cannot be reproduced. I will emphasize common pitfalls during data collection and analysis, but will not consider scientific misconduct or fraud, because their contribution to the reproducibility crisis is difficult to estimate - and they might only play a minor role (Fanelli, 2009; Collins and Tabak, 2014). The weakness of the publication system is often mentioned as another reason for the high rate of faulty and irreproducible publications. It is widely discussed that the peer review process might not be effective enough to properly evaluate the rigor of scientific work and to reject mediocre studies (Ferguson et al., 2014; Siler et al., 2015). But I still consider the peer-review process as the best, and most feasible system for scientific gatekeeping. The ongoing discussions show that while peer-reviewing is not perfect, it is constantly looking for ways to improve. From my understanding, the high rate of false positive results in the scientific literature is very likely due to a combination of bad scientific practice, a misunderstanding of statistical concepts and the observer bias (strongly provoked by the culture of ‘publish or perish’).

A major source for false positive results which I encountered during the course of this thesis, are measuring errors and batch effects. Measurement errors are systematic errors resulting from small inconsistencies between experiments. For example for FRET measurements, the fluctuations in laser intensity during microscopy, or slight differences in sample preparation, lead to different outcomes between experiments. Very similar to measurement errors are batch effects, which occur if measurements are affected by changing laboratory conditions, e.g. experiments performed on Mondays yield different outcome than on Tuesdays, because uncontrollable conditions slightly differ. This becomes a problem if the conditions vary during the course of the

experiment and correlate with an outcome of interest, leading to wrong conclusions (Leek et al., 2010). For example, a batch effect could happen when analyzing growth or transcription of *Drosophila* wing discs. Both processes show a great variation between different experiments. When testing samples of one condition in one week, and the other condition in another week, the week to week variation could result in a false correlation between the two conditions. The risk of both, measuring errors and batch effects, decreases with the knowledge of the experimenter about the experiment. If he is aware of the sources of variability in the experiments, he can adopt appropriate independent controls. If not, a convincingly low p-value could easily lead to false positive effects.

Another common source for false positives is the misuse of p-values as a definitive test to evaluate whether an effect is true or not. The problem lies in the slippery nature of the p-value, which is not as reliable or objective as generally assumed (Nuzzo, 2014). Scientific studies are regarded to be significant and true, when the p-value is below a certain threshold. But a p-value $< 0.01$ does not necessarily mean that the chance of a false positive result is $< 1\%$, as most scientists would assume. It only tells the probability that the results can be attributed by chance. To make an assumption about the underlying hypothesis one has to know the odds of the hypothesis in the first place. Let's assume, it is known from previous studies that a real positive effect is very likely to be found, with odds of 10:1. Then, a resulting p-value of 0.01 would indeed reveal a probability of 1% of being wrong. But if in another example a real effect is very implausible, e.g. an effect caused by telepathy, with an initial chance of 1:20 for an effect, then a p-value of 0.01 would still indicate a 70% chance of finding a false positive – and not a 1% chance as would be expected from a p-value of 0.01. (Nuzzo, 2014). Hence, if an effect is very unlikely in the first place, then even a low p-value does not necessarily mean that there is a real effect. Or in other words: the lower the initial likelihood of a hypothesis, the higher the risk of a false positive finding – regardless of the p-value. Because scientists love to publish with high impact and therefore tend to go for hypotheses which are new und surprising – thus unlikely – results with a low p-value could be misleading. The same is true for big data analysis, where one expects an effect only in a subset of parameters, as e.g. for the microarray in this thesis. Because we tested 20.000 genes on the microarray chip, but only expected a few of them to be affected by the treatment, the likelihood for each single gene to show a real effect is low. For this reason we still received a couple of presumably false

positive results with a low-p-value, even in all three technical replicates. Hence, the deceptive nature of the p-value could lead to questionable outcomes and interpretations that cannot be reproduced in subsequent studies.

Finally, the last fallacy I would like to discuss is p-hacking, which describes a combination of the p-value problem and the observer bias. The basis for p-hacking is the degree of freedom that scientists have when designing an experiment and planning for data collection and analysis: How much data to collect? How to compare the data? Which data to exclude? Considering relative or absolute values? … If these decisions are not made before the experiment - which is hardly ever the case in daily experimental life - then the researcher is tempted to try different combinations of comparisons and analyses. In fact, the researcher then explores experimental and analytical alternatives to find some statistically significant results. It was shown, that if statistically significant results are achieved only by testing different alternative approaches and selectively reporting them, the rate of false positive results drastically increases (Simmons et al., 2011; Simonsohn et al., 2014).

Irreproducibility in sciences is a complex problem revealing failures and misunderstandings on several levels. There is no single solution but rather a multistakeholder response is needed to address the challenging situation. As briefly mentioned in this essay, the publication system is not perfect and quite often fails to recognize and reject faulty studies. This is to some extent due to the priorities of journals to focus on new and exciting results rather than on the scientific rigor of the work. A consequence is the positive bias, which supports the publication of positive findings. Considering that most of the results of daily research have negative outcomes, most results will never be documented publicly, or they end up as false positive by selective reporting (see p-hacking). Hence, the special requirements of the publication process have to change to accept studies based on scientific rigor, rather than on novelty and relevance. This would also facilitate the publication of negative results which are essential for a scientific discussion. Also the grant reviewing process shows similar problems. For both, publication system and grand reviewing more transparency and clearly defined quality indicators would improve the process. Apart from the publication and grand reviewing process, the problem of irreproducibility could be improved based on the education standards for young scientist. Although taught in some undergraduate courses, the topic of experimental design, statistics and the

observer bias deserves more attention during academic education. When considering the bad scientific practice in many publications, the current standards are clearly not sufficient.

Finally, scientists are generally encouraged to search for new and exciting ideas to push the boundaries of our current knowledge. This brings inevitably the risk of overestimating an effect and of claiming unreliable findings. Hence, we partially have to accept the occurrence of incorrect claims and irreproducible data. A reasonable amount of skepticism and critical thinking helps to overcome this problem.

# 5. REFERENCES

Aegerter-Wilmsen, T., Aegerter, C.M., Hafen, E., Basler, K., 2007. Model for the regulation of size in the wing imaginal disc of Drosophila. Mechanisms of development 124, 318–326.

Aegerter-Wilmsen, T., Heimlicher, M.B., Smith, A.C., Reuille, P.B. de, Smith, R.S., Aegerter, C.M., Basler, K., 2012. Integrating force-sensing and signaling pathways in a model for the regulation of wing imaginal disc size. Development (Cambridge, England) 139, 3221–3231.

Affolter, M., Basler, K., 2007. The Decapentaplegic morphogen gradient: from pattern formation to growth regulation. Nature reviews. Genetics 8, 663–674.

Aigouy, B., Farhadifar, R., Staple, D.B., Sagner, A., Roper, J.-C., Julicher, F., Eaton, S., 2010. Cell flow reorients the axis of planar polarity in the wing epithelium of Drosophila. Cell 142, 773–786.

Akiyama, T., Gibson, M.C., 2015. Decapentaplegic and growth control in the developing Drosophila wing. Nature 527, 375–378.

Alexandre, C., Baena-Lopez, A., Vincent, J.-P., 2014. Patterning and growth control by membrane-tethered Wingless. Nature 505, 180–185.

Aragona, M., Panciera, T., Manfrin, A., Giulitti, S., Michielin, F., Elvassore, N., Dupont, S., Piccolo, S., 2013. A mechanical checkpoint controls multicellular growth through YAP/TAZ regulation by actin-processing factors. Cell 154, 1047–1059.

Armbrecht, G., Belavy, DL., Backström, M., Beller, G., Alexandre, C., Rizzoli, R., Felsenberg, D., 2011. Trabecular and cortical bone density and architecture inwomen after 60 days of bed rest using high-resolution pQCT: WISE 2005. J. Bone Miner. Res. 26, 2399–2410

Austen, K., Ringer, P., Mehlich, A., Chrostek-Grashoff, A., Kluger, C., Klingner, C., Sabass, B., Zent, R., Rief, M., Grashoff, C., 2015. Extracellular rigidity sensing by talin isoform-specific mechanical linkages. Nature cell biology 17, 1597–1606.

Baena-Lopez, L.A., Baonza, A., Garcia-Bellido, A., 2005. The orientation of cell divisions determines the shape of Drosophila organs. Current biology : CB 15, 1640–1644.

Bambardekar, K., Clement, R., Blanc, O., Chardes, C., Lenne, P.-F., 2015. Direct laser manipulation reveals the mechanics of cell contacts in vivo. Proceedings of the National Academy of Sciences of the United States of America 112, 1416–1421.

Baumgartner, W., Hinterdorfer, P., Ness, W., Raab, A., Vestweber, D., Schindler, H., Drenckhahn, D., 2000. Cadherin interaction probed by atomic force microscopy. Proceedings of the National Academy of Sciences of the United States of America 97, 4005–4010.

Becker, W., 2012. Fluorescence lifetime imaging--techniques and applications. Journal of microscopy 247, 119–136.

Begley, C.G., Ellis, L.M., 2012. Drug development: Raise standards for preclinical cancer research. Nature 483, 531–533.

Begley, C.G., Ioannidis, J.P.A., 2015. Reproducibility in science: improving the standard for basic and preclinical research. Circulation research 116, 116–126.

Berney, C., Danuser, G., 2003. FRET or no FRET: a quantitative comparison. Biophysical journal 84, 3992–4010.

Boehm, A.K., Saunders, A., Werner, J., Lis, J.T., 2003. Transcription factor and polymerase recruitment, modification, and movement on dhsp70 in vivo in the minutes following heat shock. Molecular and cellular biology 23, 7628–7637.

Bonewald, L.F., Johnson, M.L., 2008. Osteocytes, mechanosensing and Wnt signaling. Bone 42, 606–615.

Borghi, N., Lowndes, M., Maruthamuthu, V., Gardel, M.L., Nelson, W.J., 2010. Regulation of cell motile behavior by crosstalk between cadherin- and integrin-mediated adhesions. Proceedings of the National Academy of Sciences of the United States of America 107, 13324–13329.

Borghi, N., Sorokina, M., Shcherbakova, O.G., Weis, W.I., Pruitt, B.L., Nelson, W.J., Dunn, A.R., 2012. E-cadherin is under constitutive actomyosin-generated tension that is increased at cell-cell contacts upon externally applied stretch. Proc. Natl. Acad. Sci. USA 109, 12568–12573.

Brodland, G.W., Veldhuis, J.H., Kim, S., Perrone, M., Mashburn, D., Hutson, M.S., 2014. CellFIT: a cellular force-inference toolkit using curvilinear cell boundaries. PloS one 9, e99116.

Bryant, P.J., Levinson, P., 1985. Intrinsic growth control in the imaginal primordia of Drosophila, and the autonomous action of a lethal mutation causing overgrowth. Developmental biology 107, 355–363.

Buchmann, A., Alber, M., Zartman, J. J., 2014. Sizing it up: the mechanical feedback hypothesis of organ growth regulation. Seminars in cell & developmental biology 35, 73–81.

Buckley, C.D., Tan, J., Anderson, K.L., Hanein, D., Volkmann, N., Weis, W.I., Nelson, W.J., Dunn, A.R., 2014. Cell adhesion. The minimal cadherin-catenin complex binds to actin filaments under force. Science (New York, N.Y.) 346, 1254211.

Burke, R., Basler, K., 1996. Dpp receptors are autonomously required for cell proliferation in the entire developing Drosophila wing. Development (Cambridge, England) 122, 2261–2269.

Cai, D., Chen, S.-C., Prasad, M., He, L., Wang, X., Choesmel-Cadamuro, V., Sawyer, J.K., Danuser, G., Montell, D.J., 2014. Mechanical feedback through E-cadherin promotes direction sensing during collective cell migration. Cell 157, 1146–1159.

Campas, O., 2016. A toolbox to explore the mechanics of living embryonic tissues. Seminars in cell & developmental biology.

Campinho, P., Behrndt, M., Ranft, J., Risler, T., Minc, N., Heisenberg, C.-P., 2013. Tension-oriented cell divisions limit anisotropic tissue tension in epithelial spreading during zebrafish epiboly. Nature cell biology 15, 1405–1414.

Collins, F.S., Tabak, L.A., 2014. Policy: NIH plans to enhance reproducibility. Nature 505, 612–613.

Capaldi, A.P., Kaplan, T., Liu, Y., Habib, N., Regev, A., Friedman, N., O'Shea, E.K., 2008. Structure and function of a transcriptional network activated by the MAPK Hog1. Nature genetics 40, 1300–1306.

Chen, C.S., 1997. Geometric Control of Cell Life and Death. Science 276, 1425–1428.

Cheng, G., Tse, J., Jain, R.K., Munn, L.L., 2009. Micro-environmental mechanical stress controls tumor spheroid size and morphology by suppressing proliferation and inducing apoptosis in cancer cells. PloS one 4, e4632.

Chiou, K.K., Hufnagel, L., Shraiman, B.I., 2012. Mechanical stress inference for two dimensional cell arrays. PLoS computational biology 8, e1002512.

Christen, P., Ito, K., Ellouz, R., Boutroy, S., Sornay-Rendu, E., Chapurlat, R.D., van Rietbergen, B., 2014. Bone remodelling in humans is load-driven but not lazy. Nature communications 5, 4855.

Conlon, I., Raff, M., 1999. Size Control in Animal Development. Cell 96, 235–244.

Conway, D.E., Breckenridge, M.T., Hinde, E., Gratton, E., Chen, C.S., Schwartz, M.A., 2013. Fluid shear stress on endothelial cells modulates mechanical tension across VE-cadherin and PECAM-1. Current biology : CB 23, 1024–1030.

Crockett, J.C., Rogers, M.J., Coxon, F.P., Hocking, L.J., Helfrich, M.H., 2011. Bone remodelling at a glance. Journal of cell science 124, 991–998.

Day, S.J., Lawrence, P.A., 2000. Measuring dimensions: the regulation of size and shape. Development (Cambridge, England) 127, 2977–2987.

Desprat, N., Supatto, W., Pouille, P.-A., Beaurepaire, E., Farge, E., 2008. Tissue deformation modulates twist expression to determine anterior midgut differentiation in Drosophila embryos. Developmental cell 15, 470–477.

Dupont, S., Morsut, L., Aragona, M., Enzo, E., Giulitti, S., Cordenonsi, M., Zanconato, F., Le Digabel, J., Forcato, M., Bicciato, S., Elvassore, N., Piccolo, S., 2011. Role of YAP/TAZ in mechanotransduction. Nature 474, 179–183.

Edwards, K.A., Demsky, M., Montague, R.A., Weymouth, N., Kiehart, D.P., 1997. GFP-moesin illuminates actin cytoskeleton dynamics in living tissue and demonstrates cell shape changes during morphogenesis in Drosophila. Developmental biology 191, 103–117.

Egginton, S., 2011. In vivo shear stress response. Biochemical Society transactions, 39, 1633–1638.

Engler, A.J., Sen, S., Sweeney, H.L., Discher, D.E., 2006. Matrix elasticity directs stem cell lineage specification. Cell 126, 677–689.

Esposito, A., Wouters, F.S., 2004. Fluorescence lifetime imaging microscopy. Current protocols in cell biology / editorial board, Juan S. Bonifacino … [et al.] Chapter 4, Unit 4.14.

Fanelli, D., 2009. How many scientists fabricate and falsify research? A systematic review and meta-analysis of survey data. PloS one 4, e5738.

Fang, F.C., Casadevall, A., 2015. Competitive science: is competition ruining science? Infection and immunity 83, 1229–1233.

Ferguson, C., Marcus, A., Oransky, I., 2014. Publishing: The peer-review scam. Nature 515, 480–482.

Fernandez, B.G., Gaspar, P., Bras-Pereira, C., Jezowska, B., Rebelo, S.R., Janody, F., 2011. Actin-Capping Protein and the Hippo pathway regulate F-actin and tissue growth in Drosophila. Development (Cambridge, England) 138, 2337–2346.

Fink, J., Carpi, N., Betz, T., Betard, A., Chebah, M., Azioune, A., Bornens, M., Sykes, C., Fetler, L., Cuvelier, D., Piel, M., 2011. External forces control mitotic spindle positioning. Nature cell biology 13, 771–778.

Fletcher, G.C., Elbediwy, A., Khanal, I., Ribeiro, P.S., Tapon, N., Thompson, B.J., 2015. The Spectrin cytoskeleton regulates the Hippo signalling pathway. The EMBO journal 34, 940–954.

Fristrom, D., Chihara, C., 1978. The mechanism of evagination of imaginal discs of Drosophila melanogaster. V. Evagination of disc fragments. Developmental biology 66, 564–570.

Ganz, A., Lambert, M., Saez, A., Silberzan, P., Buguin, A., Mege, R.M., Ladoux, B., 2006. Traction forces exerted through N-cadherin contacts. Biology of the cell / under the auspices of the European Cell Biology Organization 98, 721–730.

Geiger, B., Spatz, J.P., Bershadsky, A.D., 2009. Environmental sensing through focal adhesions. Nature reviews. Molecular cell biology 10, 21–33.

Gjorevski, N., Piotrowski, A.S., Varner, V.D., Nelson, C.M., 2015. Dynamic tensile forces drive collective cell migration through three-dimensional extracellular matrices. Scientific reports 5, 11458.

Gorfinkiel, N., Arias, A.M., 2007. Requirements for adherens junction components in the interaction between epithelial tissues during dorsal closure in Drosophila. Journal of cell science 120, 3289–3298.

Gorfinkiel, N., Blanchard, G.B., Adams, R.J., Martinez Arias, A., 2009. Mechanical control of global cell behaviour during dorsal closure in Drosophila. Development (Cambridge, England) 136, 1889–1898.

Grashoff, C., Hoffman, B.D., Brenner, M.D., Zhou, R., Parsons, M., Yang, M.T., McLean, M.A., Sligar, S.G., Chen, C.S., Ha, T., Schwartz, M.A., 2010. Measuring mechanical tension across vinculin reveals regulation of focal adhesion dynamics. Nature 466, 263–266.

Green, K.J., Simpson, C.L., 2007. Desmosomes: new perspectives on a classic. The Journal of investigative dermatology 127, 2499–2515.

Guevorkian, K., Gonzalez-Rodriguez, D., Carlier, C., Dufour, S., Brochard-Wyart, F., 2011. Mechanosensitive shivering of model tissues under controlled aspiration. Proceedings of the National Academy of Sciences of the United States of America 108, 13387–13392.

Guilak, F., Cohen, D.M., Estes, B.T., Gimble, J.M., Liedtke, W., Chen, C.S., 2009. Control of stem cell fate by physical interactions with the extracellular matrix. Cell stem cell 5, 17–26.

Hamaratoglu, F., Lachapelle, A.M. de, Pyrowolakis, G., Bergmann, S., Affolter, M., 2011. Dpp signaling activity requires Pentagone to scale with tissue size in the growing Drosophila wing imaginal disc. PLoS biology.

Handke, B., Szabad, J., Lidsky, P.V., Hafen, E., Lehner, C.F., 2014. Towards long term cultivation of Drosophila wing imaginal discs in vitro. PloS one 9, e107333.

Hans, F., Dimitrov, S., 2001. Histone H3 phosphorylation and cell division. Oncogene 20, 3021–3027.

Hariharan, I.K., 2015. Organ Size Control: Lessons from Drosophila. Developmental cell 34, 255–265.

Harmansa, S., Hamaratoglu, F., Affolter, M., Caussinus, E., 2015. Dpp spreading is required for medial but not for lateral wing disc growth. Nature 527, 317–322.

Harris, A.R., Peter, L., Bellis, J., Baum, B., Kabla, A.J., Charras, G.T., 2012. Characterizing the mechanics of cultured cell monolayers. Proceedings of the National Academy of Sciences of the United States of America 109, 16449–16454.

Heath, J.P., Dunn, G.A., 1978. Cell to substratum contacts of chick fibroblasts and their relation to the microfilament system. A correlated interference-reflexion and high-voltage electron-microscope study. Journal of cell science 29, 197–212.

Heemskerk, I., Lecuit, T., LeGoff, L., 2014. Dynamic clonal analysis based on chronic in vivo imaging allows multiscale quantification of growth in the Drosophila wing disc. Development (Cambridge, England) 141, 2339–2348.

Heller, D., Hoppe, A., Restrepo, S., Gatti, L., Tournier, A.L., Tapon, N., Basler, K., Mao, Y., 2016. EpiTools: An Open-Source Image Analysis Toolkit for Quantifying Epithelial Growth Dynamics. Developmental cell 36, 103–116.

Helmlinger, G., Netti, P.A., Lichtenbeld, H.C., Melder, R.J., Jain, R.K., 1997. Solid stress inhibits the growth of multicellular tumor spheroids. Nature biotechnology 15, 778–783.

Hoefer, I.E., den Adel, B., Daemen, Mat J A P, 2013. Biomechanical factors as triggers of vascular growth. Cardiovascular research 99, 276–283.

Huang, J., Zhou, W., Dong, W., Watson, A.M., Hong, Y., 2009. From the Cover: Directed, efficient, and versatile modifications of the Drosophila genome by genomic engineering. Proceedings of the National Academy of Sciences of the United States of America 106, 8284–8289.

Huber, F., Boire, A., Lopez, M.P., Koenderink, G.H., 2015. Cytoskeletal crosstalk: when three different personalities team up. Current opinion in cell biology 32, 39–47.

Hufnagel, L., Teleman, A.A., Rouault, H., Cohen, S.M., Shraiman, B.I., 2007. On the mechanism of wing size determination in fly development Proc. Natl. Acad. Sci. USA 104, 3835–3840.

Ishihara, S., Sugimura, K., 2012. Bayesian inference of force dynamics during morphogenesis. Journal of theoretical biology 313, 201–211.

Izzard, C.S., Lochner, L.R., 1976. Cell-to-substrate contacts in living fibroblasts: an interference reflexion study with an evaluation of the technique. Journal of cell science 21, 129–159.

*Journals Unite for Reproducibility*. Editorial, 2014. Nature 515, 7

Jacobs, C.R., Temiyasathit, S., Castillo, A.B., 2010. Osteocyte mechanobiology and pericellular mechanics. Annual review of biomedical engineering 12, 369–400.

Jankovics, F., Brunner, D., 2006. Transiently reorganized microtubules are essential for zippering during dorsal closure in Drosophila melanogaster. Developmental cell 11, 375–385.

Keller, P.J., 2013. Imaging morphogenesis: technological advances and biological insights. Science (New York, N.Y.) 340, 1234168.

Klein-Nulend, J., Bacabac, R.G., Bakker, A.D., 2012. Mechanical loading and how it affects bone cells: the role of the osteocyte cytoskeleton in maintaining our skeleton. European cells & materials 24, 278–291.

Ladoux, B., Nelson, W.J., Yan, J., Mege, R.M., 2015. The mechanotransduction machinery at work at adherens junctions. Integrative biology : quantitative biosciences from nano to macro 7, 1109–1119.

Leckband, D.E., Rooij, J. de, 2014. Cadherin adhesion and mechanotransduction. Annual review of cell and developmental biology 30, 291–315.

Lecuit, T., Yap, A.S., 2015. E-cadherin junctions as active mechanical integrators in tissue dynamics. Nature cell biology 17, 533–539.

Leek, J.T., Scharpf, R.B., Bravo, H.C., Simcha, D., Langmead, B., Johnson, W.E., Geman, D., Baggerly, K., Irizarry, R.A., 2010. Tackling the widespread and critical impact of batch effects in high-throughput data. Nature reviews. Genetics 11, 733–739.

LeGoff, L., Rouault, H., Lecuit, T., 2013. A global pattern of mechanical stress polarizes cell divisions and cell shape in the growing Drosophila wing disc. Development (Cambridge, England) 140, 4051–4059.

LeGoff, L., Lecuit, T., 2015. Mechanical forces and growth in animal tissues. Cold Spring Harbor perspectives in biology.

Levayer, R., Dupont, C., Moreno, E., 2016. Tissue Crowding Induces Caspase-Dependent Competition for Space. Current biology : CB 26, 670–677.

Mao, Y., Baum, B., 2015. Tug of war--the influence of opposing physical forces on epithelial cell morphology. Developmental biology 401, 92–102.

Mao, Y., Tournier, A.L., Hoppe, A., Kester, L., Thompson, B.J., Tapon, N., 2013. Differential proliferation rates generate patterns of mechanical tension that orient tissue growth. The EMBO journal 32, 2790–2803.

Martin, A.C., Gelbart, M., Fernandez-Gonzalez, R., Kaschube, M., Wieschaus, E.F., 2010. Integration of contractile forces during tissue invagination. The Journal of cell biology 188, 735–749.

Martin, F.A., Herrera, S.C., Morata, G., 2009. Cell competition, growth and size control in the Drosophila wing imaginal disc. Development 136, 3747-56.

Martz, E., Steinberg, M.S., 1972. The role of cell-cell contact in "contact" inhibition of cell division: a review and new evidence. Journal of cellular physiology 79, 189–210.

Mateus, A.M., Martinez Arias, A., 2011. Patterned cell adhesion associated with tissue deformations during dorsal closure in Drosophila. PloS one 6, e27159.

McBeath, R., Pirone, D.M., Nelson, C.M., Bhadriraju, K., Chen, C.S., 2004. Cell shape, cytoskeletal tension, and RhoA regulate stem cell lineage commitment. Developmental cell 6, 483–495.

Meng, F., Sachs, F., 2012. Orientation-based FRET sensor for real-time imaging of cellular forces. Journal of cell science 125, 743–750.

Meng, F., Suchyna, T.M., Sachs, F., 2008. A fluorescence energy transfer-based mechanical stress sensor for specific proteins in situ. The FEBS journal 275, 3072–3087.

Metcalf, D., 1963. THE AUTONOMOUS BEHAVIOUR OF NORMAL THYMUS GRAFTS*. Immunol Cell Biol 41, 437–447.

Milan, M., Campuzano, S., Garcia-Bellido, A., 1996. Cell cycling and patterned cell proliferation in the wing primordium of Drosophila. Proc. Natl. Acad. Sci. USA 93, 640–645.

Miyamoto, T., Slone, J., Song, X., Amrein, H., 2012. A fructose receptor functions as a nutrient sensor in the Drosophila brain. Cell 151, 1113–1125.

Montell, D.J., Yoon, W.H., Starz-Gaiano, M., 2012. Group choreography: mechanisms orchestrating the collective movement of border cells. Nature reviews. Molecular cell biology 13, 631–645.

Munoz-Losa, A., Curutchet, C., Krueger, B.P., Hartsell, L.R., Mennucci, B., 2009. Fretting about FRET: failure of the ideal dipole approximation. Biophysical journal 96, 4779–4788.

Nadal, E. de, Ammerer, G., Posas, F., 2011. Controlling gene expression in response to stress. Nature reviews. Genetics 12, 833–845.

Nellen, D., Burke, R., Struhl, G., Basler, K., 1996. Direct and long-range action of a DPP morphogen gradient. Cell 85, 357–368.

Nelson, C.M., Jean, R.P., Tan, J.L., Liu, W.F., Sniadecki, N.J., Spector, A.A., Chen, C.S., 2005. Emergent patterns of growth controlled by multicellular form and mechanics. Proc. Natl. Acad. Sci. USA 102, 11594–11599.

Neufeld, T.P., de la Cruz, Aida Flor A, Johnston, L.A., Edgar, B.A., 1998. Coordination of Growth and Cell Division in the Drosophila Wing. Cell 93, 1183–1193.

Nienhaus, U., Aegerter-Wilmsen, T., Aegerter, C.M., 2009. Determination of mechanical stress distribution in Drosophila wing discs using photoelasticity. Mechanisms of development 126, 942–949.

Nienhaus, U., Aegerter-Wilmsen, T., Aegerter, C.M., 2012. In-vivo imaging of the Drosophila wing imaginal disc over time: novel insights on growth and boundary formation. PloS one 7, e47594.

Niewiadomska, P., Godt, D., Tepass, U., 1999. DE-Cadherin is required for intercellular motility during Drosophila oogenesis. The Journal of cell biology 144, 533–547.

Nowotarski, S.H., Peifer, M., 2014. Cell biology: a tense but good day for actin at cell-cell junctions. Current biology : CB 24, R688-90.

Nuzzo, R., 2014. Scientific method: statistical errors. Nature 506, 150–152.

Pelham, R. J., Wang, YL., 1997. Cell locomotion and focal adhesions are regulated by substrate flexibility. Proc. Natl. Acad. Sci. USA, 94, 13661-13665

Pope, K.L., Harris, T.J.C., 2008. Control of cell flattening and junctional remodeling during squamous epithelial morphogenesis in Drosophila. Development (Cambridge, England) 135, 2227–2238.

Prinz, F., Schlange, T., Asadullah, K., 2011. Believe it or not: how much can we rely on published data on potential drug targets? Nature reviews. Drug discovery 10, 712.

Puliafito, A., Hufnagel, L., Neveu, P., Streichan, S., Sigal, A., Fygenson, D.K., Shraiman, B.I., 2012. Collective and single cell behavior in epithelial contact inhibition. Proc. Natl. Acad. Sci. USA 109, 739–744.

Raff, M., 1998. Cell suicide for beginners. Nature 396, 119–122.

Rauskolb, C., Sun, S., Sun, G., Pan, Y., Irvine, K.D., 2014. Cytoskeletal tension inhibits Hippo signaling through an Ajuba-Warts complex. Cell 158, 143–156.

Restrepo, S., Zartman, J.J., Basler, K., 2014. Coordination of patterning and growth by the morphogen DPP. Current biology : CB 24, R245-55.

Roh-Johnson, M., Shemer, G., Higgins, C.D., McClellan, J.H., Werts, A.D., Tulu, U.S., Gao, L., Betzig, E., Kiehart, D.P., Goldstein, B., 2012. Triggering a cell shape change by exploiting preexisting actomyosin contractions. Science (New York, N.Y.) 335, 1232–1235.

Roman, B.L., Pekkan, K., 2012. Mechanotransduction in embryonic vascular development. Biomechanics and modeling in mechanobiology 11, 1149–1168.

Rooij, J. de, 2014. Cadherin adhesion controlled by cortical actin dynamics. Nature cell biology 16, 508–510.

Roth, K.A., D'Sa, C., 2001. Apoptosis and brain development. Mental retardation and developmental disabilities research reviews 7, 261–266.

Saias, L., Swoger, J., D'Angelo, A., Hayes, P., Colombelli, J., Sharpe, J., Salbreux, G., Solon, J., 2015. Decrease in Cell Volume Generates Contractile Forces Driving Dorsal Closure. Developmental cell 33, 611–621.

Salbreux, G., Charras, G., Paluch, E., 2012. Actin cortex mechanics and cellular morphogenesis. Trends in cell biology 22, 536–545.

Sansores-Garcia, L., Bossuyt, W., Wada, K.-I., Yonemura, S., Tao, C., Sasaki, H., Halder, G., 2011. Modulating F-actin organization induces organ growth by affecting the Hippo pathway. The EMBO journal 30, 2325–2335.

Schluck, T., Aegerter, C.M., 2010. Photo-elastic properties of the wing imaginal disc of Drosophila. The European physical journal. E, Soft matter 33, 111–115.

Schluck, T., Nienhaus, U., Aegerter-Wilmsen, T., Aegerter, C.M., 2013. Mechanical control of organ size in the development of the Drosophila wing disc. PloS one 8, e76171.

Schulte, F.A., Ruffoni, D., Lambers, F.M., Christen, D., Webster, D.J., Kuhn, G., Muller, R., 2013. Local mechanical stimuli regulate bone formation and resorption in mice at the tissue level. PloS one 8, e62172.

Schwank, G., Basler, K., 2010. Regulation of organ growth by morphogen gradients. Cold Spring Harbor perspectives in biology 2, a001669.

Schwank, G., Restrepo, S., Basler, K., 2008. Growth regulation by Dpp: an essential role for Brinker and a non-essential role for graded signaling levels. Development (Cambridge, England) 135, 4003–4013.

Shalem, O., Dahan, O., Levo, M., Martinez, M.R., Furman, I., Segal, E., Pilpel, Y., 2008. Transient transcriptional responses to stress are generated by opposing effects of mRNA production and degradation. Molecular systems biology 4, 223.

Shraiman, B.I., 2005. Mechanical feedback as a possible regulator of tissue growth. Proc. Natl. Acad. Sci. USA 102, 3318–3323.

Siler, K., Lee, K., Bero, L., 2015. Measuring the effectiveness of scientific gatekeeping. Proceedings of the National Academy of Sciences of the United States of America 112, 360–365.

Simmons, J.P., Nelson, L.D., Simonsohn, U., 2011. False-positive psychology: undisclosed flexibility in data collection and analysis allows presenting anything as significant. Psychological science 22, 1359–1366.

Simonsohn, U., Nelson, L.D., Simmons, J.P., 2014. P-curve: a key to the file-drawer. Journal of experimental psychology. General 143, 534–547.

Smith, M.A., Hoffman, L.M., Beckerle, M.C., 2014. LIM proteins in actin cytoskeleton mechanoresponse. Trends in cell biology 24, 575–583.

Solon, J., Kaya-Copur, A., Colombelli, J., Brunner, D., 2009. Pulsed forces timed by a ratchet-like mechanism drive directed tissue movement during dorsal closure. Cell 137, 1331–1342.

Streichan, S.J., Hoerner, C.R., Schneidt, T., Holzer, D., Hufnagel, L., 2014. Spatial constraints control cell proliferation in tissues. Proc. Natl. Acad. Sci. USA 111, 5586–5591.

Sugimura, K., Lenne, P.-F., Graner, F., 2016. Measuring forces and stresses in situ in living tissues. Development (Cambridge, England) 143, 186–196.

Takai, Y., Miyoshi, J., Ikeda, W., Ogita, H., 2008. Nectins and nectin-like molecules: roles in contact inhibition of cell movement and proliferation. Nature reviews. Molecular cell biology 9, 603–615.

Tatsumi, S., Ishii, K., Amizuka, N., Li, M., Kobayashi, T., Kohno, K., Ito, M., Takeshita, S., Ikeda, K., 2007. Targeted ablation of osteocytes induces osteoporosis with defective mechanotransduction. Cell metabolism 5, 464–75.

Tepass, U., 2012. The apical polarity protein network in Drosophila epithelial cells: regulation of polarity, junctions, morphogenesis, cell growth, and survival. Annual review of cell and developmental biology 28, 655–685.

The Economist. Trouble at the Lab. 19 October 2013. http://www.economist.com/news/briefing/21588057-scientists-think-science-self-correcting-alarming-degree-it-not-trouble. (accessed 20.10.2016)

Thompson, D.W., 1917. On Growth and Form. [With illustrations.]. University Press, Cambridge.

Tsuyama, T., Kishikawa, J.-i., Han, Y.-W., Harada, Y., Tsubouchi, A., Noji, H., Kakizuka, A., Yokoyama, K., Uemura, T., Imamura, H., 2013. In vivo fluorescent adenosine 5'-triphosphate (ATP) imaging of Drosophila melanogaster and Caenorhabditis elegans by using a genetically encoded fluorescent ATP biosensor optimized for low temperatures. Analytical chemistry 85, 7889–7896.

Twitty, V.C., Schwind, J.L., 1931. The growth of eyes and limbs transplanted heteroplastically between two species of Amblystoma. J. Exp. Zool. 59, 61–86.

Uyttewaal, M., Burian, A., Alim, K., Landrein, B., Borowska-Wykręt, D., Dedieu, A., Hamant, O., 2012. Mechanical stress acts via katanin to amplify differences in growth rate between adjacent cells in Arabidopsis. Cell, 149, 439–51.

van Rheenen, J., Langeslag, M., Jalink, K., 2004. Correcting confocal acquisition to optimize imaging of fluorescence resonance energy transfer by sensitized emission. Biophysical journal 86, 2517–2529.

VanBeek, D.B., Zwier, M.C., Shorb, J.M., Krueger, B.P., 2007. Fretting about FRET: correlation between kappa and R. Biophysical journal 92, 4168–4178.

Vico, L., Collet, P., Guignandon, A., Lafage-Proust, MH., Thomas, T., Rehaillia, M., Alexandre, C., 2011.

Effects of long-term microgravity exposure on cancellous and cortical weight-bearing bones of cosmonauts. Lancet 355, 1607–1611

Vogel, V., Sheetz, M., 2006. Local force and geometry sensing regulate cell functions. Nature reviews. Molecular cell biology 7, 265–275.

Wartlick, O.; Mumcu, P.; Kicheva, A.; Bittig, T.; Seum, C.; Julicher, F.; Gonzalez-Gaitan, M., 2011. Dynamics of Dpp signaling and proliferation control. Science 331, 1154–1159.

Wartlick, O., Mumcu, P., Julicher, F., Gonzalez-Gaitan, M., 2011. Understanding morphogenetic growth control -- lessons from flies. Nature reviews. Molecular cell biology 12, 594–604.

Wei, S.-Y., Escudero, L.M., Yu, F., Chang, L.-H., Chen, L.-Y., Ho, Y.-H., Lin, C.-M., Chou, C.-S., Chia, W., Modolell, J., Hsu, J.-C., 2005. Echinoid is a component of adherens junctions that cooperates with DE-Cadherin to mediate cell adhesion. Developmental cell 8, 493–504.

Weigmann, K., Cohen, S. M., Lehner, C. F., 1997. Cell cycle progression , growth and patterning in imaginal discs despite inhibition of cell division after inactivation of Drosophila Cdc2 kinase. Development 124, 3555–3563.

Wessels, J.T., Yamauchi, K., Hoffman, R.M., Wouters, F.S., 2010. Advances in cellular, subcellular, and nanoscale imaging in vitro and in vivo. Cytometry. Part A : the journal of the International Society for Analytical Cytology 77, 667–676.

Wyatt, T.P.J., Harris, A.R., Lam, M., Cheng, Q., Bellis, J., Dimitracopoulos, A., Kabla, A.J., Charras, G.T., Baum, B., 2015. Emergence of homeostatic epithelial packing and stress dissipation through divisions oriented along the long cell axis. Proceedings of the National Academy of Sciences of the United States of America 112, 5726–5731.

Wyatt, T., Baum, B., Charras, G., 2016. A question of time: tissue adaptation to mechanical forces. Current opinion in cell biology 38, 68–73.

You, L., Cowin, S.C., Schaffler, M.B., Weinbaum, S., 2001. A model for strain amplification in the actin cytoskeleton of osteocytes due to fluid drag on pericellular matrix. Journal of Biomechanics 34, 1375–1386.

Youvan, D.C., Silva, C.M., Bylina, E.J., Coleman, W.J., Dilworth, M.R., Yang, M.M., 1997. Calibration of Fluorescence Resonance Energy Transfer in Microscopy Using Genetically Engineered GFP Derivatives on Nickel Chelating Beads. Biotechnology.

Zartman, J., Restrepo, S., Basler, K., 2013. A high-throughput template for optimizing Drosophila organ culture with response-surface methods. Development 140, 667–674.

Zecca, M., Basler, K., Struhl, G., 1995. Sequential organizing activities of engrailed, hedgehog and decapentaplegic in the Drosophila wing. Development 121, 2265–2278.

Zecca, M., Basler, K., Struhl, G., 1996. Direct and long-range action of a wingless morphogen gradient. Cell 87, 833–844.

# 6. ACKNOWLEDEMENTS

First and foremost I would like to thank my two supervisors, Christof Aegerter and Konrad Basler, for the possibility to join their laboratories and for providing the perfect environment to independently approach my research question. I am especially grateful for their trust in my abilities and for the freedom to accept that science often just does not work out as expected.

Many thanks also to my PhD committee members Markus Affolter and Frank Schnorrer for their valuable inputs and inspiring discussions during the committee meetings.

Many thanks to all the past and present members of the Basler group, not only for their scientific support, but also for the great skiing-weekends, endless hours of table-soccer, Spanish tandems, pizza evenings, lunch breaks, all the beers and other activities together. Especially I want to thank Amarendra Badugu for being a good companion through all these years, his inspiring attitude and his enthusiasm for so many things. Additionally, I am grateful to George Hausmann for the valuable feedback and corrections of scientific texts, Marc Debrunner for embryo injections and Davide Heller for assistance with the Epitool software.

I also thank the past and present members of the Aegerter group, for the scientific support of the physics behind my project, for BBQs, dinners, beers, and the other enjoyable times. Especially, I would like to thank Sahil Puri for being the active part in our group's social life, and Flavio Lanfranconi for the great help with the stretching bench.

I also thank the members of the Brunner, Lehner and Luschnig groups for inputs and discussions during the Tuesday's progress reports. Special thanks go to Laurynas Pasakarnis for introducing me to the work on dorsal closure.

An dieser Stelle möchte ich mich ganz herzlichst bei meiner Familie, und ganz besonders bei meinen Eltern Hans und Agatha Eder, für die Unterstützung und das Vertrauen über all die Jahre hinweg bedanken.

Finally, I would like to express my great gratitude to Anna for being on my side, for the love, encouragement and patience, especially in the final month of my studies which coincided with the final month of pregnancy. And thanks to our unborn baby for the patience to let me finish the last words of this thesis.

# 7. CURRICULUM VITAE

**NAME:** EDER

**VORNAME:** Dominik

**GEBOREN:** am 17.07.1983 in Innsbruck (Österreich)

**NATIONALIÄT :** Österreich

**SCHULBILDUNG:**

| | |
|---|---|
| 1993-2001 | Bundesrealgymnasium Adolf-Pichler Platz in Innsbruck (AHS Matura) |

**AUSBILDUNG:**

| | |
|---|---|
| 2005-2008 | Bachelorstudium in Zoologie an der Universität Wien |
| 2008-2011 | Masterstudium in molekularer Zell- und Entwicklungsbiologie an der Universität Innsbruck<br><br>Masterarbeit: "*Molecular Characterization of the Two Cnidarian Homeobox Transcription Factors: HB9 and Distal-less*", unter der Leitung von Prof. Dr. Bert Hobmayer und Prof. Dr. Dirk Meyer |
| Seit 2012 | Doktorand am *Institute of Molecular Life Sciences* an der Universiät Zürich unter der Leitung von Prof. Dr. Konrad Basler und Prof. Dr. Christof Aegerter |